Molecular Diversity
https://doi.org/10.1007/s11030-022-10551-0

ORIGINAL ARTICLE

Novel 1,2,4-triazoles derived from Ibuprofen: synthesis and in vitro evaluation of their mPGES-1 inhibitory and antiproliferative activity

Bahadır Bülbül[1,2] · Kai Ding[3,4] · Chang-Guo Zhan[3,4] · Gamze Çiftçi[5] · Kemal Yelekçi[5] · Merve Gürboğa[6] · Özlem Bingöl Özakpınar[6] · Esra Aydemir[7,8] · Deniz Baybağ[7] · Fikrettin Şahin[7] · Necla Kulabaş[9] · Sinem Helvacıoğlu[10] · Mohammad Charehsaz[10] · Esra Tatar[9] · Süheyla Özbey[11] · İlkay Küçükgüzel[9]

Received: 10 June 2022 / Accepted: 17 October 2022

Abstract

Some novel triazole-bearing ketone and oxime derivatives were synthesized from Ibuprofen. In vitro cytotoxic activities of all synthesized molecules against five cancer lines (human breast cancer MCF-7, human lung cancer A549, human prostate cancer PC-3, human cervix cancer HeLa, and human chronic myelogenous leukemia K562 cell lines) were evaluated by MTT assay. In addition, mouse embryonic fibroblast cells (NIH/3T3) were also evaluated to determine the selectivity. Compounds **18, 36**, and **45** were found to be the most cytotoxic, and their IC_{50} values were in the range of 17.46–68.76 µM, against the tested cancer cells. According to the results, compounds **7** and **13** demonstrated good anti-inflammatory activity against the microsomal enzyme prostaglandin E2 synthase-1 (mPGES-1) enzyme at IC50 values of 13.6 and 4.95 µM. The low cytotoxicity and non-mutagenity of these compounds were found interesting. Also, these compounds significantly prevented tube formation in angiogenesis studies. In conclusion, the anti-inflammatory and angiogenesis inhibitory activities of these compounds without toxicity suggested that they may be promising agents in anti-inflammatory treatment and they may be supportive agents for the cancer treatment.

This research was partly presented at the 2nd International Gazi Pharma Symposium Series (GPSS 2017) on 11–13 October 2017, Ankara, Turkey, Abstract ID: 337

✉ İlkay Küçükgüzel
ikucukguzel@marmara.edu.tr

1 Department of Pharmaceutical Chemistry, Faculty of Pharmacy, Düzce University, Konuralp, Düzce, Turkey

2 Department of Pharmaceutical Chemistry, Institute of Health Sciences, Marmara University, Dragos, Kartal, 34865 Istanbul, Turkey

3 Department of Pharmaceutical Sciences, College of Pharmacy, University of Kentucky, 789 South Limestone Street, Lexington, KY 40536, USA

4 Center for Pharmaceutical Research and Innovation, College of Pharmacy, University of Kentucky, 789 South Limestone Street, Lexington, KY 40536, USA

5 Department of Bioinformatics and Genetics, Faculty of Engineering and Natural Sciences, Kadir Has University, Istanbul, Turkey

6 Department of Biochemistry, Faculty of Pharmacy, Marmara University, Haydarpaşa, 34668 Istanbul, Turkey

7 Department of Genetics and Bioengineering, Faculty of Engineering, Yeditepe University, Kayışdağı, Istanbul, Turkey

8 Department of Biomedical Engineering, Faculty of Engineering and Natural Sciences, Biruni University, Zeytinburnu 34010, Turkey

9 Department of Pharmaceutical Chemistry, Faculty of Pharmacy, Marmara University, Başıbüyük, 34854 Istanbul, Turkey

10 Department of Toxicology, Faculty of Pharmacy, Yeditepe University, Ataşehir, 34750 Istanbul, Turkey

11 Department of Physics Engineering, Faculty of Engineering, Hacettepe University, Beytepe, 06800 Ankara, Turkey

Published online: 04 November 2022

Graphical abstract

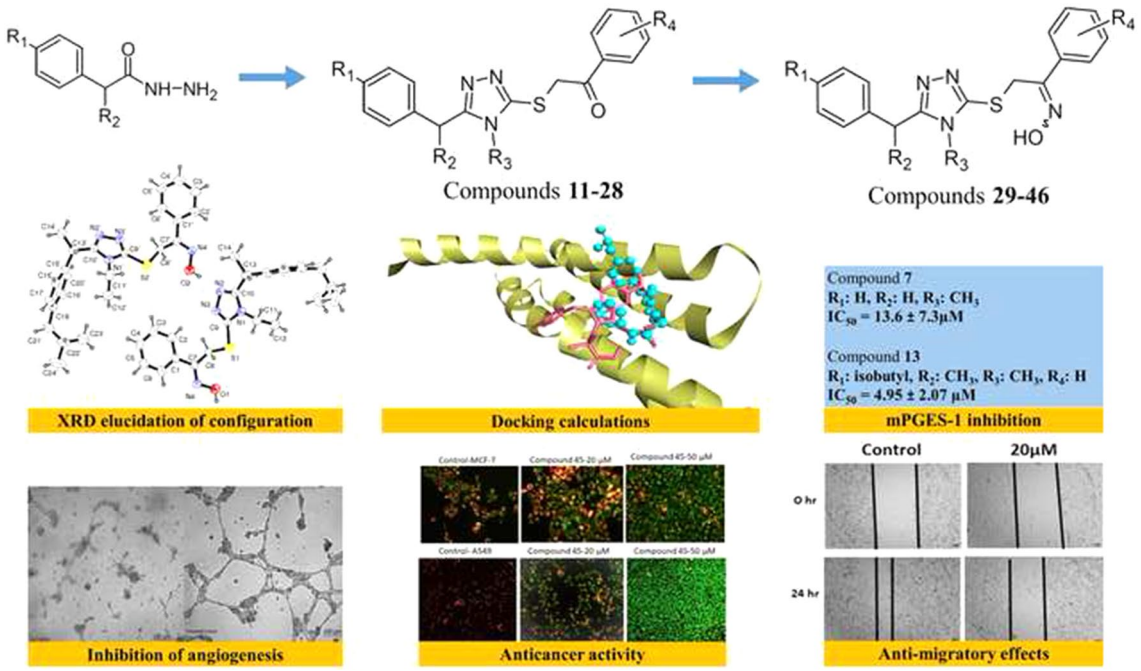

Keywords 1,2,4-Triazole · Atropisomer · Diastereotope · X-ray diffraction · Cancer · Angiogenesis · mPGES-1 · Cytotoxicity

Introduction

Cancer is recognized as an essential health issue with many types which are believed to be associated with the chronic effect of prostaglandin E2 (PGE_2) [1]. On the other hand, PGE_2 is a vital eicosanoid that plays a crucial role in homeostasis. By examining the reports on cancer biology, it can be seen that PGE_2 stimulates tumor cell proliferation, migration, and invasion [1, 2] and supports angiogenesis by increasing vascular endothelial growth factor (VEGF) production [1–3]. In addition, PGE_2 also influences cells in the tumor microenvironment and promotes tumor growth by suppressing immunosurveillance [1, 4]. According to Zhang et al., the mean metastasis of A549 cells in PGE_2 loaded mice was more than that in control mice. Contrarily, treatment with Celecoxib suppressed lung metastasis in the same experiment. The same report also shows that PGE_2 increased migration and invasion of A549 cells by wound healing and Transwell assays, which could be reversed by Celecoxib [5]. Clinical studies have noted a reduced risk for breast, lung, prostate, and colon cancers after treatment with non-steroidal anti-inflammatory drugs (NSAIDs) [1, 4–6].

Many studies focus on cyclooxygenase-2 (COX-2) expression in tumors [3–5], but there is a hidden etiology in many clinical pathologies that is co-expressed with COX-2, called microsomal prostaglandin E2 synthase-1 (mPGES-1) and in particular, PGE_2 is produced by the collaboration of COX-2 and mPGES-1 enzymes [1, 2, 6–12]. Furthermore, due to the facts mentioned above mPGES-1 has been identified as a promising target for treating inflammatory and neoplastic diseases.

Ibuprofen usage in the prophylaxis and treatment of cancer is an entirely new therapeutic approach [13–16]. To avoid the gastrointestinal damage caused by chronic drug use, the researchers focused on the search for more effective and less harmful compounds particularly obtained by derivatizing carboxylic acid function [17, 18]. One of these derivatization approaches is the cyclization to the triazole ring [19–25]. The interest of our team working on this heterocyclic ring system and its bioisosteres has turned into the search for new compounds showing anticancer anti-inflammatory effects [1, 26, 27]. The anticancer activity or mPGES-1 enzyme inhibitory effects of the main skeletons we progressively synthesize [26] were also reported by different research groups [28–30] (Fig. 1).

Following a careful literature study, selected compounds were synthesized and their structures were elucidated as well as their biological activities were tested. Molecular docking was operated for the most active compounds. This study aims to confirm the structures of the synthesized

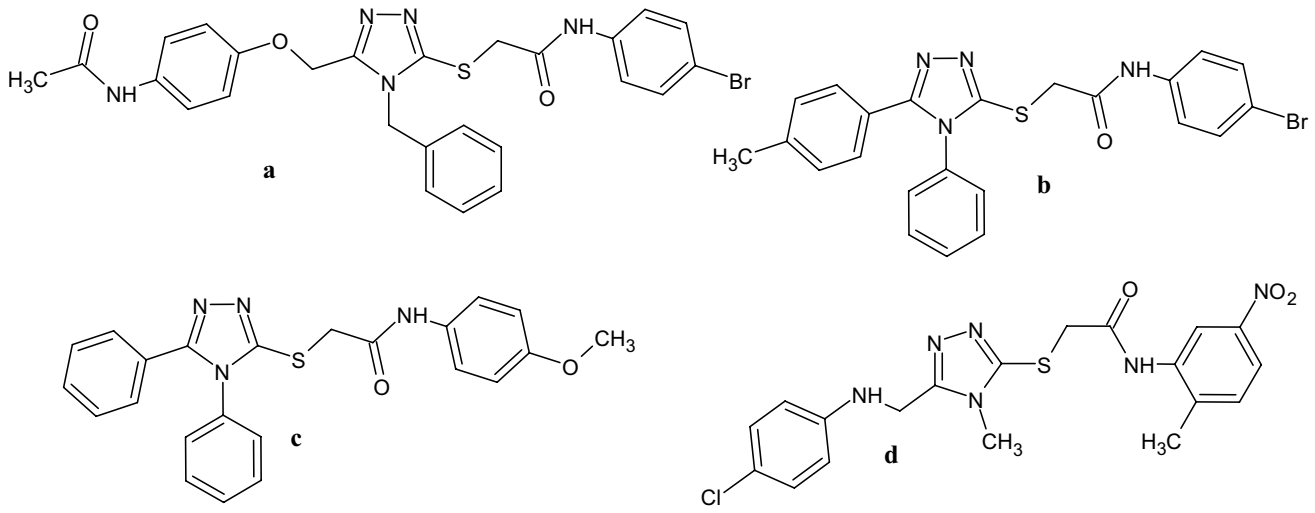

Fig. 1 1,2,4-Triazole bearing compounds with anticancer or anti-inflammatory activities

1,2,4-triazole carrying thioether compounds by spectral methods and to investigate their possible anticancer or anti-inflammatory effects.

Results and discussion

Chemistry

The primary starting material of our study was Ibuprofen. In order to support the structure determination and biological activity studies, it was decided to prepare one more series of compounds from phenylacetohydrazide (compound **1**). For the Ibuprofen-derived structures, an esterification reaction was performed first [25, 31–33]. The resulting Ibuprofen-ester (Fig. S1) was refluxed in ethanol with hydrazine monohydrate to give 2-[4-(2-methylpropyl)phenyl]propanehydrazide structure (compound **2**, Figs. S2–S4) [25, 31–34]. Then, the synthetic route given in Scheme 1 was followed to obtain the target compounds. Refluxing compound **1** (commercial phenylacetohydrazide), and compound **2** (Ibuprofen hydrazide) with methyl-/ethylisothiocyanate in ethanol yielded substituted thiosemicarbazides (compounds **3–6**, Figs. S5–S15) [25, 35–45]. All cyclization products (compound **7–10**, Figs. S16–S27) were prepared by refluxing all substituted thiosemicarbazide compounds in NaOH solution followed by acidifying the produced sodium salts with dilute solution of HCl [25, 26, 39, 42–49]. The compounds **7–10** and bromo/chloroacetophenone derivatives were reacted in acetonitrile with TEA to gain thioether compounds **11–28** (Figs. S28–S89, Table S1–S3) [50, 51]. Next, the carbonyl group was converted to oxime to obtain the compounds **29–46** in pyridine with hydroxylamine hydrochloride (Figs. S90–S152, Table S3–S5) [52].

All synthesized compounds were checked for purity using TLC, HPLC–UV/DAD, and elemental analysis. Melting point determinations and IR spectra of the synthesized compounds were operated in our laboratory. Also, ^{1}H-NMR spectra were obtained for all intermediates and target compounds except for a few intermediates consistent with the literature data. The molecular weights of all target compounds were confirmed by MS. HMBC spectra were taken for compounds **13, 14, 31**, and **32**. X-ray diffraction analysis of compound **32** was obtained to clarify the *Z/E* isomeric forms in the oxime functionality.

When the FTIR spectra of the synthesized target compounds were examined, it was seen that the triazole-3-thione tautomeric C=S stretching bands disappeared [19, 26, 41, 44, 45, 53–56] (Figs. S16, S36). Due to the hydrogen bonding in oxime derivatives, O–H stretching bands were observed in the frequency region of 3311–3078 cm^{-1}. In ketone compounds, any –OH stretching band was not found [50–57]. The exception for that observation was compound **21**, which was proven to carry crystal water, and showed an –OH stretching band at 3410 cm^{-1} (Fig. S66). Carbonyl stretching bands were not observed in compounds **7–10** and were observed in ketones between the frequency range of 1697–1647 cm^{-1}[25]. It was observed that these bands disappeared when converted to oximes. In addition, C=N and N–O stretching bands of oxime moiety were observed between 1643–1693 cm^{-1} and 950–979 cm^{-1} frequency regions, respectively [50, 52].

In the ^{1}H-NMR spectra of the target compounds, the peaks attributable to SCH_2 hydrogens were observed in the range of 4.21–4.91 ppm, but they exhibited unexpected coupling, which gave rise to AB quartets. To ensure that the chirality is the reason for these observations, compounds **11, 12, 29**, and **30** were synthesized. The peaks of SCH_2

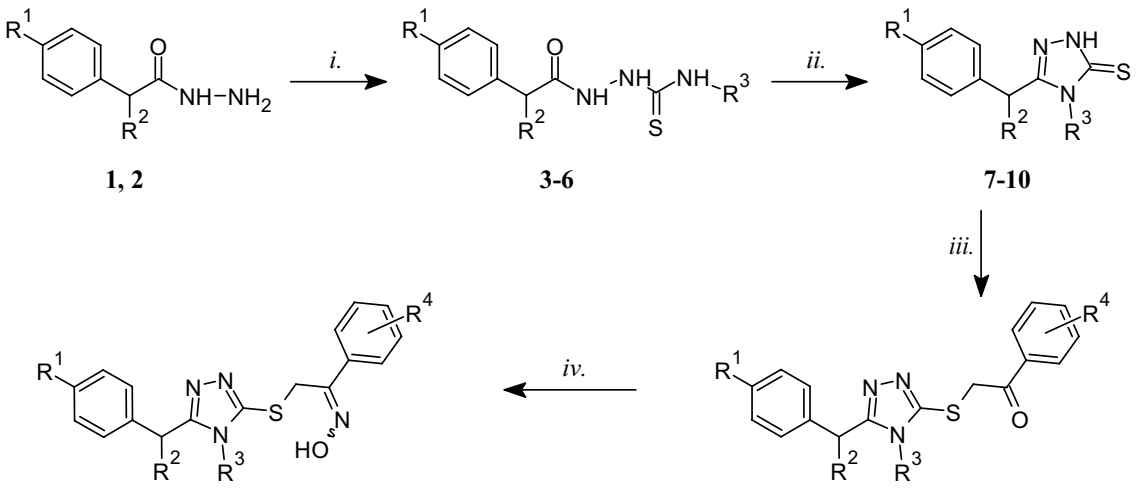

Compd	1	2	3	4	5	6	7	8	9	10
R^1	H	isobutyl	H	H	isobutyl	isobutyl	H	H	isobutyl	isobutyl
R^2	H	CH_3	H	H	CH_3	CH_3	H	H	CH_3	CH_3
R^3	-	-	CH_3	C_2H_5	CH_3	C_2H_5	CH_3	C_2H_5	CH_3	C_2H_5

11, 29: R^1: H, R^2: H, R^3: CH_3, R^4: H
12, 30: R^1: H, R^2: H, R^3: C_2H_5, R^4: H
13, 31: R^1: isobutyl R^2: CH_3, R^3: CH_3, R^4: H
14, 32: R^1: isobutyl R^2: CH_3, R^3: C_2H_5, R^4: H
15, 33: R^1: isobutyl R^2: CH_3, R^3: CH_3, R^4: 3-Cl
16, 34: R^1: isobutyl R^2: CH_3, R^3: C_2H_5, R^4: 3-Cl
17, 35: R^1: isobutyl R^2: CH_3, R^3: CH_3, R^4: 4-Cl
18, 36: R^1: isobutyl R^2: CH_3, R^3: C_2H_5, R^4: 4-Cl
19, 37: R^1: isobutyl R^2: CH_3, R^3: CH_3, R^4: 3-F
20, 38: R^1: isobutyl R^2: CH_3, R^3: C_2H_5, R^4: 3-F
21, 39: R^1: isobutyl R^2: CH_3, R^3: CH_3, R^4: 4-F
22, 40: R^1: isobutyl R^2: CH_3, R^3: C_2H_5, R^4: 4-F
23, 41: R^1: isobutyl R^2: CH_3, R^3: CH_3, R^4: 2,4-F_2
24, 42: R^1: isobutyl R^2: CH_3, R^3: C_2H_5, R^4: 2,4-F_2
25, 43: R^1: isobutyl R^2: CH_3, R^3: CH_3, R^4: 2,5-$(OCH_3)_2$
26, 44: R^1: isobutyl R^2: CH_3, R^3: C_2H_5, R^4: 2,5-$(OCH_3)_2$
27, 45: R^1: isobutyl R^2: CH_3, R^3: CH_3, R^4: 4-Br
28, 46: R^1: isobutyl R^2: CH_3, R^3: C_2H_5, R^4: 4-Br

Scheme 1 Synthetic route to compounds **1**–**46**. Key to reagents: *i* R_3NCS, EtOH; *ii* a 2N NaOH, b. 10% HCl; *iii* 2-bromo/chloroacetophenone, ACN, TEA; *iv* $NH_2OH.HCl$, pyridine

hydrogens ^{1}H-NMR spectra were observed singlet between 4.21–4.91 ppm as expected (Fig. S29, S33, S91, S95) [50, 51]. In order to understand the effect of the chirality causing this difference, a literature study was conducted. As a result, the concepts of diastereotopism and atropisomerism have emerged. Since our Ibuprofen-based compounds are racemic and have one stereogenic center, all methylene hydrogens in these structures are chemically non-equivalent and they are diastereotopic [58, 59]. In case of free rotation inhibition around one single bond, the molecule becomes atropisomeric [60–62]. According to Frączek et al., atropisomeric molecule's methylene hydrogens become chemically non-equivalent and interact with each other geminally [60].

The methylene function is adjacent to the sulfur atom with *n* electrons, and the carbonyl function with the π bond. In this case, the sulfur atom can donate electron couple by resonance. On the other hand, the carbonyl withdraws electrons from H_2C–C=O methylene inductively. Since we have a conjugation, it was thought that these interactions on the "S–(CH2)–C=O" system might cause delocalization of electrons, which would prevent free rotation and cause atropisomerism ultimately [58–60]. In light of these, ^{1}H-NMR spectra of compounds were examined, and it was observed that S–CH_2–C=O methylene protons of compounds **13–28** showed AB quartet type division (Fig. 2a). In the compounds **31–46**, these methylene protons showed singlet or AB quartet divisions due to the lower electronegativity difference between C and N atoms of oxime function (Fig. 3) [63, 64].

In conclusion, the diastereotope S–CH_2 hydrogens were observed to act in the magnetic field according to the sum of all their molecular medium's electromagnetic effects and could become atropisomers [58–60, 65]. The SCH_2 hydrogen peaks of compounds **23** and **24** were the exceptions for that divisions. The difference between these molecules' SCH_2 hydrogen peaks and the other AB quartet divisions was that each peak nail was split into two identical parts. That division pattern was thought to be caused by two fluorines in each molecule Fig. 2b. When the oxime derivatives of these compounds (compounds **41**, **42**) were examined, the peaks were observed to be complex multiplet and highly shielded. They interfered with the –CH hydrogen peaks of the Ibuprofen-derived structures (Fig. 2c).

Methylene protons of compounds **8, 12**, and **30** at the triazole N^4 position gave quartet peaks at 3.88 and 3.76 ppm

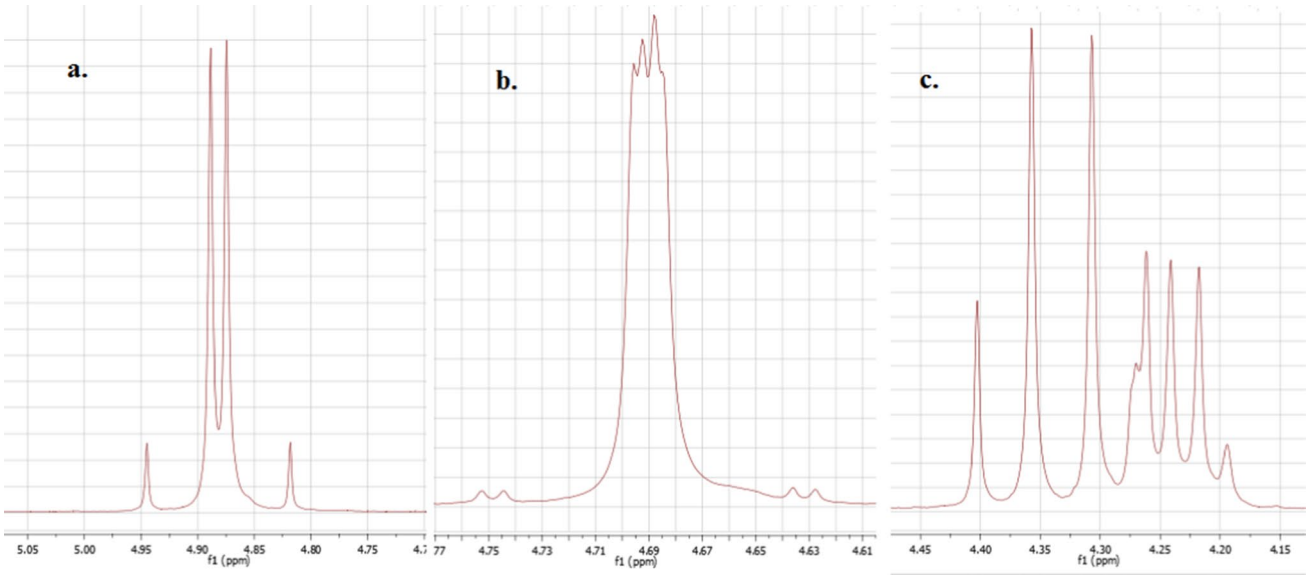

Fig. 2 **a** AB quartet coupling of compounds **13–28** due to the S–CH_2–C=O methylene protons. **b** S–CH_2–C=O methylene multiplet division of di-fluorine bearing compounds **23, 24**. **c** –(CH_2)–C=O methylene and –$CHCH_3$ multiplet division of di-fluorine bearing compounds **41**, **42**

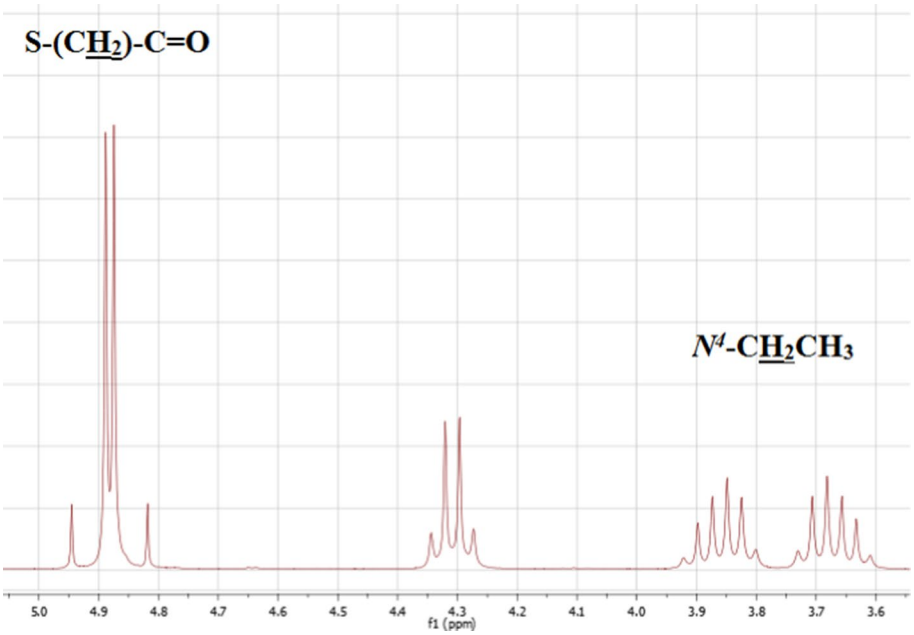

Fig. 3 S–(CH_2)–C=O methylene singlet peak and N^4–CH_2CH_3 double multiplet division of compounds **31–46**

as expected (Figs. S29, S33, S91, S95) [44, 45, 50]. However, the same methylene hydrogens were observed to give two multiplet signal groups in the range of 3.42–3.92 ppm for the compounds **10**, **14** and **32**. (Fig. 3). Similar observations were also reported by different research groups without mentioning atropisomerism [58, 59]. However, according to the earlier report by Karczmarzyk et al. [66], N^4–CH_2–CH_3 bonding of the triazoles could have an angle of 88.55° between the 1,2,4-triazole ring central plane, and the free rotation of the methylene considered to be restricted due to the intramolecular interactions [66]. In the evaluation made by considering all this information, it was concluded that the source of these extreme divisions observed are both atropisomerism and diastereotopism. (Figs. S108, S109, Table S6) [58, 59, 66].

When the ^{1}H-NMR spectra of all oxime derivatives **29–46** were examined, it was observed that the whole spectra shifted to TMS with the transition from ketone to oxime due to the lower electronegativity difference between carbon and nitrogen [50]. It was also observed that, in some spectra,

the peak area of oxime hydrogen C=N–O–H corresponds to less than 1H and had a sister peak in the shielded field (Fig. 4). According to Baji et al. [57], oxime compounds can show these sister peaks due to the *Z/E* isomeric impurity, and the sister peak: peak ratio can give us the isomeric ratio. Also, it was reported that the same sister peak pattern could be seen in the rest of the spectrum, and the sister peak: peak ratio should be the same [57]. When the remaining parts of our such spectra were examined, it was found that some of the alkyl peaks could show the same sister peak properties. Also, it has been observed that the sister peak ratio of the oxime is the same as the alkyl sister peak ratios in the same spectrum (Figs. S91, S136, Table S7).

In order to support the structure elucidation studies, HMBC spectra were taken for compounds **13, 14, 31**, and **32** due to the same main skeleton of the synthesized compounds (Fig. 5). In the HMBC spectra of compounds **13** and 31, the C-28 carbon did not interact with any of the hydrogens (Figs. S39, S101, Table S1, S4). However, when the HMBC spectra of compounds **14** and **32** were examined, it was seen that C-28 carbon interacted with the adjacent C-29 hydrogens. Likewise, C-29 carbon was coupled with only C-28 hydrogens for compounds **14** and **32** (Figs. S45, S107, Table S3, S5). C-11 carbon interacted only with the adjacent C-10 hydrogen for each compound, while the C-11 hydrogens interacted with C-5, C-10, and C-18 carbons. For the C-10 carbon, the hydrogen interactions except the C-11 hydrogens are seen in the aromatic region coming from Ibuprofen. The C-7 carbon did not show any hydrogen interactions in each spectrum. It was observed that the C-7 carbon's hydrogens coupled with the C-2 and C-8 carbons

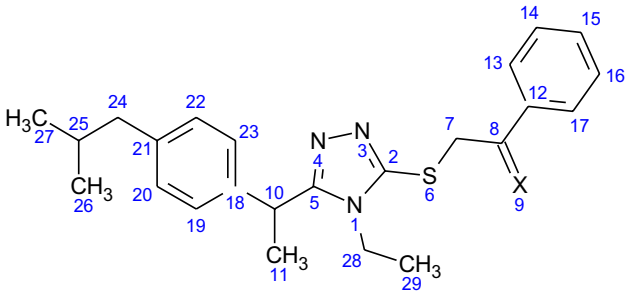

Fig. 5 Structure numbering for the HMBC and ^{13}C NMR studies

in each spectrum (Figs. S39, S45, S101, S107, Table S1, S3, S4, S5).

C-12 and C-15 ipso carbons only interacted with the acetophenone aromatic hydrogens. C-18 and C-21 carbons interacted with aromatic hydrogens of the Ibuprofen. Also, C-18 carbon, C-10, and C-11 aliphatic hydrogen interactions, and for C-21 carbon, C-24 aliphatic hydrogen interactions were observed in each spectrum. C-2 ipso carbon interacts with C-7 and C-28 hydrogens, and ipso C-5 interacts with C-10, C-11, and C-28 hydrogens in each spectrum. All these findings were evaluated to confirm the structures of the compounds **13, 14, 31,** and **32** (Fig. 5, S39, S45, S101, S107, Tables S1, S3, S4, S5).

^{13}C NMR data of compounds **13**, **14**, **31**, and **32** were obtained from the HMBC spectra. When the ^{13}C NMR data of the ketone-oxime compound pairs were compared, it was seen that most of the chemical shifts did not change, unlike ^{1}H-NMR data. The most shifting carbons in both

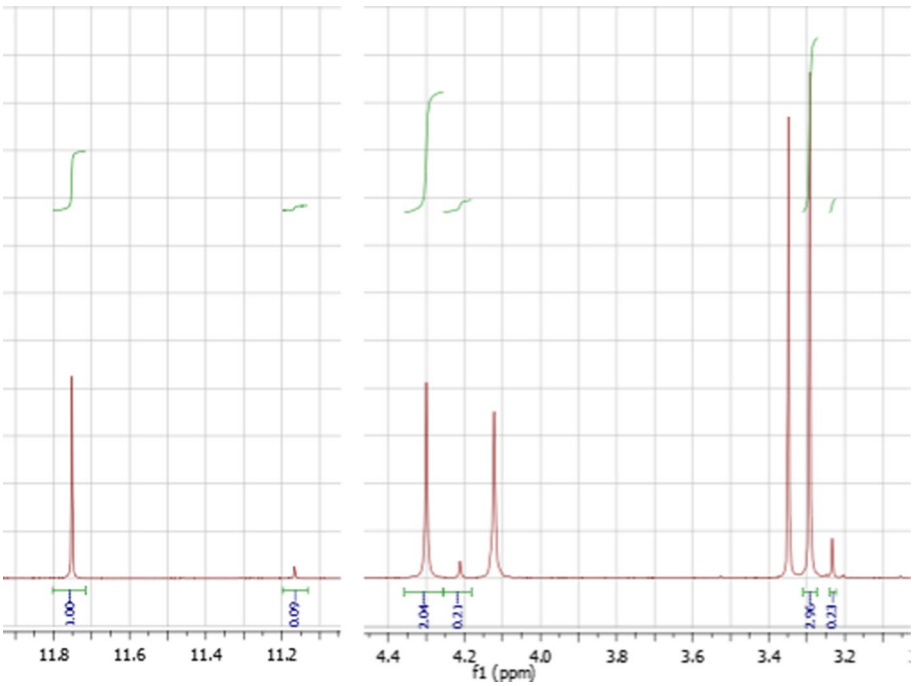

Fig. 4 ^{1}H-NMR spectrum of compound **29** cross section showing the oxime sister peak divisions

oxime spectra were C-7–8-12–13-17 carbons, which were all shielded [50]. Mainly C-8 carbon is shielded from 193 to 152 ppm, confirming the carbonyl to oxime change. C-7–12–13–17 Carbon shielding is caused by the loss of the carbonyl function's electron-withdrawing ability (Fig. 5, S38, S44, S100, S106, Table S2).

In order to elucidate the geometric isomerism of the oxime compounds synthesized in our work, the X-ray diffraction studies of compound **32** with the lowest isomeric impurity and the highest crystal quality were carried out. According to the XRD results, compound **32** was crystallized in the triclinic unit cell, and it was in the P1 space group, and there were two independent molecules in one asymmetric unit (Table S6). Results showed that compound **32** was *Z*-isomer. In the ^{1}H-NMR spectrum of the compound, the OH peak of the oxime hydrogen was seen at 11.84 ppm. When the ^{1}H-NMR spectra of all oxime compounds were examined, it was seen that the oxime –OH peaks with higher intensity are seen between the 11.57 and 11.99 range. Concerning this similarity, it was thought that all oxime compounds preferred *Z*-isomer during the synthesis or purifying processes (Fig. 6). Results also show a robust intermolecular hydrogen bonding between oxime O^2 and triazole N^2 (Fig. 6, Table S6).

The reported structural conformation, which is fixed by intramolecular interactions restricting the rotation of the triazole N^4–C$\underline{H_2}$CH$_3$ [66] is also found in our skeletons according to our XRD findings of compound **32**. Our XRD observations showed that the N^4–CH$_2$- was oriented with 80.4 and 83.4 degrees torsion angles for two independent molecules in one asymmetric unit. Also, this angular conformation was fixed by intramolecular interactions. Our thoughts about the atropisomerism for this N^4–CH$_2$– group were confirmed by these findings (Fig. 6).

As discussed before, since compound **32** is chiral, its methylenes are diastereotopic. XRD observations show that the SCH$_2$ methylene H–C–H bonding angle is 108°. The geminal interaction constant corresponding to this angle is between the 14 and 15 Hz range [63–65]. Despite these values within the Karplus Curve boundaries, the absence of geminal interaction made us think that free rotation is possible for this methylene of compound **32**.

Biological activity studies

Antiproliferative and cytotoxic activities

As mentioned before, compounds **7** [49], **8** [44, 45], **11** [67–69], and **12** [67–69] have been synthesized to support the structure determination and biological activity studies. Compounds **7–46** were screened for their antiproliferative activity against MCF-7, A549, PC-3, HeLa, K562, and NIH/3T3 cells. When selecting cancer cells to study the efficacy of synthetic inhibitors, we gave priority to cancer types in which mPGES-1 is overexpressed or for which mPGES-1 has been proven to play a role [10, 70–74]. Most of the compounds showed cytotoxic activity against the tested cell lines. The % proliferation results at 10 µM have been presented in Table S9, and the compounds with higher than 40% inhibitory activity are summarized in Table 1.

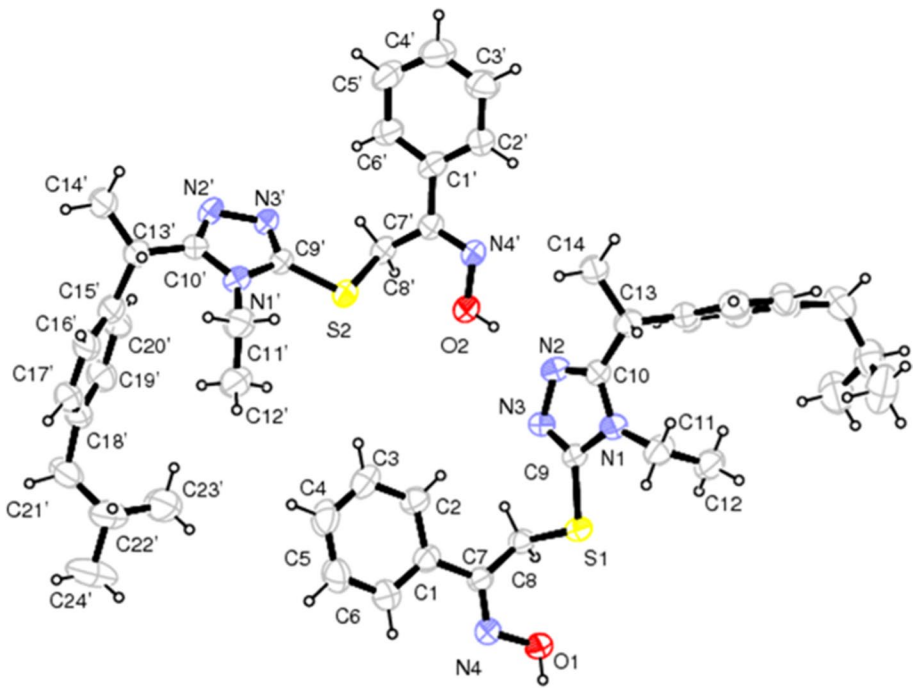

Fig. 6 The two independent molecules in the asymmetric unit of compound **32**. The displacement ellipsoids are drawn at 25% probability level

Table 1 Percent inhibition of proliferation results of compounds with higher than 40% inhibitory activity at 10 µM concentration

Compound	MCF-7	HeLa	PC-3	A549	K562	NIH3T3
10	58.16	51.44	58.53	88.17	6.62	36.43
18	83.40	89.80	92.56	89.08	56.30	71.95
27	23.84	38.55	23.09	49.46	− 1.55	47.95
28	83.20	90.50	92.15	88.70	50.48	76.00
36	0.59	89.80	93.62	88.17	60.581	65.56
39	15.48	− 1.06	40.97	4.98	13.94	3.93
45	81.82	86.95	90.81	87.29	71.26	82.38

These compounds were selected to determine IC_{50} values in respective cell lines. The results of these IC_{50} studies are also presented in the Table 2. According to these results, selectivity indexes were calculated between 0.34 and 1.97. Compound **45** showed the best IC_{50} values for the MCF-7 and A549 cell lines. The values were 14.66 µM and 20.14 µM; the selectivity indexes were 1.97 and 1.43, respectively. The second best was compound **36**. Its IC_{50} value for the HeLa cell line was 19.40 µM, and the selectivity index was 1.20. The third molecule was compound **28**, and it showed the best results for PC-3 and K562 cell lines. The results were 32.15 µM and 38.15 µM, and the selectivity indexes were 0.90 and 0.75, respectively.

Apoptosis studies

Biochemical and morphological methods demonstrated the apoptotic effects of compound **45** on A549 and MCF-7 cells. First of all, Annexin V staining was performed to detect early apoptosis in cells [75, 76]. This method is based on phosphatidylserine, which is found in the inner part of healthy cell membranes, and rises to the outer part of the cell in apoptotic cells. During the early period of apoptosis, phosphatidylserine, which is located on the inner surface of the plasma membrane, rises to the cell surface with the disruption of the phospholipid asymmetry in the membrane. Annexin V, an anticoagulant protein, binds with high sensitivity to phosphatidylserine. In this way, it is possible to detect cells undergoing apoptosis with annexin V at an early stage [75, 76]. When the results obtained were evaluated, it was determined that Compound **45** induced early apoptosis in both cell lines in a dose-dependent manner. On the other hand, this effect was more pronounced, especially on MCF-7 cells (Fig. 7).

Caspases are proteases that initiate and terminate apoptotic cell death. The activity of these enzymes, which are synthesized as inactive zymogens, is strictly protected. Caspase enzymes, which become active when the cell receives a death signal, cause activation or inactivation of various substrates involved in cell signaling. In apoptotic cell death, there are two processes carried out by the cysteine protease family known as caspases: the extrinsic (mitochondrial) pathway initiated by Caspase-8 and the activation of intrinsic pathways triggered by caspase-9, triggering cell death. The most commonly measured caspase activity at the end of extrinsic or intrinsic apoptotic processes is the caspase-3 enzyme [75–77]. In this study, we determined the activities of caspase 8, 9, and 3 enzymes to indicate which apoptotic pathway of compound **45** on A549 and MCF-7 cells. The analysis determined that compound **45** triggered internal and external apoptotic pathways in both cell lines (Fig. 8). Furthermore, caspase-3 activity increased due to the activation of both caspase enzymes.

The activity of the internal apoptotic pathway was confirmed by JC-1 staining (Fig. 9). JC-1 is a dye used in determination of mitochondrial membrane polarization. The JC-1 dye aggregates in mitochondria in healthy cells, giving it a red fluorescent color. In apoptotic cells, however, since the mitochondrial membrane potential has collapsed, the JC-1 dye cannot accumulate in the mitochondria and remains in monomeric form in the cytoplasm, giving a green fluorescent color. Compound **45** triggered apoptosis through the internal apoptotic pathway, especially in the A549 cell line.

Table 2 IC_{50} (µM) values of compounds with higher than 40% inhibitory activity

Compound	IC_{50} (µM)					
	MCF-7	HeLa	PC-3	A549	K562	NIH3t3
10	33.26	42.25	74.40	45.45	–	45.28
18	17.46	34.81	**29.79**	24.49	**36.45**	25.39
27	–	93.77	–	121.83	–	54.73
28	18.35	37.56	32.15	31.19	38.15	28.62
36	–	**19.40**	31.37	28.34	68.76	23.40
39	–	–	57.47	–	–	32.29
45	**14.66**	32.06	32.70	**20.14**	49.20	28.95

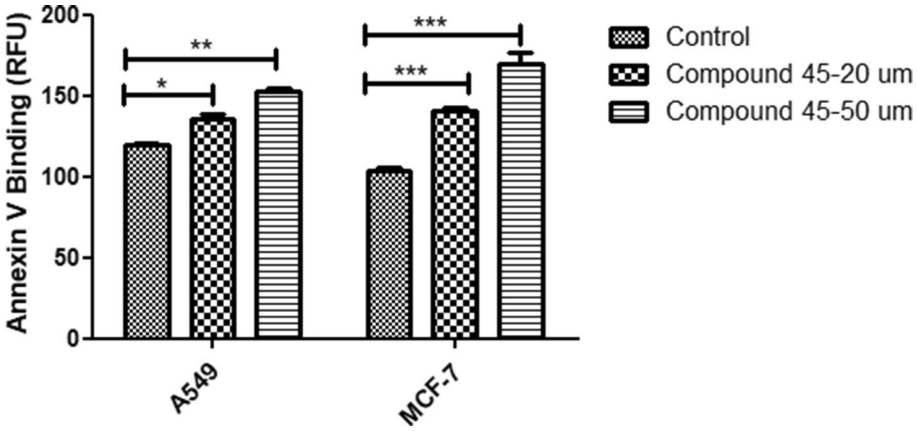

Fig. 7 The effects of compound 45 on early apoptosis at MCF-7 and A549 cells. ***$p < 0.001$, **$p < 0.01$, *$p < 0.5$ vs control

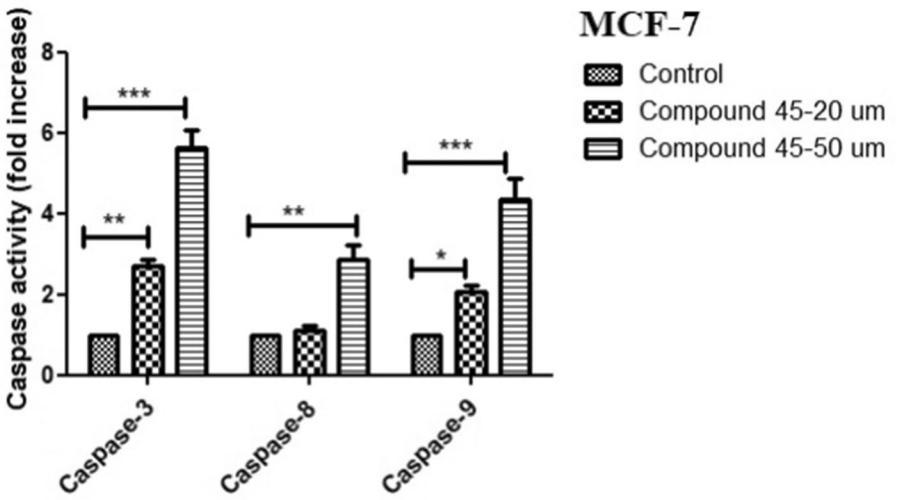

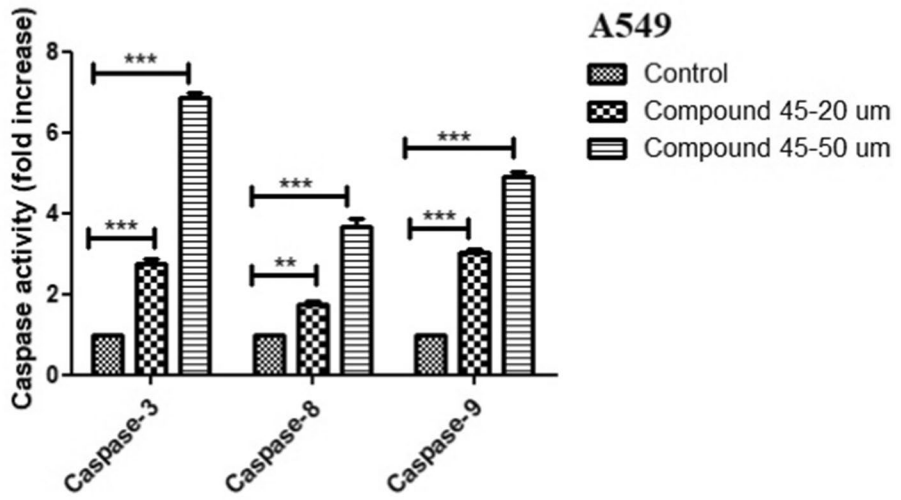

Fig. 8 The results of caspase enzymes activities. ***$p < 0.001$, **$p < 0.01$, *$p < 0.5$ vs control

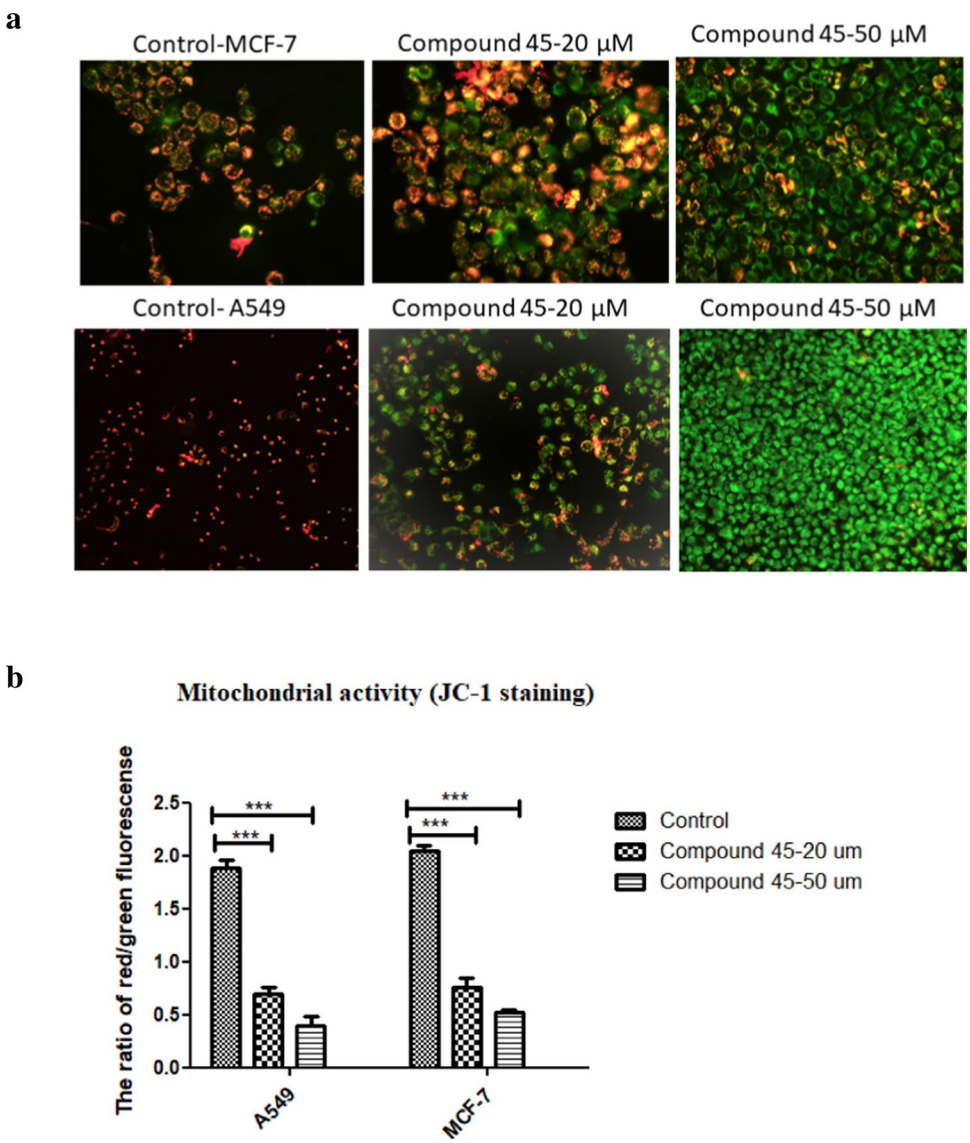

Fig. 9 **A** JC-1 staining images after 48-h treatments with 20 and 50 µM of compound **45**. **B** Red/green fluorescence intensity for JC-1 staining of MCF-7 and A549 cells after treatment of compound **45** at different concentrations. ***$p < 0.001$ vs control

Cell migration assay

A wound healing assay was applied to determine the inhibitory effect of compound **45** on cell migration. Cell migration for wound healing assay was taken for 0 h and 24 h. The wound healing assay proved that compound **45** inhibited A549 and MCF-7 cell migration dose-dependent (Fig. 10).

Inhibition of mPGES-1 enzyme and COX-1/2 enzymes

Compounds **7–46** were tested for their inhibitory activity against mPGES-1 at a concentration of 10 µM. Most of the synthesized compounds showed mild mPGES-1 inhibitory activity. The compounds that showed higher inhibition than 70% (compound **7, 13**) were further screened for the IC_{50} values. Compound **4b** and **MK-886** were used as the standard to compare. Compound **4b** [5-{[3-Chloro-4-(4-Cyclohexylbutoxy)phenyl]methylidene}-1,3-diazinane-2,4,6-trione] is a potent mPGES-1 inhibitor developed by the Zhan's group [78], and **MK-886** is also another well-recognized inhibitor [1]. IC50 values of **MK-886** and reference compound **4b** were found as 2.58 ± 0.48 and 0.034 ± 0.014 µM, respectively. The results are presented in Table 3.

As a next step to determine the anti-inflammatory activity, compounds with promising inhibitory activity against mPGES-1 (compound **7, 13**) were tested to determine whether they have a significant inhibition profile against COX-1 and COX-2. The test was applied at 10 and 100 µM concentrations. COX-2 inhibition values were significantly higher than the COX-1 inhibitions at both concentrations for each compound. Since the mPEGS-1 and COX-2 enzymes are colocalized, these similar results were reasonable. It was

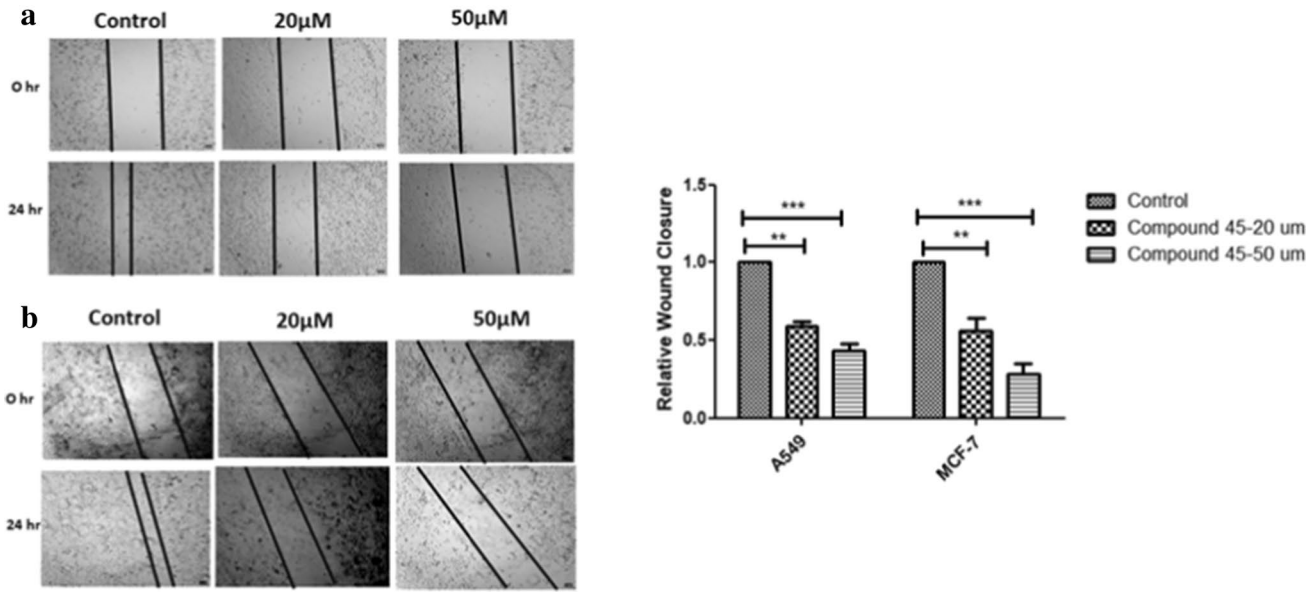

Fig. 10 The anti-migratory effects of compound **45** on MCF-7 breast cancer (**A**) and A549 lung cancer (**B**) cells. Monolayer scratch assays demonstrated that compound **45** inhibited the migratory potential in MCF-7 and A549 cells depending on dose and time (Magnification, × 10). ***$p < 0.001$, **$p < 0.01$ vs control

also observed that the COX inhibition values did not change with the concentration increase (Table 4).

Measurement of angiogenesis by the tube formation assay

Tube formation assay is a practical test to determine the stage of angiogenesis. The assay is based on the ability of endothelial cells to form three-dimensional capillary-like structures and measuring the ability of compounds which promote or inhibit the formation of these tubes [79]. Due to the reported relationship between inhibition and deletion of the mPGES-1 enzyme and angiogenesis [11, 80], the matrigel tube formation assay was performed for compounds **7** and **13**. As shown in Fig. 11, compounds **7** and **13** prevented tube formation significantly.

To reveal the mechanism under this prevention, the viability of HUVEC cells was measured in a dose-dependent manner (5 nM–10 μM). At all doses, compound-treated cell viability values are equal to untreated cells. These results indicated that compounds **7** and **13** had no effect on cell viability but on tube formation (Fig. 12).

Mutagenicity studies

Genotoxicity testing is a critical component of the safety assessment of xenobiotics. It is designed to detect genetic damage, which may be reflected in the tumorigenic or heritable mutation potential of the materials [81]. In this study, results of the mutagenicity assay showed that none of the tested concentrations of compounds **7** and **13** induced a significant increase in the revertant number of TA98, TA100, and TA102 strains, indicating no mutagenicity to the tested strains with and without metabolic activation (S9 fraction).

Table 5 represents the mutagenicity assay results induced by compounds **7** and **13** in the tested strains with and without metabolic activation. For both tested compounds, any of the tested concentrations did not significantly increase the revertant colony numbers, indicating no mutagenicity in tested strains ($p > 0.05$).

In silico studies

Molecular docking and conformation analysis

The structure of the mPGES-1 enzyme forms a homotrimer, but only one monomer is active at a time in the open conformation of the enzyme used for modeling studies. Glutathione (GSH) is the cofactor for the catalytic conversion of mPGES-1 that catalyzes the isomerization of PGH_2 to PGE_2. GSH binds to the active site of the mPGES-1 enzyme in a U-shaped conformation by hydrogen bonds, hydrophobic interactions, and polar interactions. The U-shaped conformation of the designed inhibitors is essential for efficient inhibition of the mPGES-1 enzyme. Most of the mPGES-1 inhibitors also interact with glutathione (GSH) when interacting with the active site residues of the enzyme [82]. Therefore, docking studies were performed using the active site of the

Table 3 Percent inhibitions of compounds **7–46** against mPGES-1

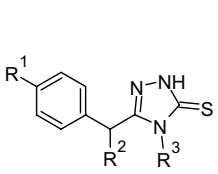

7-10

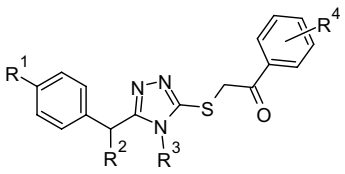

11-28

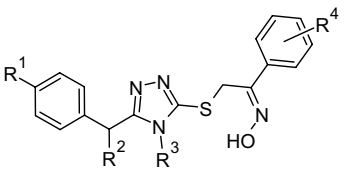

29-46

Compound	R^1	R^2	R^3	R^4	% Inhibition at 10 μM[a]	IC_{50} (μM, Mean ± SD)[b]
7	H	H	CH_3	–	**75 ± 23**	**13.6 ± 7.3**
8	H	H	C_2H_5	–	55 ± 18	
9	Isobutyl	CH_3	CH_3	–	0	
10	Isobutyl	CH_3	C_2H_5	–	62 ± 4.9	
11	H	H	CH_3	H	0	
12	H	H	C_2H_5	H	0	
13	Isobutyl	CH_3	CH_3	H	**73 ± 21**	**4.95 ± 2.07**
14	Isobutyl	CH_3	C_2H_5	H	5.0 ± 6.9	
15	Isobutyl	CH_3	CH_3	3-Cl	0	
16	Isobutyl	CH_3	C_2H_5	3-Cl	0	
17	Isobutyl	CH_3	CH_3	4-Cl	38 ± 12	
18	Isobutyl	CH_3	C_2H_5	4-Cl	57 ± 9.1	
19	Isobutyl	CH_3	CH_3	3-F	0	
20	Isobutyl	CH_3	C_2H_5	3-F	0	
21	Isobutyl	CH_3	CH_3	4-F	30 ± 6.7	
22	Isobutyl	CH_3	C_2H_5	4-F	0	
23	Isobutyl	CH_3	CH_3	2,4-F_2	0	
24	Isobutyl	CH_3	C_2H_5	2,4-F_2	0	
25	Isobutyl	CH_3	CH_3	2,5-$(OCH_3)_2$	0	
26	Isobutyl	CH_3	C_2H_5	2,5-$(OCH_3)_2$	45 ± 8.7	
27	Isobutyl	CH_3	CH_3	4-Br	33 ± 1.3	
28	Isobutyl	CH_3	C_2H_5	4-Br	45 ± 5.7	
29	H	H	CH_3	H	0	
30	H	H	C_2H_5	H	0	
31	Isobutyl	CH_3	CH_3	H	2.9 ± 0.5	
32	Isobutyl	CH_3	C_2H_5	H	0	
33	Isobutyl	CH_3	CH_3	3-Cl	0	
34	Isobutyl	CH_3	C_2H_5	3-Cl	0	
35	Isobutyl	CH_3	CH_3	4-Cl	50 ± 7.6	
36	Isobutyl	CH_3	C_2H_5	4-Cl	47 ± 4.7	
37	Isobutyl	CH_3	CH_3	3-F	27 ± 7.1	
38	Isobutyl	CH_3	C_2H_5	3-F	0	
39	Isobutyl	CH_3	CH_3	4-F	18 ± 2.8	
40	Isobutyl	CH_3	C_2H_5	4-F	26 ± 12	
41	Isobutyl	CH_3	CH_3	2,4-F_2	38 ± 7.2	
42	Isobutyl	CH_3	C_2H_5	2,4-F_2	20 ± 1.4	
43	Isobutyl	CH_3	CH_3	2,5-$(OCH_3)_2$	37 ± 2.3	
44	Isobutyl	CH_3	C_2H_5	2,5-$(OCH_3)_2$	0	
45	Isobutyl	CH_3	CH_3	4-Br	0	
46	Isobutyl	CH_3	C_2H_5	4-Br	0	
MK-886[c]						2.58 ± 0.48
4b[c]						0.034 ± 0.014

Table 3 (continued)

[a]Data are expressed as means ± SD of single determinations obtained in triplicate. Compounds that caused an inhibition greater than 70% were further screened at a concentration of 1 μM. Data are expressed as means ± SD of single determinations obtained in duplicate

[b]IC_{50} values were determined only for the compounds that showed ≥ 70% inhibition at 10 μM. Data are expressed as means ± SD of single determinations obtained in triplicate

[c]Compounds **MK-886** [1] and **4b** [78] were used as reference compounds for the determination of IC_{50} values. **MK-886** is a well-recognized inhibitor against mPGES-1 and **4b** is the inhibitor developed by Zhan's Lab

mPGES-1 enzyme in the presence of glutathione (GSH). The resulting docking studies suggested that the most active compounds were compounds **7** (Fig. S153) and **13** (Fig. S154), which retain the U-shape conformations supporting the enzyme inhibition assay. Among the compounds showing the best enzyme inhibition was compound **7**, which carries 1,2,4 triazole-3 thione moiety and exhibits thione-thiol tautomers. The tautomer formation is a reversible process that plays an essential role in biological systems [83]. For compound **7**, docking studies also showed that the thione form's binding energy and binding pose are more significant than that of the thiol form. Therefore, the thione form has been used in this study.

Interaction modes and binding energies of inhibitors with binding site residues of enzymes are given in Table 6. When the interaction types and binding energies of compound **7** are compared with the reference compounds, the hydrophobic interaction of TYR130 (pi-pi stacking) in both reference compounds and compound **7** for mPGES-1 was seen to be familiar to all. This mutual interaction contributes significantly to the binding energy. There are many hydrophobic interactions and hydrogen bonds for COX-1 in compound **7**, but they do not contribute to binding energy as potent as reference compounds. No co-interactions with reference compounds for COX-2 were found in compound **7**. The observed hydrophobic and hydrogen bond interactions were observed specific to the molecules. When the interaction types and binding energies of compound **13**, according to Table 6, were compared with the reference compounds, the hydrophobic interaction of TYR130 (pi-pi stacking) in both reference compounds, compound **7**, and compound **13** for mPGES-1 was common to all. It is possible to observe here that this typical interaction contributes to binding energy significantly. In addition, hydrogen bonds formed with ASN74 and ARG73 in compound **13** were also found in reference compounds. Hydrogen bonding with ARG120 and pi–Cation interaction with ARG120 for COX-1 in compound **13** positively affected the binding. No co-interactions were found with reference compounds for COX-2 in compound **13** as for compound **7**. On the other hand, this compound provided close binding energy to reference compounds with strong hydrogen bonds with the active site.

The positions of the active site of the mPGES-1 enzyme with compounds **13** (blue) and **MK-886** (pink) are shown in Fig. 13a. Accordingly, compound **13** showed activity at a position close to **MK-886** in the active site of the mPGES-1 enzyme. The positions of the active site of the mPGES-1 enzyme with compounds **13** (blue) and **4b** (orange) are shown in Fig. 13b. Accordingly, compound **13** showed activity at a close position between **4b** and **MK-886**. However, when these binding positions were compared, it was observed that compound **13** binds with **4b** in a more similar position. As a result of this positioning, binding energies and poses of **4b** and compound **13** were similar. The positioning and poses of **MK-886**, which seemed different from compounds **13** and **4b**, positively affected the binding energy.

In silico ADMET studies

The ADME properties of compounds **7–46** calculated using SwissADME (http://www.swissadme.ch/) online tools are given in Table S7. Lipinski's rule suggests that molecular weight < 500 daltons, partition coefficient (Log P) < 5, H-bond acceptors < 10, H-bond donors < 5 [84]. Result details of the in silico ADMET studies concerning the Veber's rule [85], in silico toxicity risks [86], and intestinal absorption [87] are presented in supplementary file under the same heading.

Conclusion

According to the results, compounds **10, 18, 27, 28, 36, 39**, and **45** showed the highest cytotoxic activity against the studied cancer cell lines. However, these also showed toxic effects on the healthy NIH/3T3 cell line. According to their high cytotoxicity and selectivity indexes, 28, 36, and 45 were the most promising among these compounds. No cytotoxic activity was observed for compounds **7** and **8**, which do not carry isobutyl or methyl residues. For the Ibuprofen-derived triazole compounds, an ethyl group at the triazole N^4 position increased the cytotoxicity. The ten compounds showed moderate cytotoxic activity against MCF-7, HeLa, PC-3, and A549 cell lines. Among the triazole N^4 methyl-bearing compounds, only **27** and **39** showed cytotoxic activity. The brome-bearing compound **27** showed only 49.46% inhibition against the A549 cell line, but its selectivity was very low. Compound **39** carried fluoride at the same location and showed 40.97% inhibition against the PC-3 cell line. In addition, it inhibited the NIH /3T3cells by only 3.93%,

offering the highest selectivity. When all these results were examined, it was seen that the alkyl residues from Ibuprofen were found to be necessary for cytotoxicity. It is also noteworthy about the length of the alkyl chain of the triazole; as the N^4 substitution gets bigger, the cytotoxicity increases, but the selectivity decreases. The presence of halogen at the acetophenone's para position was evaluated to affect the cytotoxicity positively. As the halogen became smaller, it was observed that the toxicity and activity decreased, and the selectivity increased.

Compound **45**, which had the best IC_{50} values against A549 and MCF-7 cells, was selected for apoptosis experiments. It was determined that compound **45** dose-dependently induced apoptosis on both cell lines. In addition, compound **45** also inhibited cell migration in a dose-dependent manner. Considering these results, it can be proposed that compound **45** could be a lead compound for further development.

Remarkably, the most promising compounds (compounds **7** and **13**) in terms of anti-inflammatory activity were also low in cytotoxicity. They also exhibited antiangiogenesis potential without toxicity over HUVEC cells. Also, they were found to be non-mutagenic over *S. typhimurium* strains. Although molecular modeling studies of compounds **7** and **13** agreed well with the experimental results, interactions of **13** were found more potent than **7**. According to these findings, these molecules were evaluated as new candidates for further investigations in anti-inflammatory drug research.

Experimental

Chemistry

All solvents and reagents were obtained from commercial sources and used without purification. All melting points (°C uncorrected) were determined using Thermo Scientific 9300 melting point apparatus. Elemental analyses were obtained using Leco CHNS-932. Infrared spectra were recorded on a Shimadzu FTIR 8400S, and data are expressed in wavenumbers $\bar{\nu}$ (cm^{-1}). NMR spectra were recorded on Brüker AVANCE-DPX 400 at 300 MHz for ^{1}H-NMR, 300 MHz, and 75 MHz for HMBC. The chemical shifts were expressed in δ (ppm) downfield from tetramethylsilane (TMS) using DMSO d_6 as solvent. The liquid chromatographic system consisted of an Agilent technologies 1100 series instrument equipped with a quaternary solvent delivery system and a model Agilent series G1315 A photodiode array detector. A Rheodyne syringe loading sample injector with a 50 ml sample loop was used to inject the analytes. Chromatographic data were collected and processed using Agilent ChemStation Plus software. The separation was performed at ambient temperature using a reversed-phase ZORBAX C8 (250 × 4 mm) column. The mobile phase -1- was prepared by mixing acetonitrile and water (80:20 v/v during 0–10 min), the mobile phase -2- was prepared by mixing acetonitrile and pH 4.7 phosphate buffer solution (60:40 v/v during 0–10 min), and subsequently degassed by ultrasonication, prior to use. Solvent delivery was employed at a flow

Table 4 COX % inhibitory activities of the studied compounds

Compound	COX-1		COX-2		COX-1/COX-2	
	10 μM	100 μM	10 μM	100 μM	10 μM	100 μM
7	64.01	67.11	83.45	85.64	0.76	0.78
13	53.37	57.54	82.70	83.20	0.64	0.69

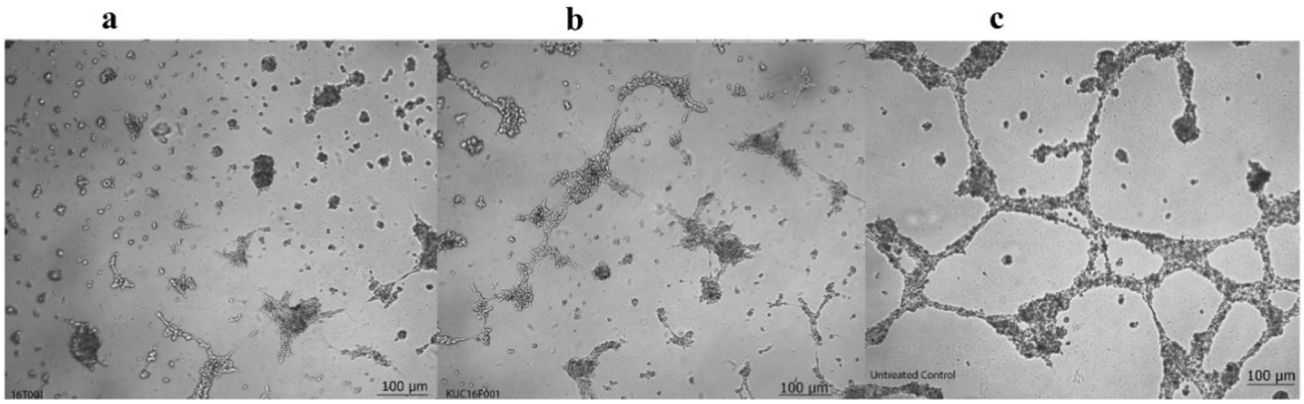

Fig. 11 Inhibition of tube formation by mPGES-1 inhibitors compounds **7** and **13** in HUVEC cells. **a** cells treated with compound **7**; **b** cells treated with compound **13**; **c** untreated cells

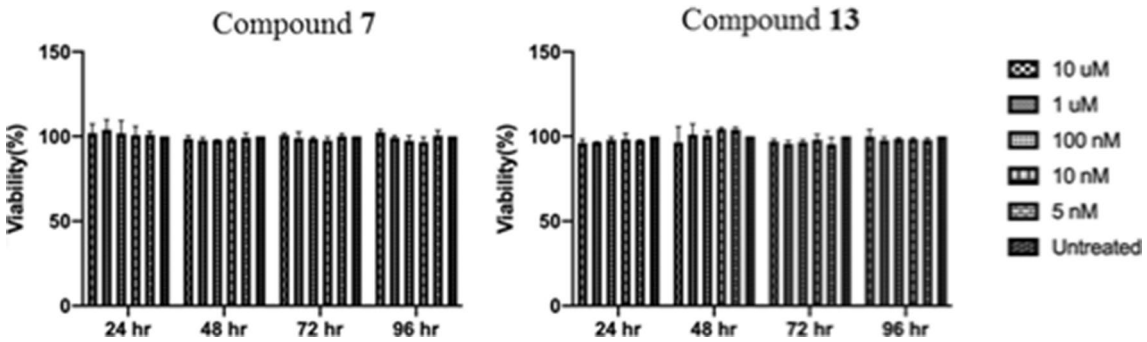

Fig. 12 Cytotoxicity testing of compounds **7** and **13** on HUVEC cells

Table 5 Mutagenicity of samples in *Salmonella typhimurium* TA98, TA100, and TA102 strains

Strains	Number of revertant/plate					
	TA98		TA100		TA102	
Samples	13	7	13	7	13	7
Without S9[a]						
Dose (μg/plate)						
1000	29.5 ± 9.2	20.5 ± 2.1	124.3 ± 9.5	120.0 ± 14.3	358.5 ± 12.0	364.0 ± 9.9
100	29.0 ± 2.8	24.5 ± 2.1	121.0 ± 9.5	122.0 ± 8.2	368.5 ± 21.9	368.0 ± 36.8
10	24.5 ± 6.4	21.5 ± 7.8	127.0 ± 4.0	116.5 ± 27.6	350.0 ± 14.1	370.0 ± 12.7
1	29.5 ± 2.1	22.0 ± 4.2	126.0 ± 6.6	128.5 ± 3.5	366.0 ± 25.5	349.5 ± 12.0
With S9[b]						
Dose (μg/plate)						
1000	32.8 ± 6.2	30.0 ± 4.6	144.0 ± 1.4	148.0 ± 12.7	371.5 ± 9.2	361.5 ± 10.6
100	32.3 ± 4.1	29.0 ± 5.6	140.0 ± 14.1	145.5 ± 10.6	360.5 ± 16.3	374.0 ± 9.9
10	32.0 ± 5.2	31.5 ± 2.1	146.5 ± 7.8	138.5 ± 6.4	375.0 ± 5.7	368.5 ± 24.7
1	33.5 ± 6.6	29.0 ± 7.5	139.5 ± 2.1	142.0 ± 19.8	368.5 ± 28.3	373.0 ± 1.4

*Dunnett's multiple comparison test was carried out for statistical analysis

[a]NPD (20 μg/plate), SA (1 μg/plate), and MMC (0.5 μg/plate) were used as positive mutagens without S9. 2-AA (10 μg/plate) was used as positive mutagen for with S9 experiment. In the experiment without S9 activation, revertant colony numbers in negative control groups were 22.2 ± 5.2, 120.8 ± 7.8 and 386.0 ± 25.5 for TA98, TA100 a,nd TA102 strains, respectively.

[b]In the experiment with S9 activation, revertant colony numbers in negative control groups were 31.8 ± 5.4, 138.5 ± 12.8, and 377.5 ± 4.9 for TA98, TA100, and TA102 strains, respectively. In the experiment without S9 activation, revertant colony numbers in positive control groups were 843.5 ± 26.2, 986.5 ± 106.4, and 928.7 ± 68.0 for TA98, TA100, and TA102 strains, respectively. In the experiment with S9 activation, revertant colony numbers in positive control groups were 804.5 ± 50.2, 1610.0 ± 99.0, and 1036.3 ± 78.6 for TA98, TA100, and TA102 strains, respectively

rate of 1 ml min^{-1}. Detection of the analytes was carried out at 254 nm. XRD studies were performed by Rigaku (r-axis rapid 2, DW Micro Max 007) device.

Synthesis of ethyl-2-[4-(2-methylpropyl)phenyl] propanoate (CAS: 41283–72-1) [25, 31–33]

Ibuprofen (20 mmol) was dissolved in 20 ml of ethanol. After adding 1 ml of concentrated sulfuric acid, it was boiled under reflux for 3 h. After 3 h, the reaction vessel is cooled to room temperature. The reaction medium was taken into the ice bath and neutralized with 5% sodium bicarbonate. It was then extracted with diethyl ether and filtered. The filtrate is dried with anhydrous sodium sulfate. The pure substance is obtained by evaporating the solvent [30, 31, 40]. It was obtained as a colorless liquid, yielding 90%. IR cm^{-1}: 1732 (ester C=O), 1199, 1159 (ester C–O).

Table 6 Interaction types and binding energies of inhibitors with binding site residues of enzymes

Compound	Enzyme	Binding energy (kcal/mol)	Number of H-bond	Distance of H-bonds (Å)	H-bonds interactions	Hydrofobic interactions
MK-886	mPGES-1	− 7.38	1	3.28	ARG73:S	TYR130 (pi–pi stacking)(2)
						GLU77 (pi-anion)
	COX-1	− 8.00	1	3.27	TYR355:H(CH3)	VAL116(pi-sigma)
						SER353(pi-sigma)
						PHE518(pi-sigma)
						PHE518(pi-sulfur)
	COX-2	− 6.34				ASN87(pi-sigma)
4b	mPGES-1	− 6.74	2	3.01	ASN74:O	TYR130 (pi-pi stacking)
				3.27	ARG126:Cl	HIS113(halogen)
	COX-1	− 9.34	3	2.03	TYR385:O	VAL349(pi-sigma)
				1.93	MET522:H(NH)	ALA527(pi-sigma)
				2.93	ALA527:O	MET522(pi-sulfur)
	COX-2	− 7.49	2	2.04	THR88:O	TYR91(pi-pi stacking)
				3.61	PRO514:O	ASN87(pi-sigma)
7	mPGES-1	− 5.04	1	2.63	ARG126:Triazole(N)	TYR130 (pi-pi stacking)
						TYR130 (pi-sigma)
	COX-1	− 6.42	1	1.98	LEU352:H(NH)	ILE523(pi-sigma)
						GLY526(amide-pi stacking)
						HIS90(pi-sulfur)
						MET522(pi-sulfur)
	COX-2	− 5.28	1	2.08	LYS511:H(NH)	TYR475(pi-sulfur)
13	mPGES-1	− 6.71	2	3.39	ASN74:Triazole(N)	TYR130 (pi–pi stacking)
				2.65	ARG73:O	ARG126(pi-Cation)
	COX-1	− 8.52	1	2.01	ARG120:O	TYR355(pi-sulfur)
						ARG120(pi-Cation)
	COX-2	− 6.49	2	2.44	ASN87:Triazole	
				2.47	THR88:Phenyl	

Synthesis of 2-[4-(2-Methylpropyl)phenyl]propane-hydrazyde (2) (CAS: 127222-69-9) [25, 31–34]

Ibuprofen ethyl ester (10 mmol) and hydrazine monohydrate (0.040 mol) were taken into a flask. 10 ml of ethanol was added, and the mixture was refluxed for 8 h. The reaction was terminated by pouring onto the ice. The precipitate was washed three times with distilled water. The crude product was recrystallized from petroleum ether and obtained as a white shiny solid [31–34]. HPLC tR (min): 4.03, Mp: 80 °C, yield 90%. IR cm^{-1}: 3269, 3207, 3176 (N–H), 1639 (hydrazide C=O). ^{1}H-NMR (300 MHz, DMSO d_6): δ 0.84 (6H, d, $J = 6.60$ Hz, $CH(C\underline{H}_3)_2$), 1.31 (3H, d, $J = 7.20$ Hz, $CH(C\underline{H}_3)$), 1.72–1.85 (1H, m, $C\underline{H}(CH_3)_2$), 2.39 (2H, d, $J = 6.90$ Hz, $CH(C\underline{H}_2)$), 2.51 ($CD_2\underline{H}SOCD_3$), 3.42 (DMSO d_6 $\underline{H}_2O$), 3.47–3.56 (1H, m, $C\underline{H}(CH_3)$), 4.17 (2H, d, $J = 3.60$ Hz, $NHN\underline{H}_2$, exchangeable with D_2O), 7.06 and 7.21 (4H, 2d, $J = 8.10$ Hz $C_6\underline{H}_4$), 9.15 (1H, s, $N\underline{H}NH_2$). Anal. Calcd. For $C_{13}H_{20}N_2O$: C, 70.87; H, 9.15; N, 12.72. Found: C, 70.69; H, 8.87; N, 12.67.

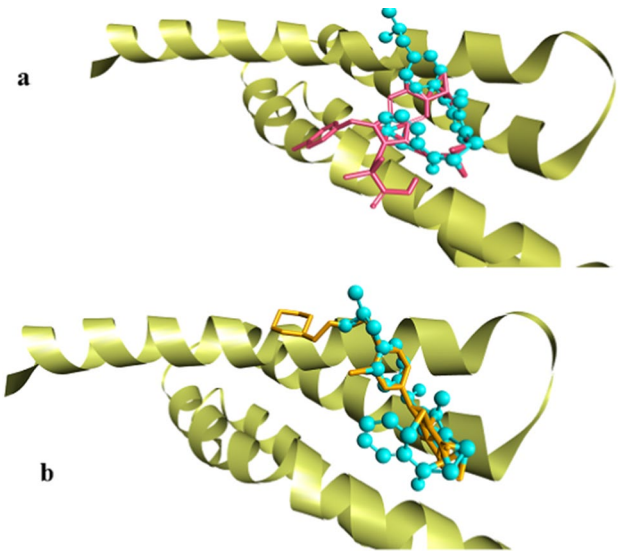

Fig. 13 3D images of the active site of the mPGES-1 enzyme, and compound **13** (blue) with **MK-886** (pink) (**a**) and **4b** (orange) (**b**)

Synthesis of 1,4-disubstituted thiosemicarbazide derivatives

The corresponding hydrazide (0.020 mol) and methyl or ethylisothiocyanate (0.020 mol) were weighed into a flask, and 40 ml of ethanol was added. It was refluxed for 3 h. The reaction was stopped by pouring onto the ice. The precipitate was washed twice with distilled water and dried. Next, it was washed twice with petroleum ether, dried, and crystallized from ethanol.

N-Methyl-2-(phenylacetyl)hydrazine-1-Carbothioamide (3) (CAS: 51291-26-0) [42, 43]

It was obtained as white solid and recrystallized from ethanol, HPLC t_R (min): 2.99, Mp: 162 °C, yield 60%. IR cm^{-1}: 3165 (N–H), 1693 (hydrazide C=O), 1236 (C=S). ^{1}H-NMR (300 MHz, DMSO d_6): δ 2.51 ($CD_2\underline{H}SOCD_3$), 2.88 (3H, d, J = 4.50 Hz, C=SNHC$\underline{H}_3$), 3.38 (DMSO d_6 $\underline{H}_2O$), 3.47 (2H, s, ArC$\underline{H}_2$C=O), 7.17–7.34 (5H, m, $C_6\underline{H}_5$), 7.97 (1H, d, J = 4.20 Hz, S = CN$\underline{H}$CH$_3$), 9.22 (1H, s, C=ONHN$\underline{H}$C=S), 9.93 (1H, s, C=ON$\underline{H}$NHC=S). Anal. Calcd. for $C_{10}H_{13}N_3OS$,1/5 H_2O: C, 52.93; H, 5.95; N, 18.52; S, 14.13. Found: C, 53.10; H, 5.28; N, 19.01; S, 14.10.

N-ethyl-2-(phenylacetyl)hydrazine-1-carbothioamide (4) (CAS: 31409-13-9) [43–45]

It was obtained as white solid and recrystallized from ethanol, HPLC t_R (min): 3.27, Mp: 156 °C, yield 40%. IR cm^{-1}: 3300, 3142 (N–H), 1691 (hydrazide C=O), 1220 (C=S). ^{1}H-NMR (300 MHz, DMSO d_6): δ 1,06 (3H, t, J = 7.20 and 6.90 Hz, NHCH$_2$C$\underline{H}_3$), 2.51 ($CD_2\underline{H}SOCD_3$), 3.38 (DMSO d_6, $\underline{H}_2O$), 3.41–3.51 (4H, m, ArC$\underline{H}_2$C=O, and C=SNHC$\underline{H}_2$), 7.17–7.34 (5H, m, $C_6\underline{H}_5$), 7.93 (1H, t, J = 5.40 Hz, S = CN$\underline{H}$CH$_2$CH$_3$), 9.17 (1H, s, C=ONHN$\underline{H}$C=S), 9.92 (1H, s C=ON$\underline{H}$NHC=S). Anal. Calcd. for $C_{11}H_{15}N_3OS$: C, 55.67; H, 6.37; N, 17.71; S, 13.51. Found: C, 55.18; H, 5.77; N, 17.93; S, 13.42.

N-methyl-2-{2-[4-(2-methylpropyl)phenyl]propanoyl} hydrazine-1-carbothioamide (5)(CAS: 2473569-92-3) [25]

It was obtained as white solid and recrystallized from ethanol, HPLC t_R (min): 3.29, Mp: 163–165 °C, yield 90%. IR cm^{-1}: 3518, 3456, 3146 (N–H), 1672 (hydrazide C=O), 1219 (C=S). ^{1}H-NMR (300 MHz, DMSO d_6): δ 0.85 (6H, d, J = 6.60 Hz, CH(C$\underline{H}_3$)$_2$), 1.36 (3H, d, J = 7.20 Hz, CH(C$\underline{H}_3$), 1.73–1.86 (1H, m, C$\underline{H}$(CH$_3$)$_2$), 2.40 (2H, d, J = 6.90 Hz, CH(C$\underline{H}_2$)), 2.51 ($CD_2\underline{H}SOCD_3$), 2.86 (3H, d, J = 4.20 Hz, C=SNHC$\underline{H}_3$), 3.42 (DMSO d_6, $\underline{H}_2O$), 3.59 (1H, q, J = 7.00 Hz, C$\underline{H}$(CH$_3$)), 7.08 (2H, d, J = 8.10 Hz $C_6\underline{H}_4$), 7.23 (2H, d, J = 7.80 Hz, $C_6\underline{H}_4$), 7.75 (1H, d, J = 3.60 Hz, S = CN$\underline{H}$CH$_3$), 9.17 (1H, s, C=ONHN$\underline{H}$C=S), 9.83 (1H, s, C=ON$\underline{H}$NHC=S). Anal. Calcd. For $C_{15}H_{23}N_3OS$, 4/5 H_2O: C, 58.52; H, 8.05; N, 13.65; S, 10.42. Found: C, 58.10; H, 7.38; N, 13.59; S, 10.29.

N-ethyl-2-{2-[4-(2-methylpropyl)phenyl]propanoyl}hydrazine-1-carbothioamide (6) (CAS: 184706-13-6) [41]

It was obtained as white solid and recrystallized from ethanol, HPLC t_R (min): 3.49, Mp: 152 °C, yield 70%. IR cm^{-1}: 3298, 3176 (N–H), 1672 (hydrazide C=O), 1217 (C=S). Anal. Calcd. For $C_{16}H_{25}N_3OS$,1/3 H_2O: C, 61.31; H, 8.25; N, 13.41; S, 10.23. Found: C, 61.59; H, 7.50; N, 13.59; S, 10.51.

Synthesis of 1,4-dihydro-3*H*-1,2,4-triazol-3-thione derivatives

The corresponding thiosemicarbazide (10 mmol) was dissolved in sodium hydroxide solution (37.5 ml, 2 N). The mixture was refluxed for 4 h. In the end, the reaction vessel was left to cool down to room temperature. It is neutralized with a 2 N hydrochloric acid solution. The precipitate is filtered and washed twice with distilled water. After drying, it is crystallized from ethanol.

5-Benzyl-4-methyl-2,4-dihydro-3H-1,2,4-triazole-3-thione (7) (CAS: 51291-31-7) [49]

It was obtained as white solid and recrystallized from ethanol, HPLC t_R (min): 3.53, Mp: 157 °C, yield 50%. IR cm^{-1}: 3084 (N–H), 2758 (S–H), 1600 (C=N), 1282 (C=S). ^{1}H-NMR (300 MHz, DMSO d_6): δ 2.51 ($CD_2\underline{H}SOCD_3$), 3.31 (3H, s, NC$\underline{H}_3$), 3.38 (DMSO d_6, $\underline{H}_2O$), 4.11 (2H, s, ArC$\underline{H}_2$), 7.22–7.38 (5H, m, $C_6\underline{H}_5$), 13.60 (1H, s, N$\underline{H}$). Anal. Calcd. For $C_{10}H_{11}N_3S$,1/6H_2O: C, 57.67; H, 5.48; N, 20.17; S, 15.39. Found: C, 57.77; H, 4.99; N, 20.62; S, 15.06.

5-Benzyl-4-ethyl-2,4-dihidro-3H-1,2,4-triazole-3-thione (8) (CAS: 31405-22-8) [44, 45, 66]

It was obtained as white solid and recrystallized from ethanol, HPLC t_R (min): 3.94, Mp: 159 °C, yield 40%. IR cm^{-1}: 3095 (N–H), 2766 (S–H), 1658 (C=N), 1280 (C=S). ^{1}H-NMR (300 MHz, DMSO d_6): δ 0.93 (3H, t, J = 7.2 Hz, CH$_2$C$\underline{H}_3$), 2.51 ($CD_2\underline{H}SOCD_3$), 3.38 (DMSO d_6, $\underline{H}_2O$), 3.88 (2H, q, J = 7.10 Hz, NC$\underline{H}_2$CH$_3$), 4.13 (2H, s, ArC$\underline{H}_2$), 7.25–7.38 (5H, m, $C_6\underline{H}_5$), 13.60 (1H, s, N$\underline{H}$). Anal. Calcd. For $C_{11}H_{13}N_3S$: C, 60.24; H, 5.97; N, 19.16; S, 14.62. Found: C, 59.93; H, 5.54; N, 19.38; S, 14.12.

4-Methyl-5-{1-[4-(2-methylpropyl)phenyl]ethyl}-2,4-dihydro-3H-1,2,4-triazole-3-thione (9)(CAS:2641122-43-0) [25]

It was obtained as white solid and recrystallized from ethanol, HPLC t_R (min): 3.90, Mp: 173 °C**,** yield 86%. IR cm^{-1}: 3091 (N–H), 2750 (S–H), 1689 (C=N), 1267 (C=S). ^{1}H-NMR (300 MHz, DMSO d_6): δ 0.83 (6H, d, $J = 6.60$ Hz, $CH(C\underline{H}_3)_2$), 1.52 (3H, d, $J = 6.90$ Hz, $CH(C\underline{H}_3)$), 1.72–1.86 (1H, m, $C\underline{H}(CH_3)_2$), 2.40 (2H, d, $J = 7.20$ Hz, $CH(C\underline{H}_2)$), 2.51 ($CD_2\underline{H}SOCD_3$), 3.14 (3H, s, $NC\underline{H}_3$), 3.42 (DMSO d_6 $\underline{H}_2O$), 4.27 (1H, q, $J = 7.10$ Hz, $C\underline{H}(CH_3)$), 7.12 (4H, s, $C_6\underline{H}_4$), 13.65 (1H, s, N<u>H</u>). Anal. Calcd. For $C_{15}H_{21}N_3S$: C, 65.41; H, 7.69; N, 15.26; S, 11.64. Found: C, 65.62; H, 7.05; N, 15.29; S, 10.78.

4-Ethyl-5-{1-[4-(2-methylpropyl)phenyl]ethyl}-2,4-dihydro-3H-1,2,4-triazole-3-thione (10)

It was obtained as white solid and recrystallized from ethanol, HPLC t_R (min): 4.26, Mp: 131–132 °C**,** yield 60%. IR cm^{-1}: 3084 (N–H), 2764 (S–H), 1612 (C=N), 1278 (C=S). ^{1}H-NMR (300 MHz, DMSO d_6): δ 0.71 (3H, t, $J = 7.20$ Hz, $CH_2C\underline{H}_3$), 0.81 (6H, d, $J = 6.60$ Hz, $CH(C\underline{H}_3)_2$), 1.52 (3H, d, $J = 6.90$ Hz, $CH(C\underline{H}_3)$), 1.71–1.85 (1H, m, $C\underline{H}(CH_3)_2$), 2.40 (2H, d, $J = 6.90$ Hz, $CH(C\underline{H}_2)$, 2.51 ($CD_2\underline{H}SOCD_3$), 3.42 (DMSO d_6, $\underline{H}_2O$), 3.60–3.72 3.76–3.88 (2H, 2 m, $NC\underline{H}_2$), 4.29 (1H, q, $J = 7.00$ Hz, $C\underline{H}(CH_3)$), 7.13 (4H, s, $C_6\underline{H}_4$), 13.64 (1H, s, N<u>H</u>). Anal. Calcd. For $C_{16}H_{23}N_3S$: C, 66.39; H, 8.01; N, 14.52; S, 11.08. Found: C, 66.24; H, 7.45; N, 14.55; S, 11.26.

Synthesis of 2-[(4*H*-1,2,4-triazol-3-yl)sulphanyl] ethane-1-one derivatives (11–35)

The corresponding 2,4-dihydro-3H-triazole-3-thione (4 mmol) was dissolved in 50 ml acetonitrile. Next, Triethylamine (4.80 mmol/0.670 ml) was added to the solution. The mixture was refluxed for 1 h. Next, the corresponding 2-bromo-1-phenylethan-1-one derivative was added to the medium (4 mmol). The mixture was refluxed for 6 h. The solvent was then evaporated to dryness under reduced pressure. The precipitate was dissolved in diethyl ether and filtered. The solid material precipitated from diethyl ether was recrystallized from 80% ethanol.

2-[(5-Benzyl-4-methyl-4H-1,2,4-triazole-3-yl) sulphanyl]-1-phenylethane-1-on (11) (CAS: 332934-32-4) [67–69]

It was obtained as white solid, recrystallized from diethylether initially, and 80% ethanol latterly, HPLC t_R (min): 5.15, Mp: 157 °C, yield 40%. IR cm^{-1}: 1685 (C=O), 1645 (C=N), 723 (C-S). ^{1}H-NMR (300 MHz, DMSO d_6): δ 2.51 ($CD_2\underline{H}SOCD_3$), 3.38 (DMSO d_6 $\underline{H}_2O$), 3.40 (3H, s, $NC\underline{H}_3$), 4.15 (2H, s, $ArC\underline{H}_2$), 4.82 (2H, s, $SC\underline{H}_2C{=}O$), 7.18–7.36 (5H, m, $C_6\underline{H}_5$), 7.52–7.58 (2H, m, $C_6\underline{H}_5$), 7.65–7.71 (1H, m, $C_6\underline{H}_5$), 7.99 (2H, dd, $J = 8.40$, 1.20 Hz, $C_6\underline{H}_5$). HRMS (EI^+) (*m*/*z*): calculated for $C_{18}H_{17}N_3OS$ $(M+H)^+$ 322.1009, found 322.1021. Anal. Calcd. For $C_{18}H_{17}N_3OS.1/3H_2O$: C, 65.63; H, 5.41; N, 12.76; S, 9.73. Found: C, 66.19; H, 4.93; N, 13.11; S, 9.48.

2-[(5-Benzyl-4-ethyl-4H-1,2,4-triazole-3-yl) sulphanyl]-1-phenylethane-1-on (12) (CAS: 663158-45-0) [68, 69]

It was obtained as white solid, recrystallized from diethylether initially, and 80% ethanol latterly, HPLC t_R (min): 6.13, Mp: 138 °C, yield 30%. IR cm^{-1}: 1685 (C=O), 1645 (C=N), 719 (C-S). ^{1}H-NMR (300 MHz, DMSO d_6): δ 0.95 (3H, t, $J = 7.20$ Hz $NCH_2C\underline{H}_3$), 2.51 ($CD_2\underline{H}SOCD_3$), 3.38 (DMSO d_6 $\underline{H}_2O$), 3.88 (2H, q, $J = 7.20$ Hz, $NC\underline{H}_2CH_3$), 4.17 (2H, s, $ArC\underline{H}_2$), 4.91 (2H, s, $SC\underline{H}_2C{=}O$), 7.22–7.36 (5H, m, $C_6\underline{H}_5$), 7.53–7.58 (2H, m, $C_6\underline{H}_5$), 7.66–7.72 (1H, m, $C_6\underline{H}_5$), 7.99–8.03 (2H, m, $C_6\underline{H}_5$). HRMS (EI^+) (*m*/*z*): calculated for $C_{19}H_{19}N_3OS$ $(M+H)^+$ 336.1165, found 336.1189. Anal. Calcd. For $C_{19}H_{19}N_3OS.1/3H_2O$: C, 66.45; H, 5.77; N, 12.23; S, 9.34. Found: C, 66.52; H, 5.11; N, 12.54; S, 9.01.

1-Phenyl-2-({4-methyl-5-[1-(4-isobutylphenyl) ethyl]-4H-1,2,4-triazole-3-yl} sulphanyl)ethan-1-one (13)

It was obtained as white solid, recrystallized from diethylether initially, and 80% ethanol latterly, HPLC t_R (min): 4.68, Mp: 107 °C, yield 60%. IR cm^{-1}: 1693 (C=O), 1645 (C=N), 746 (C-S). ^{1}H-NMR (300 MHz, DMSO d_6): δ 0.84 (6H, d, $J = 6.60$ Hz, $CH(C\underline{H}_3)_2$), 1.57 (3H, d, $J = 7.20$ Hz, $CH(C\underline{H}_3)$), 1.72–1.86 (1H, m, $C\underline{H}(CH_3)_2$), 2.40 (2H, d, $J = 7.20$ Hz, $CH(C\underline{H}_2)$), 2.51 ($CD_2\underline{H}SOCD_3$), 3.24 (3H, s, $NC\underline{H}_3$), 3.40 (DMSO d_6 $\underline{H}_2O$), 4.23 (1H, q, $J = 7.00$ Hz, $C\underline{H}(CH_3)$), 4.81 (2H, ABq, $\Delta\delta_{AB} = 0.038$, $J = 16.83$ Hz, $SC\underline{H}_2C{=}O$), 7.09 (4H, s, $C_6\underline{H}_4$), 7.51–7.56 (2H, m, $C_6\underline{H}_4$), 7.64–7.70 (1H, m, $C_6\underline{H}_4$), 7.97–8.00 (2H, m, $C_6\underline{H}_4$). ppm; ^{13}C NMR (75.47 MHz, DMSO d_6): δ 20.90, 22.13, 29.56, 29.89, 35.47, 40.52, 44.15, 126.83, 128.38, 128.75, 129.29, 133.67, 135.17, 139.38, 139.62, 148.83, 157.97, 193.41. HRMS (EI^+) (*m*/*z*): calculated for $C_{23}H_{27}N_3OS$ $(M+H)^+$ 392.1791, found 392.1808. Anal. Calcd. For $C_{23}H_{27}N_3OS.1/3H_2O$: C, 69.14; H, 6.98; N, 10.52; S, 8.03. Found: C, 69.29; H, 6.57; N, 10.69; S, 8.07.

1-Phenyl-2-({4-ethyl-5-[1-(4-isobutylphenyl) ethyl]-4H-1,2,4-triazole-3-yl}sulphanyl) ethane-1-one (14)

It was obtained as white solid, recrystallized from diethyl-ether initially, and 80% ethanol latterly, HPLC t_R (min): 5.20, Mp: 115 °C, yield 50%. IR cm^{-1}: 1689 (C=O), 1651 (C=N), 748 (C-S). ^{1}H-NMR (300 MHz, DMSO d_6): δ 0.75 (3H, t, $J=7.20$ and 6.90 Hz, $CH_2C\underline{H}_3$), 0.82 (6H, d, $J=6.60$ Hz, $CH(C\underline{H}_3)_2$), 1.58 (3H, d, $J=7.20$ Hz, $CH(C\underline{H}_3)$), 1.71–1.85 (1H, m, $C\underline{H}(CH_3)_2$), 2.40 (2H, d, $J=7.20$ Hz, $CH(C\underline{H}_2)$), 2.51 ($CD_2\underline{H}SOCD_3$), 3.40 (DMSO d_6 $\underline{H}_2O$), 3.61–3.73 and 3.80–3.92 (2H, 2 m, $NC\underline{H}_2$), 4.31 (1H, q, $J=7.00$ Hz, $C\underline{H}(CH_3)$), 4.90 (2H, ABq, $\Delta\delta_{AB}=0.037$, $J=17.13$ Hz, $SC\underline{H}_2C{=}O$), 7.11 (4H, s, $C_6\underline{H}_4$), 7.52–7.57 (2H, m, $C_6\underline{H}_4$), 7.65–7.71 (1H, m, $C_6\underline{H}_4$), 7.99–8.02 (2H, m, $C_6\underline{H}_4$). ppm; ^{13}C NMR (75.47 MHz, DMSO d_6): δ 14.15, 21.29, 22.04, 29.57, 35.43, 38.27, 40.43, 44.11, 126.88, 128.36, 128.76, 129.31, 133.67, 135.27, 139.68, 140.08, 148.50, 157.42, 193.31. HRMS (EI^+) (*m*/*z*): calculated for $C_{24}H_{29}N_3OS$ $(M+H)^+$ 406.1947, found 406.1988. Anal. Calcd. For $C_{24}H_{29}N_3OS$: C, 70.73; H, 7.17; N, 10.31; S, 7.87. Found: C, 70.37; H, 6.59; N, 10.26; S, 7.43.

1-(3–Chlorophenyl)-2-({4-methyl-5-[1-(4-isobutylphenyl) ethyl]-4H-1,2,4-triazole -3- yl}sulphanyl)ethane-1-one (15)

It was obtained as white solid, recrystallized from diethyl-ether initially, and 80% ethanol latterly, HPLC t_R (min): 5.75, Mp: 144 °C, yield 60%. IR cm^{-1}: 1683 (C=O), 1651 (C=N), 727 (C-S). ^{1}H-NMR (300 MHz, DMSO d_6): δ 0.84 (6H, d, $J=6.60$ Hz, $CH(C\underline{H}_3)_2$), 1.57 (3H, d, $J=6.90$ Hz, $CH(C\underline{H}_3)$), 1.73–1.86 (1H, m, $C\underline{H}(CH_3)_2$), 2.40 (2H, d, $J=7.20$ Hz, $CH(C\underline{H}_2)$), 2.50 ($CD_2\underline{H}SOCD_3$), 3.25 (3H, s, $NC\underline{H}_3$), 3.34 (DMSO d_6 $\underline{H}_2O$), 4.29 (1H, q, $J=7.00$ Hz, $C\underline{H}(CH_3)$), 4.80 (2H, ABq, $\Delta\delta_{AB}=0.037$, $J=16.83$ Hz, $SC\underline{H}_2C{=}O$), 7.06–7.12 (4H, m, $C_6\underline{H}_4$), 7.58 (1H, t, $J=7.80$ Hz, $C_6\underline{H}_4$), 7.74–7.77 (1H, m, $C_6\underline{H}_4$), 7.92–7.96 (1H, m, $C_6\underline{H}_4$), 8.01 (1H, t, $J=1.50$ and 1.80 Hz, $C_6\underline{H}_4$). LC–MS (EI^-) (*m*/*z*): calculated for $C_{23}H_{26}ClN_3OS$ $(M-H)^-$ 426, found 426. Anal. Calcd. For $C_{23}H_{26}ClN_3OS.1/3H_2O$: C, 63.65; H, 6.19; N, 9.68; S, 7.39. Found: C, 64.02; H, 6.86; N, 9.94; S, 7.54.

1-(3–Chlorophenyl)-2-({4-ethyl-5-[1-(4-isobutylphenyl) ethyl]-4H-1,2,4-triazole-3-yl} sulphanyl)ethane-1-one (16)

It was obtained as white solid, recrystallized from diethyl-ether initially, and 80% ethanol latterly, HPLC t_R (min): 6.59, Mp: 89 °C, yield 50%. IR cm^{-1}: 1693 (C=O), 1660 (C=N), 729 (C-S). ^{1}H-NMR (300 MHz, DMSO d_6): δ 0.76 (3H, t, $J=7.20$ Hz $CH_2C\underline{H}_3$), 0.83 (6H, d, $J=6.60$ Hz, $CH(C\underline{H}_3)_2$), 1.58 (3H, d, $J=6.90$ Hz, $CH(C\underline{H}_3)$), 1.72–1.85 (1H, m, $C\underline{H}(CH_3)_2$), 2.40 (2H, d, $J=7.20$ Hz, $CH(C\underline{H}_2)$), 2.51 ($CD_2\underline{H}SOCD_3$), 3.35 (DMSO d_6 $\underline{H}_2O$), 3.61–3.73 3.80–3.92 (2H, 2 m, $NC\underline{H}_2$), 4.31 (1H, q, $J=7.00$ Hz, $C\underline{H}(CH_3)$), 4.89 (2H, ABq, $\Delta\delta_{AB}=0.042$, $J=16.80$ Hz, $SC\underline{H}_2C{=}O$), 7.11 (4H, s, $C_6\underline{H}_4$), 7.59 (1H, t, $J=8.10$ and 7.80 Hz, $C_6\underline{H}_4$), 7.74–7.78 (1H, m, $C_6\underline{H}_4$), 7.95–7.98 (1H, m, $C_6\underline{H}_4$), 8.02 (1H, t, $J=1.80$ Hz, $C_6\underline{H}_4$). LC–MS (EI^-) (*m*/*z*): calculated for $C_{24}H_{28}ClN_3OS$ $(M-H)^-$ 440, found 440. Anal. Calcd. For $C_{24}H_{28}ClN_3OS.1/3H_2O$: C, 64.34; H, 6.45; N, 9.38; S, 7.16. Found: C, 64.53; H, 5.94; N, 9.49; S, 7.18.

1-(4–Chlorophenyl)-2-({4-methyl-5-[1-(4-isobutylphenyl) ethyl]-4H-1,2,4-triazole -3-yl}sulphanyl)ethane-1-one (17)

It was obtained as white solid, recrystallized from diethyl-ether initially, and 80% ethanol latterly, HPLC t_R (min): 5.65, Mp: 148 °C, yield 60%. IR cm^{-1}: 1672 (C=O), 1637 (C=N), 729 (C-S). ^{1}H-NMR (300 MHz, DMSO d_6): δ 0.84 (6H, d, $J=6.60$ Hz, $CH(C\underline{H}_3)_2$), 1.57 (3H, d, $J=6.90$ Hz, $CH(C\underline{H}_3)$), 1.73–1.86 (1H, m, $C\underline{H}(CH_3)_2$), 2.40 (2H, d, $J=7.20$ Hz, $CH(C\underline{H}_2)$), 2.51 ($CD_2\underline{H}SOCD_3$), 3.24 (3H, s, $NC\underline{H}_3$), 3.42 (DMSO d_6 $\underline{H}_2O$), 4.28 (1H, q, $J=7.00$ Hz, $C\underline{H}(CH_3)$), 4.77 (2H, ABq, $\Delta\delta_{AB}=0.033$, $J=16.82$ Hz, $SC\underline{H}_2C{=}O$), 7.07 and 7.10 (4H, 2d, $J=8.40$ Hz, $C_6\underline{H}_4$), 7.61 and 7.99 (4H, 2d, $J=8.70$ Hz, $C_6\underline{H}_4$). LC–MS (EI^-) (*m*/*z*): calculated for $C_{23}H_{26}ClN_3OS$ $(M-H)^-$ 426, found 426. Anal. Calcd. For $C_{23}H_{26}ClN_3OS$: C, 64.54; H, 6.12; N, 9.82; S, 7.49. Found: C, 64.37; H, 5.60; N, 9.73; S, 7.13.

1-(4–Chlorophenyl)-2-({4-ethyl-5-[1-(4-isobutylphenyl) ethyl]-4H-1,2,4-triazole-3-yl} sulphanyl)ethane-1-one (18)

It was obtained as white solid, recrystallized from diethy-lether initially, and 80% ethanol latterly, HPLC t_R (min): 6.27, Mp: 125 °C, yield 50%. IR cm^{-1}: 1670 (C=O), 1645 (C=N), 759 (C-S). ^{1}H-NMR (300 MHz, DMSO d_6): δ 0.73 (3H, t, $J=7.20$ Hz, $CH_2C\underline{H}_3$), 0.82 (6H, d, $J=6.60$ Hz, $CH(C\underline{H}_3)_2$), 1.57 (3H, d, $J=6.90$ Hz, $CH(C\underline{H}_3)$), 1.71–1.85 (1H, m, $C\underline{H}(CH_3)_2$), 2.39 (2H, d, $J=7.20$ Hz, $CH(C\underline{H}_2)$), 2.51 ($CD_2\underline{H}SOCD_3$), 3.42 (DMSO d_6 $\underline{H}_2O$), 3.60–3.72 3.79–3.91 (2H, 2 m, $NC\underline{H}_2$), 4.30 (1H, q, $J=7.00$ Hz, $C\underline{H}(CH_3)$), 4.86 (2H, ABq, $\Delta\delta_{AB}=0.033$, $J=16.80$ Hz, $SC\underline{H}_2C{=}O$), 7.10 (4H, s, $C_6\underline{H}_4$), 7.62 and 8.01(4H, 2d, $J=8.70$ Hz $C_6\underline{H}_4$). LC–MS (EI^-) (*m*/*z*): calculated for $C_{24}H_{28}ClN_3OS$ $(M-H)^-$ 440, found 440. Anal. Calcd. For $C_{24}H_{28}ClN_3OS.1/3H_2O$: C, 64.34; H, 6.45; N, 9.38; S, 7.16. Found: C, 64.21; H, 5.99; N, 9.37; S, 6.91.

1-(3-Fluorophenyl)-2-({4-methyl-5-[1-(4-isobutylphenyl) ethyl]-4H-1,2,4-triazole-3-yl}sulphanyl)ethane-1-one (19)

It was obtained as white solid, recrystallized from diethy-lether initially, and 80% ethanol latterly, HPLC t_R (min):

5.19, Mp: 140 °C, yield 60%. IR cm^{-1}: 1681 (C=O), 1653 (C=N), 729 (C-S). ^{1}H-NMR (300 MHz, DMSO d_6): δ 0.84 (6H, d, $J = 6.60$ Hz, CH(C$\underline{H}_3$)$_2$), 1.57 (3H, d, $J = 6.90$ Hz, CH(C$\underline{H}_3$)), 1.73–1.87 (1H, m, C$\underline{H}$(CH$_3$)$_2$), 2.40 (2H, d, $J = 7.20$ Hz, CH(C$\underline{H}_2$)), 2.51 ($CD_2\underline{H}SOCD_3$), 3.25 (3H, s, NC$\underline{H}_3$), 3.35 (DMSO d_6 $\underline{H}_2$O), 4.29 (1H, q, $J = 7.00$ Hz, C$\underline{H}$(CH$_3$)), 4.79 (2H, ABq, $\Delta\delta_{AB} = 0.039$, $J = 16.80$ Hz, SC$\underline{H}_2$C=O), 7.07 and 7.11 (4H, 2d, $J = 8.40$ Hz, $C_6\underline{H}_4$), 7.51–7.64 (2H, m, $C_6\underline{H}_4$), 7.76–7.80 (1H, m, $C_6\underline{H}_4$), 7.83–7.86 (1H, m, $C_6\underline{H}_4$). LC–MS (EI^-) (*m/z*): calculated for $C_{23}H_{26}FN_3OS$ $(M-H)^-$ 410, found 410. Anal. Calcd. For $C_{23}H_{26}FN_3OS.1/4H_2O$: C, 66.40; H, 6.42; N, 10.10; S, 7.77. Found: C, 66.73; H, 5.95; N, 10.25; S, 7.77.

1-(3-Fluorophenyl)-2-({4-ethyl-5-[1-(4-isobutylphenyl) ethyl]-4H-1,2,4-triazole-3-yl}sulphanyl)ethane-1-one (20)

It was obtained as white solid, recrystallized from diethylether initially, and 80% ethanol latterly, HPLC t_R (min): 5.76, Mp: 108 °C, yield 40%. IR cm^{-1}: 1693 (C=O), 1608 (C=N), 742 (C-S). ^{1}H-NMR (300 MHz, DMSO d_6): δ 0.76 (3H, t, $J = 7.20$ and 6.90 Hz, $CH_2C\underline{H}_3$), 0.83 (6H, d, $J = 6.60$ Hz, CH(C$\underline{H}_3$)$_2$), 1.58 (3H, d, $J = 7.20$ Hz, CH(C$\underline{H}_3$)), 1.72–1.85 (1H, m, C$\underline{H}$(CH$_3$)$_2$), 2.40 (2H, d, $J = 7.20$ Hz, CH(C$\underline{H}_2$)), 2.51 ($CD_2\underline{H}SOCD_3$), 3.35 (DMSO d_6 $\underline{H}_2$O), 3.61–3.73 3.80–3.92 (2H, 2 m, NC$\underline{H}_2$), 4.30 (1H, q, $J = 7.10$ Hz, C$\underline{H}$(CH$_3$)), 4.88 (2H, ABq, $\Delta\delta_{AB} = 0.041$, $J = 17.10$ Hz, SC$\underline{H}_2$C=O), 7.11 (4H, s, $C_6\underline{H}_4$), 7.52–7.66 (2H, m, C_6H_4), 7.78–7.82 (1H, m, Hz $C_6\underline{H}_4$), 7.85–7.88 (1H, m, $C_6\underline{H}_4$). LC–MS (EI^-) (*m/z*): calculated for $C_{24}H_{28}FN_3OS$ $(M-H)^-$ 424, found 424. Anal. Calcd. For $C_{24}H_{28}FN_3OS$: C, 67.74; H, 6.63; N, 9.87; S, 7.53. Found: C, 67.58; H, 6.64; N, 10.00; S, 7.56.

1-(4-Fluorophenyl)-2-({4-methyl-5-[1-(4-isobutylphenyl) ethyl]-4H-1,2,4-triazole-3-yl}sulphanyl)ethane-1-one (21)

It was obtained as white solid, recrystallized from diethylether initially, and 80% ethanol latterly, HPLC t_R (min): 5.03, Mp: 122 °C, yield 60%. IR cm^{-1}: 1681 (C=O), 1622 (C=N), 713 (C-S). ^{1}H-NMR (300 MHz, DMSO d_6): δ 0.84 (6H, d, $J = 6.60$ Hz, CH(C$\underline{H}_3$)$_2$), 1.57 (3H, d, $J = 6.90$ Hz, CH(C$\underline{H}_3$)), 1.73–1.86 (1H, m, C$\underline{H}$(CH$_3$)$_2$), 2.40 (2H, d, $J = 7.20$ Hz, CH(C$\underline{H}_2$)), 2.50 ($CD_2\underline{H}SOCD_3$), 3.24 (3H, s, NC$\underline{H}_3$), 3.34 (DMSO d_6 $\underline{H}_2$O), 4.29 (1H, q, $J = 7.00$ Hz, C$\underline{H}$(CH$_3$)), 4.79 (2H, ABq, $\Delta\delta_{AB} = 0.033$, $J = 16.50$ Hz, SC$\underline{H}_2$C=O), 7.07 and 7.11 (4H, 2d, $J = 8.70$ Hz, $C_6\underline{H}_4$), 7.37 (2H, t, $J = 8.70$ and 9.00 Hz, $C_6\underline{H}_4$), 8.04–9.11 (2H, m, $C_6\underline{H}_4$). LC–MS (EI^-) (*m/z*): calculated for $C_{23}H_{26}FN_3OS$ $(M-H)^-$ 410, found 410. Anal. Calcd. For $C_{23}H_{26}FN_3OS.1/3H_2O$: C, 66.16; H, 6.44; N, 10.06; S, 7.68. Found: C, 66.28; H, 5.89; N, 10.28; S, 7.71.

1-(4-Fluorophenyl)-2-({4-ethyl-5-[1-(4-isobutylphenyl) ethyl]-4H-1,2,4-triazole-3-yl} sulphanyl)ethane-1-one (22)

It was obtained as white solid, recrystallized from diethylether initially, and 80% ethanol latterly, HPLC t_R (min): 5.55, Mp: 134 °C, yield 55%. IR cm^{-1}: 1691 (C=O), 1620 (C=N), 758 (C-S). ^{1}H-NMR (300 MHz, DMSO d_6): δ 0.75 (3H, t, $J = 7.20$ Hz, $CH_2C\underline{H}_3$), 0.82 (6H, d, $J = 6.60$ Hz, CH(C$\underline{H}_3$)$_2$), 1.58 (3H, d, $J = 6.90$ Hz, CH(C$\underline{H}_3$)), 1.72–1.85 (1H, m, C$\underline{H}$(CH$_3$)$_2$), 2.40 (2H, d, $J = 7.20$ Hz, CH(C$\underline{H}_2$)), 2.51 ($CD_2\underline{H}SOCD_3$), 3.36 (DMSO d_6 $\underline{H}_2$O), 3.61–3.73 3.80–3.92 (2H, 2 m, NC$\underline{H}_2$), 4.31 (1H, q, $J = 7.00$ Hz, C$\underline{H}$(CH$_3$)), 4.88 (2H, ABq, $\Delta\delta_{AB} = 0.035$, $J = 16.80$ Hz, SC$\underline{H}_2$C=O), 7.11 (4H, s, $C_6\underline{H}_4$), 7.39 (2H, t, $J = 8.70$ and 9.00 Hz, $C_6\underline{H}_4$), 8.06–8.12 (2H, m, $C_6\underline{H}_4$). LC–MS (EI^-) (*m/z*): calculated for $C_{24}H_{28}FN_3OS$ $(M-H)^-$ 424, found 424. Anal. Calcd. For $C_{24}H_{28}FN_3OS$: C, 67.74; H, 6.63; N, 9.87; S, 7.53. Found: C, 67.83; H, 6.39; N, 9.94; S, 7.07.

1-(2,4-Difluorophenyl)-2-({4-methyl-5-[1-(4-isobutylphenyl) ethyl]-4H-1,2,4-triazole-3-yl}sulphanyl)ethane-1-one (23)

It was obtained as white solid, recrystallized from diethylether initially, and 80% ethanol latterly, HPLC t_R (min): 5.12, Mp: 108 °C, yield 50%. IR cm^{-1}: 1693 (C=O), 1681, (C=N), 758 (C-S). ^{1}H-NMR (300 MHz, DMSO d_6): δ 0.84 (6H, d, $J = 6.60$ Hz, CH(C$\underline{H}_3$)$_2$), 1.57 (3H, d, $J = 6.90$ Hz, CH(C$\underline{H}_3$)), 1.73–1.86 (1H, m, C$\underline{H}$(CH$_3$)$_2$), 2.40 (2H, d, $J = 7.20$ Hz, CH(C$\underline{H}_2$)), 2.51 ($CD_2\underline{H}SOCD_3$), 3.24 (3H, s, NC$\underline{H}_3$), 3.35 (DMSO d_6 $\underline{H}_2$O), 4.29 (1H, q, $J = 7.00$ Hz, C$\underline{H}$(CH$_3$)), 4.63–4.75 (2H, m, SC$\underline{H}_2$C=O), 7.06–7.13 (4H, m, $C_6\underline{H}_4$), 7.23–7.29 (1H, m, $C_6\underline{H}_3$), 7.43–7.51 (1H, m, $C_6\underline{H}_3$), 7.92–8.00 (1H, m, $C_6\underline{H}_3$). LC–MS (EI^-) (*m/z*): calculated for $C_{23}H_{25}F_2N_3OS$ $(M-H)^-$ 428, found 428. Anal. Calcd. For $C_{23}H_{25}F_2N_3OS$: C, 64.31; H, 6.63; N, 9.87; S, 7.53. Found: C, 64.37; H, 5.68; N, 9.85; S, 7.65.

1-(2,4-Difluorophenyl)-2-({4-ethyl-5-[1-(4-isobutylphenyl) ethyl]-4H-1,2,4-triazole-3-yl}sulphanyl)ethane-1-one (24)

It was obtained as white solid, recrystallized from diethylether initially, and 80% ethanol latterly, HPLC t_R (min): 5.62, Mp: 92 °C, yield 50%. IR cm^{-1}: 1697 (C=O), 1610 (C=N), 761 (C-S). ^{1}H-NMR (300 MHz, DMSO d_6): δ 0.75 (3H, t, $J = 7.20$ Hz, $CH_2C\underline{H}_3$), 0.82 (6H, d, $J = 6.60$ Hz, CH(C$\underline{H}_3$)$_2$), 1.58 (3H, d, $J = 6.90$ Hz, CH(C$\underline{H}_3$)), 1.72–1.85 (1H, m, C$\underline{H}$(CH$_3$)$_2$), 2.40 (2H, d, $J = 7.20$ Hz, CH(C$\underline{H}_2$)), 2.51 ($CD_2\underline{H}SOCD_3$), 3.35 (DMSO d_6 $\underline{H}_2$O), 3.60–3.72 3.79–3.91 (2H, 2 m, NC$\underline{H}_2$), 4.31 (1H, q, $J = 7.00$ Hz, C$\underline{H}$(CH$_3$)), 4.71–4.83 (2H, m, SC$\underline{H}_2$C=O), 7.11 (4H, s, $C_6\underline{H}_4$), 7.24–7.30 (1H, m, Hz $C_6\underline{H}_3$), 7.44–7.52 (1H, m, $C_6\underline{H}_3$), 7.93–8.01 (1H, m, $C_6\underline{H}_3$). LC–MS (EI^-) (*m/z*): calculated for $C_{24}H_{27}F_2N_3OS$ $(M-H)^-$ 442, found 442. Anal.

Calcd. For $C_{24}H_{27}F_2N_3OS.1/2H_2O$: C, 63.69; H, 6.24; N, 9.28; S, 7.09. Found: C, 63.78; H, 5.58; N, 9.64; S, 7.12.

1-(2,5-Dimethoxyphenyl)-2-({4-methyl-5-[1-(4-isobutylphenyl)ethyl]-4H-1,2,4- triazole-3-yl}sulphanyl)ethane-1-one (25)

It was obtained as white solid, recrystallized from diethylether initially, and 80% ethanol latterly, HPLC t_R (min): 5.78, Mp: 107 °C, yield 50%. IR cm^{-1}: 1647 (C=O), 1608 (C=N), 709 (C-S). ^{1}H-NMR (300 MHz, DMSO d_6): δ 0.84 (6H, d, J = 6.60 Hz, CH(C$\underline{H}_3$)$_2$), 1.58 (3H, d, J = 7.20 Hz, CH(C$\underline{H}_3$)), 1.73–1.86 (1H, m, C$\underline{H}$(CH$_3$)$_2$), 2.40 (2H, d, J = 7.20 Hz, CH(C$\underline{H}_2$)), 2.51 ($CD_2\underline{H}SOCD_3$), 3.22 (3H, s, NC$\underline{H}_3$), 3.35 (DMSO d_6 $\underline{H}_2O$), 3.73 (3H, s, OC$\underline{H}_3$), 3.85 (3H, s, OC$\underline{H}_3$), 4.29 (1H, q, J = 7.10 Hz, C$\underline{H}$(CH$_3$)), 4.62 (2H, ABq, $\Delta\delta_{AB}$ = 0.022, J = 16.80 Hz SC$\underline{H}_2$C=O), 7.07 and 7.11 (4H, 2d, J = 8.70 Hz, $C_6\underline{H}_4$), 7.14–7.22 (3H, m, $C_6\underline{H}_3$). LC–MS (EI^-) (*m/z*): calculated for $C_{25}H_{31}N_3O_3S$ $(M-H)^-$ 452, found 452. Anal. Calcd. For $C_{25}H_{31}N_3O_3S.1/3H_2O$: C, 65.33; H, 6.94; N, 9.14; S, 6.98. Found: C, 65.22; H, 6.29; N, 9.32; S, 6.98.

1-(2,5-Dimethoxyphenyl)-2-({4-ethyl-5-[1-(4-isobuthylphenyl)ethyl]-4H-1,2,4-triazole-3-yl}sulphanyl)ethane-1-one (26)

It was obtained as white solid, recrystallized from diethylether initially, and 80% ethanol latterly, HPLC t_R (min): 5.62, Mp: 83 °C, yield 40%. IR cm^{-1}: 1647 (C=O), 1608 (C=N), 756 (C-S). ^{1}H-NMR (300 MHz, DMSO d_6): δ 0.74 (3H, t, J = 7.20 and 6.90 Hz CH$_2$C$\underline{H}_3$), 0.82 (6H, d, J = 6.60 Hz, CH(C$\underline{H}_3$)$_2$), 1.58 (3H, d, J = 6.90 Hz, CH(C$\underline{H}_3$)), 1.72–1.85 (1H, m, C$\underline{H}$(CH$_3$)$_2$), 2.40 (2H, d, J = 7.20 Hz, CH(C$\underline{H}_2$)), 2.51 ($CD_2\underline{H}SOCD_3$), 3.35 (DMSO d_6 $\underline{H}_2O$), 3.58–3.70 3.77–3.90 (2H, 2 m, NC$\underline{H}_2$), 3.74 (3H, s, OC$\underline{H}_3$), 3.87 (3H, s, OC$\underline{H}_3$), 4.30 (1H, q, J = 7.00 Hz, C$\underline{H}$(CH$_3$)), 4.71 (2H, ABq, $\Delta\delta_{AB}$ = 0.022, J = 17.10 Hz, SC$\underline{H}_2$C=O), 7.10 (4H, s, $C_6\underline{H}_4$), 7.14–7.22 (3H, m, $C_6\underline{H}_3$). LC–MS (EI^-) (*m/z*): calculated for $C_{26}H_{33}N_3O_3S$ $(M-H)^-$ 466, found 466. Anal. Calcd. For $C_{26}H_{33}N_3O_3S$: C, 66.78; H, 7.11; N, 8.99; S, 6.86. Found: C, 66.31; H, 6.96; N, 9.13; S, 6.82.

1-(4-Bromophenyl)-2-({4-methyl-5-[1-(4-isobutylphenyl)ethyl]-4H-1,2,4-triazole-3-yl}sulphanyl)ethane-1-one (27)

It was obtained as white solid, recrystallized from diethylether initially, and 80% ethanol latterly, HPLC t_R (min): 5.83, Mp: 146 °C, yield 45%. IR cm^{-1}: 1674 (C=O), 1645 (C=N), 729 (C-S). ^{1}H-NMR (300 MHz, DMSO d_6): δ 0.84 (6H, d, J = 6.60 Hz, CH(C$\underline{H}_3$)$_2$), 1.57 (3H, d, J = 6.90 Hz, CH(C$\underline{H}_3$)), 1.72–1.86 (1H, m, C$\underline{H}$(CH$_3$)$_2$), 2.40 (2H, d, J = 7.20 Hz, CH(C$\underline{H}_2$)), 2.51 ($CD_2\underline{H}SOCD_3$), 3.24 (3H, s, NC$\underline{H}_3$), 3.42 (DMSO d_6 $\underline{H}_2O$), 4.28 (1H, q, J = 7.00 Hz, C$\underline{H}$(CH$_3$)), 4.76 (2H, ABq, $\Delta\delta_{AB}$ = 0.033, J = 16.50 Hz, SC$\underline{H}_2$C=O), 7.05–7.12 (4H, m, $C_6\underline{H}_4$), 7.75 and 7.91 (4H, 2d, J = 8.70 Hz $C_6\underline{H}_4$). LC–MS (EI^-) (*m/z*): calculated for $C_{23}H_{26}BrN_3OS$ $(M-H)^-$ 470, found 470. Anal. Calcd. For $C_{23}H_{26}BrN_3OS$: C, 58.47; H, 5.55; N, 8.89; S, 6.79. Found: C, 58.20; H, 5.20; N, 8.90; S, 6.54.

1-(4-Bromophenyl)-2-({4-ethyl-5-[1-(4-isobutylphenyl)ethyl]-4H-1,2,4-triazole-3-yl}sulphanyl)ethane-1-one (28)

It was obtained as white solid, recrystallized from diethylether initially, and 80% ethanol latterly, HPLC t_R (min): 6.43, Mp: 126 °C, yield 50%. IR cm^{-1}: 1674 (C=O), 1645 (C=N), 763 (C-S). ^{1}H-NMR (300 MHz, DMSO d_6): δ 0.75 (3H, t, J = 7.20 Hz, CH$_2$C$\underline{H}_3$), 0.82 (6H, d, J = 6.60 Hz, CH(C$\underline{H}_3$)$_2$), 1.57 (3H, d, J = 6.90 Hz, CH(C$\underline{H}_3$)), 1.71–1.85 (1H, m, C$\underline{H}$(CH$_3$)$_2$), 2.39 (2H, d, J = 7.20 Hz, CH(C$\underline{H}_2$)), 2.51 ($CD_2\underline{H}SOCD_3$), 3.42 (DMSO d_6 $\underline{H}_2O$), 3.60–3.72 3.79–3.91 (2H, 2 m, NC$\underline{H}_2$), 4.29 (1H, q, J = 7.00 Hz, C$\underline{H}$(CH$_3$)), 4.85 (2H, ABq, $\Delta\delta_{AB}$ = 0.033, J = 17.12 Hz, SC$\underline{H}_2$C=O), 7.10 (4H, s, $C_6\underline{H}_4$), 7.76 and 7.93 (4H, 2d, J = 8.40 and 8.70 Hz, $C_6\underline{H}_4$). LC–MS (EI^+) (*m/z*): calculated for $C_{24}H_{28}BrN_3OS$ $(M+H)^+$ 485, found 485. Anal. Calcd. For $C_{24}H_{28}BrN_3OS$: C, 59.26; H, 5.80; N, 8.64; S, 6.59. Found: C, 58.94; H, 5.52; N, 8.58; S, 6.17.

Synthesis of *N*-{(1*Z*)-2-[(5-benzyl-4-alkyl-4*H*-1,2,4-triazol-3-yl)sulphanyl]-1-phenylethylidene}hydroxylamine derivatives (29–46)

Compounds **11–28** (2 mmol), hydroxylamine hydrochloride (6 mmol), and pyridine (6 mmol) were placed in a flask. The mixture was dissolved in 25 ml of ethanol and refluxed for 18 h. The solvent was evaporated to dryness under reduced pressure. The precipitate was washed twice with distilled water and crystallized from 80% ethanol.

N-{(1Z)-1-Phenyl-2-[(5-benzyl-4-methyl-4H-1,2,4-triazole-3-yl)sulphanyl]-1-ethylidene}hydroxylamine (29)

It was obtained as white solid, recrystallized from 80% ethanol, HPLC t_R (min): 4.11, Mp: 187 °C, yield 40%. IR cm^{-1}: 3140 (oxime -OH), 1668 (oxime C=N), 1600 (C=N), 952 (oxime N–O), 731 (C-S). ^{1}H-NMR (300 MHz) (DMSO d_6): δ 2.51 ($CD_2\underline{H}SOCD_3$), 3.23 and 3.29 (3H, 2 s, NC$\underline{H}_3$), 3.35 (DMSO d_6 $\underline{H}_2O$), 4.12 (2H, s, ArC$\underline{H}_2$), 4.21 and 4.30 (2H, 2 s, SC$\underline{H}_2$C=O), 7.16–7.33 (5H, m, $C_6\underline{H}_5$), 7.35–7.41 (3H, m, $C_6\underline{H}_5$), 7.60–7.63 (2H, m, $C_6\underline{H}_5$), 11.17 and 11.75 (1H, 2 s, C=N–O$\underline{H}$). HRMS (EI^+) (*m/z*): calculated for

$C_{18}H_{18}N_4OS$ M^+ 338.1196, found 338.1246. Anal. Calcd. For $C_{18}H_{18}N_4OS.1/4H_2O$: C, 63.04; H, 5.44; N, 16.34; S, 9.35. Found: C, 63.34; H, 5.39; N, 16.66; S, 9.42.

N-{(1Z)-1-Phenyl-2-[(5-benzyl-4-ethyl-4H-1,2,4-triazole-3-yl)sulphanyl]-1-ethylidene} hydroxylamine (30)

It was obtained as white solid, recrystallized from 80% ethanol, HPLC t_R (min): 4.67, Mp: 169 °C, yield %40. IR cm^{-1}: 3105 (oxime -OH, hydrogen bonded), 1681 (oxime C=N), 1604 (C=N), 950 (oxime N–O), 729 (C-S). ^{1}H-NMR (300 MHz) (DMSO d_6): δ 0.85 (3H, t, J = 7.20 Hz $NCH_2C\underline{H}_3$), 2.51 ($CD_2\underline{H}SOCD_3$), 3.35 (DMSO d_6 $\underline{H}_2O$), 3.76 (2H, q, J = 7.20 Hz, $NC\underline{H}_2CH_3$), 4.15 (2H, s, $ArC\underline{H}_2$), 4.39 (2H, s, $SC\underline{H}_2C{=}O$), 7.20–7.33 (5H, m, $C_6\underline{H}_5$), 7.34–7.39 (3H, m, $C_6\underline{H}_5$), 7.62–7.65 (2H, m, $C_6\underline{H}_5$), 11.81 (1H, s, C=N–O$\underline{H}$). HRMS (EI^+) (*m*/*z*): calculated for $C_{19}H_{20}N_4OS$ M^+ 352.1358, found 352.1339. Anal. Calcd. For $C_{19}H_{20}N_4OS$: C, 64.75; H, 5.72; N, 15.90; S, 9.10. Found: C, 64.24; H, 5.38; N, 15.95; S, 9.08.

N-[(1Z)-1-Phenyl-2-({4-methyl-5-[1-(4-isobutylphenyl) ethyl]-4H-1,2,4-triazole-3-yl} sulphanyl)ethylidene] hydroxylamine (31)

It was obtained as white solid, recrystallized from 80% ethanol, HPLC t_R (min): 3.86, Mp: 164 °C, yield %40. IR cm^{-1}: 3103 (oxime -OH, hydrogen bonded), 1689 (oxime C=N), 1614 (C=N), 958 (oxime N–O), 729 (C-S). ^{1}H-NMR (300 MHz) (DMSO d_6): δ 0.83 (6H, d, J = 6.60 Hz, $CH(C\underline{H}_3)_2$), 1.57 (3H, d, J = 6.90 Hz, $CH(C\underline{H}_3)$), 1.72–1.86 (1H, m, $C\underline{H}(CH_3)_2$), 2.39 (2H, d, J = 7.20 Hz, $CH(C\underline{H}_2)$), 2.51 ($CD_2\underline{H}SOCD_3$), 3.12 (3H, s, $NC\underline{H}_3$), 3.40 (DMSO d_6 $\underline{H}_2O$), 4.22 (1H, q, J = 7.10 Hz, $C\underline{H}(CH_3)$), 4.29 (2H, s, $SC\underline{H}_2C{=}NOH$), 7.05 and 7.09 (4H, 2d, J = 8.40 Hz, $C_6\underline{H}_4$), 7.30–7.38 (3H, m, $C_6\underline{H}_4$), 7.57–7.60 (2H, m, $C_6\underline{H}_4$), 11.76 (1H, s, C=NO$\underline{H}$). ppm; ^{13}C NMR (75.47 MHz, DMSO d_6): δ 20.90, 22.13, 26.13, 29.56, 29.88, 35.64, 44.15, 125.72, 126.84, 128.38, 128.98, 129.29, 134.23, 139.27, 139.56, 148.65, 152.16, 158.15. HRMS (EI^+) (*m*/*z*): calculated for $C_{23}H_{28}N_4OS$ M^+ 408.1978, found 408.1993. Anal. Calcd. For $C_{23}H_{28}N_4OS$: C, 67.61; H, 6.91; N, 13.71; S, 7.85. Found: C, 67.13; H, 6.55; N, 13.71; S, 7.75.

N-[(1Z)-1-Phenyl-2-({4-ethyl-5-[1-(4-isobutylphenyl) ethyl]-4H-1,2,4-triazole-3-yl} sulphanyl)ethylidene] hydroxylamine (32)

It was obtained as white solid, recrystallized from 80% ethanol, HPLC t_R (min): 4.20, Mp: 128 °C, yield %45. IR cm^{-1}: 3109 (oxime -OH, hydrogen bonded), 1681 (oxime C=N), 1645 (C=N), 960 (oxime N–O), 759 (C-S). ^{1}H-NMR (300 MHz) (DMSO d_6): δ 0.64 (3H, t, J = 7.20 Hz, $CH_2C\underline{H}_3$), 0.81 (6H, d, J = 6.60 Hz, $CH(C\underline{H}_3)_2$), 1.59 (3H, d, J = 6.90 Hz, $CH(C\underline{H}_3)$), 1.70–1.83 (1H, m, $C\underline{H}(CH_3)_2$), 2.38 (2H, d, J = 7.20 Hz, $CH(C\underline{H}_2)$), 2.51 ($CD_2\underline{H}SOCD_3$), 3.41 (DMSO d_6 $\underline{H}_2O$), 3.49–3.61 3.66–3.78 (2H, 2 m, $C\underline{H}_2CH_3$), 4.24 (1H, q, J = 7.00 Hz, $C\underline{H}(CH_3)$), 4.39 (2H s, $SC\underline{H}_2C{=}NOH$)), 7.09 (4H, s, $C_6\underline{H}_4$), 7.32–7.36 (3H, m, $C_6\underline{H}_4$), 7.60–7.63 (2H, m, $C_6\underline{H}_4$), 11.84 (1H, s, C=N–O$\underline{H}$). ppm; ^{13}C NMR (75.47 MHz, DMSO d_6): δ 14.22, 21.35, 22.03, 26.26, 29.57, 35.57, 38.20, 44.11, 125.74, 126.86, 128.41, 129.01, 129.29, 134.25, 139.62, 139.99, 148.50, 152.30, 157.56. HRMS (EI^+) (*m*/*z*): calculated for $C_{24}H_{30}N_4OS$ M^+ 422.2134, found 422.2120. Anal. Calcd. For $C_{24}H_{30}N_4OS$: C, 66.79; H, 7.24; N, 12.98; S, 7.43. Found: C, 66.45; H, 6.75; N, 13.03; S, 7.47.

N-[(1Z)-1-(3–Chlorophenyl)-2-({4-methyl-5-[1-(4-isobutylphenyl)ethyl]-4H-1,2,4-triazole-3-yl}sulphanyl)ethylidene] hydroxylamine (33)

It was obtained as white solid, recrystallized from 80% ethanol, HPLC t_R (min): 4.63, Mp: 126 °C, yield %45. IR cm^{-1}: 3097 (oxime –OH, hydrogen bonded), 1689 (oxime C=N), 1614 (C=N), 970 (oxime N–O), 705 (C-S). ^{1}H-NMR (300 MHz) (DMSO d_6): δ 0.84 (6H, d, J = 6.60 Hz $CH(C\underline{H}_3)_2$), 1.57 (3H, d, J = 6.90 Hz, $CH(C\underline{H}_3)$), 1.72–1.86 (1H, m, $C\underline{H}(CH_3)_2$), 2.40 (2H, d, J = 7.20 Hz, $CH(C\underline{H}_2)$), 2.50 ($CD_2\underline{H}SOCD_3$), 3.34 (DMSO d_6 $\underline{H}_2O$), 3.15 (3H, s, $NC\underline{H}_3$), 4.23 (1H, q, J = 7.00 Hz, $C\underline{H}CH_3$), 4.27 (2H, ABq, $\Delta\delta_{AB}$ = 0.028, J = 13.20 Hz, $SC\underline{H}_2C{=}O$), 7.04 and 7.09 (4H, 2d, $C_6\underline{H}_4$, J = 8.10 and 8.40 Hz), 7.37 (1H, t, J = 7.80 Hz, $C_6\underline{H}_4$), 7.42–7.46 (1H, m, C_6H_4), 7.53–7.57 (1H, m, $C_6\underline{H}_4$), 7.64 (1H, t, J = 1.80 and 1.50 Hz, $C_6\underline{H}_4$), 11.32 and 11.90 (2 s, 1H, C=N–O$\underline{H}$). LC–MS (EI^-) (*m*/*z*): calculated for $C_{23}H_{27}ClN_4OS$ $(M-H)^-$ 441, found 441. Anal. Calcd. For $C_{23}H_{27}ClN_4OS$: C, 62.36; H, 6.14; N, 12.65; S, 7.24. Found: C, 62.31; H, 6.34; N, 12.89; S, 7.41.

N-[(1Z)-1-(3–Chlorophenyl)-2-({4-ethyl-5-[1-(4-isobutylphenyl)ethyl]-4H-1,2,4-triazole-3-yl}sulphanyl)ethylidene] hydroxylamine (34)

It was obtained as white solid, recrystallized from 80% ethanol, HPLC t_R (min): 5.17, Mp: 101 °C, yield %30. IR cm^{-1}: 3093 (oxime –OH, hydrogen bonded), 1693 (oxime C=N), 1614 (C=N), 976 (oxime N–O), 680 (C-S). ^{1}H-NMR (300 MHz) (DMSO d_6): δ 0.64 (3H, t, J = 7.20 and 6.90 Hz, $CH_2C\underline{H}_3$), 0.82 (6H, d, J = 6.60 Hz $CH(C\underline{H}_3)_2$), 1.59 (3H, d, J = 7.20 Hz, $CH(C\underline{H}_3)$), 1.71–1.85 (1H, m, $C\underline{H}(CH_3)_2$), 2.39 (2H, d, J = 7.20 Hz, $CH(C\underline{H}_2)$), 2.51 ($CD_2\underline{H}SOCD_3$), 3.35 (DMSO d_6 $\underline{H}_2O$), 3.50–3.62 3.69–3.81 (2H, 2 m, $C\underline{H}_2CH_3$), 4.25 (1H, q, J = 7.00 Hz, $C\underline{H}CH_3$), 4.36 (2H, s, $SC\underline{H}_2C{=}O$), 7.08 (4H, s, $C_6\underline{H}_4$), 7.39 (1H, t, J = 7.80 Hz, $C_6\underline{H}_4$), 7.43–7.47 (1H, m, $C_6\underline{H}_4$), 7.55–7.58 (1H, m, $C_6\underline{H}_4$), 7.64 (1H, t, J = 1.80 and 1.50 Hz, $C_6\underline{H}_4$), 11.99 (1H, s, C=N–O$\underline{H}$). LC–MS (EI^-)

(*m*/*z*): calculated for $C_{24}H_{29}ClN_4OS$ $(M-H)^-$ 455, found 455. Anal. Calcd. For $C_{24}H_{29}ClN_4OS.1/3H_2O$: C, 62.25; H, 6.46; N, 12.10; S, 6.92. Found: C, 62.00; H, 6.28; N, 12.47; S, 6.90.

N-[(1Z)-1-(4–Chlorophenyl)-2-({4-methyl-5-[1-(4-isobutylphenyl)ethyl]-4H-1,2,4-triazole-3-yl}sulphanyl)ethylidene] hydroxylamine (35)

It was obtained as white solid, recrystallized from 80% ethanol, HPLC t_R (min): 4.65, Mp: 156 °C, yield %35. IR cm^{-1}: 3095 (oxime –OH, hydrogen bonded), 1693 (oxime C=N), 1612 (C=N), 960 (oxime N–O), 707(C-S). ^{1}H-NMR (300 MHz) (DMSO d_6): δ 0.83 (6H, d, $J=6.60$ Hz $CH(C\underline{H}_3)_2$), 1.57 (3H, d, $J=7.20$ Hz, $CHC\underline{H}_3$), 1.72–1.86 (1H, m, $C\underline{H}(CH_3)_2$), 2.39 (2H, d, $J=6.90$ Hz, $CH(C\underline{H}_2)$), 2.51 ($CD_2\underline{H}SOCD_3$), 3.14 (3H, s, $NC\underline{H}_3$)), 3.42 (DMSO d_6 $\underline{H}_2O$), 4.21 (1H, q, $J=6.90$ Hz, $C\underline{H}CH_3$)), 4.25 (2H, s, $SC\underline{H}_2C$=NOH), 7.04 and 7.09 (4H, 2d, $J=8.40$ Hz, $C_6\underline{H}_4$), 7.39 and 7.59 (4H, 2d, $J=8.70$ Hz $C_6\underline{H}_4$), 11.86 (1H, s, C=N–O$\underline{H}$). LC–MS (EI^-) (*m*/*z*): calculated for $C_{23}H_{27}ClN_4OS$ $(M-H)^-$ 441, found 441. Anal. Calcd. For $C_{23}H_{27}ClN_4OS$: C, 62.36; H, 6.14; N, 12.65; S, 7.24. Found: C, 62.15; H, 6.09; N, 12.84; S, 7.30.

N-[(1Z)-1-(4–Chlorophenyl)-2-({4-ethyl-5-[1-(4-isobutylphenyl)ethyl]-4H-1,2,4-triazole-3-yl}sulphanyl)ethylidene] hydroxylamine (36)

It was obtained as white solid, recrystallized from 80% ethanol, HPLC t_R (min): 5.11, Mp: 96 °C, yield %30. IR cm^{-1}: 3107 (oxime –OH, hydrogen bonded), 1681 (oxime C=N), 1626, 1608 (C=N), 960 (oxime N–O), 702 (C-S). ^{1}H-NMR (300 MHz) (DMSO d_6): δ 0.62 (3H, t, $J=7.20$ Hz, $CH_2C\underline{H}_3$), 0.81 (6H, d, $J=6.60$ Hz, $CH(C\underline{H}_3)_2$), 1.58 (3H, d, $J=6.90$ Hz, $CH(C\underline{H}_3)$), 1.71–1.84 (1H, m, $C\underline{H}(CH_3)_2$), 2.39 (2H, d, $J=7.20$ Hz, $CH(C\underline{H}_2)$), 2.51 ($CD_2\underline{H}SOCD_3$), 3.42 (DMSO d_6 $\underline{H}_2O$), 3.52–3.61 3.67–3.79 (2H, 2 m, $NC\underline{H}_2CH_3$), 4.23 (1H, q, $J=6.90$ Hz, $C\underline{H}(CH_3)$), 4.35 (2H, s, $SC\underline{H}_2C$=NOH), 7.08 (4H, s, $C_6\underline{H}_4$), 7.40 and 7.60 (4H, 2d, $J=8.70$ Hz, $C_6\underline{H}_4$), 11.93 (1H, s, C=N–O$\underline{H}$). LC–MS (EI^-) (*m*/*z*): calculated for $C_{24}H_{29}ClN_4OS$ $(M-H)^-$ 455, found 455. Anal. Calcd. For $C_{24}H_{29}ClN_4OS.1/4H_2O$: C, 62.46; H, 6.44; N, 12.14; S, 6.95. Found: C, 62.58; H, 5.96; N, 12.08; S, 6.52.

N-[(1Z)-1-(3-Fluorophenyl)-2-({4-ethyl-5-[1-(4-isobutylphenyl)ethyl]-4H-1,2,4-triazole-3-yl}sulphanyl)ethylidene] hydroxylamine (37)

It was obtained as white solid, recrystallized from 80% ethanol, HPLC t_R (min): 4.28, Mp: 150 °C, yield %40. IR cm^{-1}: 3095 (oxime –OH, hydrogen bonded), 1691 (oxime C=N), 1616 (C=N), 979 (oxime N–O), 729 (C-S). ^{1}H-NMR (300 MHz) (DMSO d_6): δ 0.84 (6H, d, $J=6.60$ Hz $CH(C\underline{H}_3)_2$), 1.57 (3H, d, $J=6.90$ Hz, $CH(C\underline{H}_3)$, 1.73–1.86 (1H, m, $C\underline{H}(CH_3)_2$), 2.40 (2H, d, $J=7.20$ Hz, $CH(C\underline{H}_2)$), 2.51 ($CD_2\underline{H}SOCD_3$), 3.15 (3H, s, $NC\underline{H}_3$), 3.38 (DMSO d_6 $\underline{H}_2O$), 4.23 (1H, q, $J=7.00$ Hz, $C\underline{H}CH_3$), 4.27 (2H, ABq, $\Delta\delta_{AB}=0.022$, $J=13.20$ Hz, $SC\underline{H}_2C$=O), 7.05 and 7.09 (4H, 2d, $J=8.40$ Hz, $C_6\underline{H}_4$), 7.18–7.25 (1H, m, $C_6\underline{H}_4$), 7.35–7.45 (3H, m, $C_6\underline{H}_4$), 11.90 (1H, s, C=N–O$\underline{H}$). LC–MS (EI^-) (*m*/*z*): calculated for $C_{23}H_{27}FN_4OS$ $(M-H)^-$ 425, found 425. Anal. Calcd. For $C_{23}H_{27}FN_4OS.1/3H_2O$: C, 63.86; H, 6.45; N, 12.95; S, 7.41. Found: C, 63.96; H, 6.01; N, 13.23; S, 7.48.

N-[(1Z)-1-(3-Fluorophenyl)-2-({4-ethyl-5-[1-(4-isobutylphenyl)ethyl]-4H-1,2,4-triazole-3-yl}sulphanyl)ethylidene] hydroxylamine (38)

It was obtained as white solid, recrystallized from 80% ethanol, HPLC t_R (min): 4.67, Mp: 143 °C, yield %30. IR cm^{-1}: 3082 (oxime –OH, hydrogen bonded), 1681 (oxime C=N), 1614 (C=N), 979 (oxime N–O), 746 (C-S). ^{1}H-NMR (300 MHz) (DMSO d_6): δ 0.64 (3H, t, $J=7.20$ Hz, $CH_2C\underline{H}_3$), 0.82 (6H, d, $J=6.60$ Hz $CH(C\underline{H}_3)_2$), 1.59 (3H, d, $J=6.90$ Hz, $CH(C\underline{H}_3)$, 1.71–1.85 (1H, m, $C\underline{H}(CH_3)_2$), 2.39 (2H, d, $J=7.20$ Hz, $CH(C\underline{H}_2)$, 2.51 ($CD_2\underline{H}SOCD_3$), 3.35 (DMSO d_6 $\underline{H}_2O$), 3.50–3.62 3.69–3.81 (2H, 2 m, $C\underline{H}_2CH_3$), 4.25 (1H, q, $J=7.00$ Hz, $C\underline{H}CH_3$), 4.37 (2H, s, $SC\underline{H}_2C$=O), 7.08 (4H, s, $C_6\underline{H}_4$), 7.19–7.26 (1H, m, $C_6\underline{H}_4$), 7.35–7.47 (3H, m, $C_6\underline{H}_4$), 11.36 and 11.98 (1H, 2 s, C=N–O$\underline{H}$). LC–MS (EI^-) (*m*/*z*): calculated for $C_{24}H_{29}FN_4OS$ $(M-H)^-$ 439, found 439. Anal. Calcd. For $C_{24}H_{29}FN_4OS.1/3H_2O$: C, 64.55; H, 6.70; N, 12.55; S, 7.18. Found: C, 64.05; H, 6.27; N, 12.82; S, 7.20.

N-[(1Z)-1-(4-Fluorophenyl)-2-({4-methyl-5-[1-(4-isobutylphenyl)ethyl]-4H-1,2,4-triazole-3-yl}sulphanyl)ethylidene] hydroxylamine (39)

It was obtained as white solid, recrystallized from 80% ethanol, HPLC t_R (min): 4.21, Mp: 149 °C, yield %30. IR cm^{-1}: 3109 (oxime –OH, hydrogen bonded), 1681 (oxime C=N), 1600 (C=N), 962 (oxime N–O), 709 (C-S). ^{1}H-NMR (300 MHz) (DMSO d_6): δ 0.84 (6H, d, $J=6.60$ Hz, $CH(C\underline{H}_3)_2$), 1.57 (3H, d, $J=7.20$ Hz, $CH(C\underline{H}_3)$), 1.73–1.86 (1H, m, $C\underline{H}(CH_3)_2$), 2.40 (2H, d, $J=7.20$ Hz, $CHC\underline{H}_2$), 2.50 ($CD_2\underline{H}SOCD_3$), 3.14 (3H, s, $NC\underline{H}_3$), 3.34 (DMSO d_6 $\underline{H}_2O$), 4.23 (1H, q, $J=7.00$ Hz, $C\underline{H}CH_3$), 4.27 (2H, s, $SC\underline{H}_2C$=NOH), 7.05 and 7.10 (4H, 2d, $J=8.40$ Hz, $C_6\underline{H}_4$), 7.17 (2H, t, $J=9.00$ and 8.70 Hz, $C_6\underline{H}_4$), 7.64 (2H, dd, $J=9.00$ and 5.40 Hz, $C_6\underline{H}_4$), 11.23 and 11.74 (1H, 2 s, C=NO$\underline{H}$). LC–MS (EI^-) (*m*/*z*): calculated for $C_{23}H_{27}FN_4OS$ $(M-H)^-$ 425, found 425. Anal. Calcd. For $C_{23}H_{27}FN_4OS$: C,

64.76; H, 6.38; N, 13.13; S, 7.52. Found: C, 64.46; H, 6.48; N, 13.14; S, 7.57.

N-[(1Z)-1-(4-Fluorophenyl)-2-({4-ethyl-5-[1-(4-isobutylphenyl)ethyl]-4H-1,2,4-triazole-3-yl}sulphanyl)ethylidene] hydroxylamine (40)

It was obtained as white solid, recrystallized from 80% ethanol, HPLC t_R (min): 4.57, Mp: 130 °C, yield %40. IR cm^{-1}: 3078 (oxime –OH, hydrogen bonded), 1660 (oxime C=N), 1610 (C=N), 966 (oxime N–O), 732 (C-S). ^{1}H-NMR (300 MHz) (DMSO d_6): δ 0.63 (3H, t, J = 7.20 and 6.90 Hz, $CH_2C\underline{H}_3$), 0.81 (6H, d, J = 6.30 Hz, $CH(C\underline{H}_3)_2$), 1.58 (3H, d, J = 7.20 Hz, $CH(C\underline{H}_3)$), 1.71–1.84 (1H, m, $C\underline{H}(CH_3)_2$), 2.39 (2H, d, J = 7.20 Hz, $CH(C\underline{H}_2)$), 2.51 ($CD_2\underline{H}SOCD_3$), 3.38 (DMSO d_6 $\underline{H}_2O$), 3.49–3.61 3.67–3.79 (2H, 2 m, $NC\underline{H}_2CH_3$), 4.25 (1H, q, J = 7.00 Hz, $C\underline{H}(CH_3)$), 4.36 (2H s, $SC\underline{H}_2C$=NOH), 7.08 (4H, s, $C_6\underline{H}_4$), 7.18 (2H, t, J = 9.00 and 8.70 Hz, $C_6\underline{H}_4$), 7.64 (2H, dd, J = 9.00 and 5.70 Hz $C_6\underline{H}_4$), 11.28 and 11.82 (1H, 2 s, C=N–O$\underline{H}$). LC–MS (EI^-) (*m/z*): calculated for $C_{24}H_{29}FN_4OS$ $(M-H)^-$ 439, found 439. Anal. Calcd. For $C_{24}H_{29}FN_4OS$: C, 65.43; H, 6.63; N, 12.72; S, 7.28. Found: C, 65.23; H, 6.12; N, 12.77; S, 7.04.

N-[(1Z)-1-(2,4-Difluorophenyl)-2-({4-methyl-5-[1-(4-isobutylphenyl)ethyl]-4H-1,2,4-triazole-3-yl}sulphanyl) ethylidene] hydroxylamine (41)

It was obtained as white solid, recrystallized from 80% ethanol, HPLC t_R (min): 4.20, Mp: 103 °C, yield %30. IR cm^{-1}: 3311 (oxime –OH), 1681 (oxime C=N), 1612 (C=N), 972 (oxime N–O), 715 (C-S). ^{1}H-NMR (300 MHz) (DMSO d_6): δ 0.84 (6H, d, J = 6.60 Hz, $CH(C\underline{H}_3)_2$), 1.56, 1.57 (3H, 2d, J = 6.90 and 6.90 Hz, $CH(C\underline{H}_3)$), 1.73–1.87 (1H, m, $C\underline{H}(CH_3)_2$), 2.40 (2H, d, J = 7.20 Hz, $CH(C\underline{H}_2)$), 2.51 ($CD_2\underline{H}SOCD_3$.), 3.11 and 3.14 (3H, 2 s, $NC\underline{H}_3$), 3.35 (DMSO d_6 $\underline{H}_2O$), 4.18–4.30 (3H, m, $C\underline{H}(CH_3)$, and $SC\underline{H}_2C$=NOH), 6.97–7.12 (5H, m, $C_6\underline{H}_3$, and $C_6\underline{H}_4$,), 7.20–7.29 (1H, m, $C_6\underline{H}_3$), 7.38–7.47 (1H, m, $C_6\underline{H}_3$), 11.35 and 11.94 (1H, 2 s, C=NO$\underline{H}$). LC–MS (EI^+) (*m/z*): calculated for $C_{23}H_{26}F_2N_4OS$ $(M+H)^+$ 445, found 445. Anal. Calcd. For $C_{23}H_{26}F_2N_4OS.3/2H_2O$: C, 58.58; H, 6.20; N, 11.88; S, 6.80. Found: C, 58.60; H, 5.75; N, 12.30; S, 6.88.

N-[(1Z)-1-(2,4-Difluorophenyl)-2-({4-ethyl-5-[1-(4-isobutylphenyl)ethyl]-4H-1,2,4-triazole-3-yl}sulphanyl)ethylidene] hydroxylamine (42)

It was obtained as white solid, recrystallized from 80% ethanol, HPLC t_R (min): 4.58, Mp: 142 °C, yield %40. IR cm^{-1}: 3122 (oxime –OH, hydrogen bonded), 1643 (oxime C=N), 1612 (C=N), 972 (oxime N–O), 759 (C-S). ^{1}H-NMR (300 MHz) (DMSO d_6): δ 0.60 (3H, t, J = 7.20 Hz, $CH_2C\underline{H}_3$), 0.82 (6H, d, J = 6.60 Hz, $CH(C\underline{H}_3)_2$), 1.56 (3H, d, J = 6.90 Hz, $CH(C\underline{H}_3)$), 1.72–1.85 (1H, m, $C\underline{H}(CH_3)_2$), 2.40 (2H, d, J = 6.90 Hz, $CH(C\underline{H}_2)$), 2.51 ($CD_2\underline{H}SOCD_3$), 3.35 (DMSO d_6 $\underline{H}_2O$), 3.44–3.57 3.63–3.76 (2H, 2 m, $NC\underline{H}_2CH_3$), 4.19–4.40 (3H, m, $C\underline{H}(CH_3)$ and $SC\underline{H}_2C$=O), 6.99–7.12 (5H, m, $C_6\underline{H}_3$ and C_6H_4), 7.20–7.29 (1H, m, $C_6\underline{H}_3$,), 7.37–7.45 (1H, m, $C_6\underline{H}_3$,), 11.38 and 11.98 (1H, 2 s, C=N–O$\underline{H}$). LC–MS (EI^+) (*m/z*): calculated for $C_{24}H_{28}F_2N_4OS$ $(M+H)^+$ 459, found 459. Anal. Calcd. For $C_{24}H_{28}F_2N_4OS$: C, 62.86; H, 6.15; N, 12.22; S, 6.99. Found: C, 62.56; H, 5.61; N, 12.33; S, 6.86.

N-[(1Z)-1-(2,5-Dimethoxyphenyl)-2-({4-methyl-5-[1-(4-isobutylphenyl)ethyl]-4H- 1,2,4-triazole-3-yl}sulphanyl) ethylidene] hydroxylamine (43)

It was obtained as white solid, recrystallized from 80% ethanol, HPLC t_R (min): 4.15, Mp: 150 °C, yield %50. IR cm^{-1}: 3122 (oxime –OH, hydrogen bonded), 1681 (oxime C=N), 1612 (C=N), 976 (oxime N–O), 705 (C-S). ^{1}H-NMR (300 MHz) (DMSO d_6): δ 0.84 (6H, d, J = 6.60 Hz, $CH(C\underline{H}_3)_2$), 1.56 (3H, d, J = 7.20 Hz, $CH(C\underline{H}_3)$), 1.72–1.86 (1H, m, $C\underline{H}(CH_3)_2$), 2.40 (2H, d, J = 7.20 Hz, $CH(C\underline{H}_2)$), 2.51 ($CD_2\underline{H}SOCD_3$), 3.10 (3H, s, $NC\underline{H}_3$), 3.38 (DMSO d_6 $\underline{H}_2O$), 3.66 (3H, s, $OC\underline{H}_3$), 3.69 (3H, s, $OC\underline{H}_3$), 4.16–4.24 (1H, m, $C\underline{H}(CH_3)$), 4.22 (2H, ABq, $\Delta\delta_{AB} = 0.017$, J = 13.20 Hz, $SC\underline{H}_2C$=NOH), 6.73–6.77 (1H, m, $C_6\underline{H}_3$), 6.83–6.94 (2H, m, $C_6\underline{H}_3$), 7.04 and 7.09 (4H, 2d, J = 8.10 Hz, $C_6\underline{H}_4$), 10.94 and 11.57 (1H, 2 s, C=NO$\underline{H}$). LC–MS (EI^+) (*m/z*): calculated for $C_{25}H_{32}N_4O_3S$ $(M+H)^+$ 469, found 469. Anal. Calcd. For $C_{25}H_{32}N_4O_3S$: C, 64.08; H, 6.88; N, 11.96; S, 6.84. Found: C, 63.54; H, 6.54; N, 12.17; S, 6.80.

N-[(1Z)-1-(2,5-Dimethoxyphenyl)-2-({4-ethyl-5-[1-(4-isobutylphenyl)ethyl]-4H-1,2,4-triazole-3-yl}sulphanyl) ethylidene] hydroxylamine (44)

It was obtained as white solid, recrystallized from 80% ethanol, HPLC t_R (min): 4.67, Mp: 126 °C, yield %40. IR cm^{-1}: 3120 (oxime –OH, hydrogen bonded), 1683 (oxime C=N), 1631 (C=N), 970 (oxime N–O), 723 (C-S). ^{1}H-NMR (300 MHz) (DMSO d_6): δ 0.61 (3H, t, J = 7.20 Hz, $CH_2C\underline{H}_3$), 0.82 (6H, d, J = 6.60 Hz, $CH(C\underline{H}_3)_2$), 1.57 (3H, d, J = 6.90 Hz, $CH(C\underline{H}_3)$), 1.71–1.85 (1H, m, $C\underline{H}(CH_3)_2$), 2.39 (2H, d, J = 7.20 Hz, $CH(C\underline{H}_2)$), 2.51 ($CD_2\underline{H}SOCD_3$), 3.35 (DMSO d_6 $\underline{H}_2O$), 3.42–3.55 3.62–3.75 (2H, 2 m, $NC\underline{H}_2$), 3.68 (6H, s, $OC\underline{H}_3$), 4.21 (1H, q, J = 7.00 Hz, $C\underline{H}(CH_3)$), 4.31 (2H s, $SC\underline{H}_2C$=NOH)), 6.72–6.73 (1H, m, $C_6\underline{H}_3$), 6.88–6.95 (2H, m, $C_6\underline{H}_3$), 7.08 (4H, s, $C_6\underline{H}_4$), 10.97 and 11.61 (1H, 2 s, C=N–O$\underline{H}$). LC–MS (EI^+) (*m/z*): calculated for $C_{26}H_{34}N_4O_3S$ $(M+H)^+$ 483, found 483. Anal. Calcd. For

$C_{26}H_{34}N_4O_3S.1H_2O$: C, 62.37; H, 7.25; N, 11.19; S, 6.40. Found: C, 62.69; H, 7.55; N, 11.66; S, 6.58.

N-[(1Z)-1-(4-Bromophenyl)-2-({4-methyl-5-[1-(4-isobutylphenyl)ethyl]-4H-1,2,4-triazole-3-yl}sulphanyl)ethylidene] hydroxylamine (45)

It was obtained as white solid, recrystallized from 80% ethanol, HPLC t_R (min): 4.78, Mp: 160 °C, yield %33. IR cm^{-1}: 3095 (oxime –OH, hydrogen bonded), 1681 (oxime C=N), 1612 (C=N), 960 (oxime N–O), 707 (C-S). ^{1}H-NMR (300 MHz) (DMSO d_6): δ 0.84 (6H, d, J = 6.60 Hz, $CH(C\underline{H}_3)_2$), 1.57 (3H, d, J = 7.20 Hz, $CH(C\underline{H}_3)$), 1.73–1.86 (1H, m, $C\underline{H}(CH_3)_2$), 2.40 (2H, d, J = 6.90 Hz, $CH(C\underline{H}_2)$), 2.51 ($CD_2\underline{H}SOCD_3$), 3.14 (3H, s, $NC\underline{H}_3$), 3.37 (DMSO d_6 $\underline{H}_2O$), 4.19–4.25 (1H, m, $C\underline{H}(CH_3)$), 4.26 (2H, s, $SC\underline{H}_2C$=NOH), 7.03–7.11 (4H, m, $C_6\underline{H}_4$), 7.53 (4H, s, $C_6\underline{H}_4$), 11.30 and 11.86 (1H, 2 s, C=NO$\underline{H}$). LC–MS (EI^+) (m/z): calculated for $C_{23}H_{27}BrN_4OS$ $(M+H)^+$ 487, found 487. Anal. Calcd. For $C_{23}H_{27}BrN_4OS$: C, 56.67; H, 5.58; N, 11.49; S, 6.58. Found: C, 56.41; H, 5.03; N, 11.40; S, 6.22.

N-[(1Z)-1-(4-Bromophenil)-2-({4-ethyl-5-[1-(4-isobutylphenyl)ethyl]-4H-1,2,4-triazole-3-yl}sulphanyl)ethylidene] hydroxylamine (46)

It was obtained as white solid, recrystallized from 80% ethanol, HPLC t_R (min): 5.26, Mp: 153 °C, yield %50. IR cm^{-1}: 3084 (oxime –OH, hydrogen bonded), 1681 (oxime C=N), 1606 (C=N), 968 (oxime N–O), 738 (C-S). ^{1}H-NMR (300 MHz) (DMSO d_6): δ 0.62 (3H, t, J = 7.20 Hz, $CH_2C\underline{H}_3$), 0.81 (6H, d, J = 6.60 Hz, $CH(C\underline{H}_3)_2$), 1.58 (3H, d, J = 7.20 Hz, $CH(C\underline{H}_3)$), 1.71–1.84 (1H, m, $C\underline{H}(CH_3)_2$), 2.39 (2H, d, J = 7.20 Hz, $CH(C\underline{H}_2)$), 2.51 ($CD_2\underline{H}SOCD_3$), 3.38 (DMSO d_6 $\underline{H}_2O$), 3.50–3.61 3.67–3.79 (2H, 2 m, $NC\underline{H}_2CH_3$), 4.24 (1H, q, J = 6.90 Hz, $C\underline{H}(CH_3)$), 4.34 (2H s, $SC\underline{H}_2C$=NOH), 7.08 (4H, s, $C_6\underline{H}_4$), 7.54 (4H, s, $C_6\underline{H}_4$), 11.34 and 11.94 (1H, 2 s, C=N–O$\underline{H}$). LC–MS (EI^-) (m/z): calculated for $C_{24}H_{29}BrN_4S$ $(M-H)^-$ 499, found 499. Anal. Calcd. For $C_{24}H_{29}BrN_4S$: C, 57.48; H, 5.83; N, 11.17; S, 6.39. Found: C, 57.63; H, 5.46; N, 11.16; S, 6.22.

Biological methods

Cell culture

In this study, human breast cancer (MCF-7), human lung cancer (A549), human prostate cancer (PC-3), human cervix cancer (HeLa), human chronic myelogenous leukemia (K562), and mouse embryonic fibroblast (NIH/3T3) cells were used. Cells were cultured in Dulbecco's modified eagle medium (DMEM) (Gibco, Rockville, MD, USA) containing 10% fetal bovine serum (FBS) (Gibco, Rockville, MD, USA) and maintained in a 37 °C, 5% CO2 incubator. Cell passage was conducted at 80–90% confluence.

Cell viability assay

Cell viability was determined by the 3-(4,5-dimethylthiazol-2-yl)-2,5-diphenyltetrazolium bromide (MTT) assay. Briefly, the cells (1 × 104 cells/well) were seeded onto 96-well plates and incubated overnight. Then, the cells were treated with different concentrations (1–50 μM) of compounds for 48 h. After the incubation period, MTT was added into each well to a final concentration of 0.5 mg/mL and incubated for 4 h. The culture medium was then removed, and 100μL of the SDS buffer was added to solubilize the purple formazan product. A microplate reader measured absorption at wavelengths of 570 and 630 nm (Biotek, Winooski, VT, USA).

Annexin V binding

After treatment, the cells were pre-incubated on ice for 30 min. Then, cells were centrifuged and resuspended in cold PBS. After incubation with annexin V for 30 min at room temperature, the cells were washed and fixed in PFA. The fluorescence intensity was measured using a fluorospectrophotometer [75, 76].

Caspase enzymes activity

The caspase colorimetric assay kits measured Caspase-3, 8, and 9 activities following the procedure provided by the manufacturer (Millipore, USA). Briefly, treated (50 and 100 μM) and untreated cells were collected after 24 h and resuspended in a chilled lysis buffer for 15 min. Next, centrifugation with high speed was performed, and the supernatants were collected and used for caspase activation assays. Before samples were incubated at 37 °C for 2 h, reaction buffer, DTT and DEVD-p-NA, Ac-IETD-p-NA, and Ac-LEHD-p-NA substrates for caspase-3, 8, and 9, respectively, were added. The principle was that caspase-3 derived from cellular lysate recognizes the sequence Asp-Glu-Val-Asp (DEVD). The assay is based on spectrophotometric detection of the chromophore p-nitroaniline (p-NA) after cleavage from the labeled substrate (DEVD-p-NA). The p-NA light emission can be quantified using a microtiter plate reader at 405 nm. Comparison of the absorbance of p-NA from an apoptotic sample with an untreated control sample allows determination of the fold increase in caspase-3, 8, and 9 activities [75–77].

Determination of mitochondrial membrane potential (MMP)

The loss of MMP was detected by the JC-1 mitochondrial membrane potential (MMP) kit (MitoPT JC-1, Immunochemistry Technologies, LLC). The lipophilic cation JC-1 is widely used in apoptosis studies to monitor mitochondrial health. The membrane-permeant JC-1 dye exhibits potential-dependent accumulation in mitochondria, indicated by a fluorescence emission shift from green (~ 529 nm) to red (~ 590 nm). Depending on MMP, JC-1 forms J-aggregates associated with a significant shift in emission (590 nm). Color dye changes reversibly from orange to green as mitochondrial membranes become depolarized. For JC-1 staining, after the incubation of compounds, cell suspensions were adjusted to a density of 0.5 × 106 cells/ml and incubated in an assay buffer with JC-1 (10 µg/ml) for 15 min at 37° C in the dark. The cells were collected by centrifugation at 1000 rpm for 10 min. A fluorescence Elisa reader read the plate at 510 and 585 nm wavelengths. Finally, 585/510 values were calculated to determine the changes in MMP.

Wound healing assay

The effects of Compound **45** on migration and motility of cancer cells were examined using a wound healing assay. Cells were seeded in six-well dishes to achieve approximately 90% confluence. Using a sterile 200-µL pipette tip, a straight scratch simulating a wound in a monolayer was made. After scratching, wells were gently washed with PBS to remove the detached cells, and a fresh serum-free medium was added. MCF-7 and A549 cells were treated with the vehicle (untreated cells), 20 µM and 50 µM Compound **45**. Then, the plates were incubated at 37 °C, and the speed of cell movement across the gap was observed. Digital documentation at the same position was made after scratching at time zero (T0) and 24 h and captured by a computer-imaging system (Leica DC300F camera). The effects on cell migration and motility were estimated using ImageJ software (National Institutes of Health, Bethesda, MD, USA). The area of the remaining wound was determined as the ratio between the residual area at a given time point and the original wound area (T0) × 100.

Microsomal PGES-1 and COX-1/2 enzyme inhibition assays

Preparation of mPGES-1 enzymes

The cloning of mPGES-1 enzyme and the preparation of protein followed the same protocols as described in our previous reports [88]. Briefly, FreeStyle Max Expression system was used to express wild-type human mPGES-1 enzymes. FreeStyle 293-F cells were cultured following manufacturer's manual in FreeStyle 293 expression medium on orbit rotate shaker in 8% CO2 incubator at 37 °C. Cells were transfected with 1.5 µg/mL of mPGES-1/pcDNA3 construct using FreeStyle Max reagent at a cell density of 1 × 106 for two days. Transfected cells were collected, washed, and sonicated in TSES buffer (15 mM Tris–HCl, pH 8.0 plus 0.25 M sucrose, 0.1 mM EDTA and 1 mM DTT) on ice. The broken cells were first centrifuged at 12.500 µg for 10 min. The supernatant was further centrifuged at 105,000 µg for 1 h at 4 ºC. The residual pellet was washed and homogenized in PBS buffer. The crude microsomal mPGES-1 was aliquoted and stored at − 80 °C before use [27].

Activity assay using a recombinant mPGES-1

The enzyme activity assay was performed using the same protocol as described in our previous reports [27, 78, 89–91]. Briefly, the mPGES-1–Catalyzed reaction was performed in 1.5 mL microcentrifuge tubes with reaction mixture of 0.2 Na_2HPO_4/NaH_2PO_4, pH 7.2 (10 µL); 2.5 mM GSH (2.5 µL), diluted microsomal human mPGES-1 enzyme (80 µg/mL, 1 µL), inhibitor in DMSO solution (1 µL); 0.31 mM PGH_2 in DMF (5 µL), and distilled deionized water in a final volume of 100 µL. An inhibitor was incubated with the enzyme for 15 min at ambient temperature followed by the addition of substrate PGH_2 (stored in dry ice). The enzymatic reaction was started immediately upon the addition of PGH_2. After 1 min of reaction, solution (40 mg/mL $SnCl_2$ in absolute ethanol, 10 µL) was added to cease the reaction by converting excess PGH_2 to $PGF_{2\alpha}$. The produced PGE_2 from the enzymatic reaction was quantified by the PGE_2 enzyme immunoassay as described earlier [92].

COX-1/2 enzyme activity assay

The inhibitory potential of all synthesized compounds on COX-1 and COX-2 enzymes was evaluated using a colorimetric COX Inhibitor Screening Kit (Cayman Chemical, Ann Arbor, MI, USA). The samples and control were dissolved in the DMSO and diluted with the reaction buffer to their final concentrations. DMSO served as a negative control for 100% initial activity. We have also tested for inhibitor interference by adding the inhibitor to a boiled enzyme sample as a control. The assay was conducted in duplicate.

Tube formation assay

Matrigel was thawed at 4 °C the night before the experiment. 48-well plates were coated with matrigel and let it polymerize at 37 °C for 1 h. Cells were seeded onto the wells at

a density of 250 × 103/well in culture media consisting of two different compounds (**7** and **13**) in each and incubated at normal culturing conditions for 10 h. Images for each compound well were captured under an inverted microscope and analyzed.

Mutagenicity studies

Chemicals

Sodium azide (SA), 4-nitro-o-phenylenediamine (NPD), mitomycin C (MMC), 2-aminoanthracene (2-AA), biotin, histidine, nicotinamide adenine dinucleotide phosphate (NADP), glucose-6-phosphate, ampicillin trihydrate, agar, and dimethyl sulfoxide (DMSO) were supplied from Sigma Chemical Company (St Louis, Missouri, USA). The nutrient broth was supplied from HiMedia Laboratories Ltd (Mumbai, Maharashtra, India). The post-mitochondrial fraction (S9) and bacteria were purchased from the Moltox molecular toxicology, Inc (North Carolina, USA).

Mutagenicity assay

The tester strains employed were *Salmonella typhimurium* TA98, TA100 and TA102. TA98 detects frameshift and TA100 detects base pair mutagens. TA102 detects a variety of oxidants and other agents as mutagens, which are not detected by the other tester strains. Compounds **7** and **13** were dissolved in DMSO and different concentrations up to 1000 µg/plate (1, 10, 100, and 1000 µg/plate) were used for mutagenicity assay. The solubility in the final treatment mixture was used for determining the highest concentration of test substances according to OECD guideline [93].

Briefly, for each plate to be treated in the absence of metabolic activation, a 2.0 mL of top agar was added to a sterile glass 13 mm culture tube; 0.05 mL aliquot of negative, positive, or test chemical solution; 0.50 mL of phosphate buffer (0.2 M, pH 7.4); and finally, 0.10 mL of the appropriate bacterial culture were added to each tube. To evaluate the impact of test samples metabolites, instead of phosphate buffer, 0.50 mL of S9 mix was added immediately prior to the addition of bacterial culture in the experiment with metabolic activation. The tube contents were immediately vortex mixed and then transferred to the surface of the minimal glucose agar plates, inverted, and placed at 37 °C for 48 h in dark and revertant colonies were counted after incubation [94].

Statistical analysis

In mutagenicity assay, results were expressed as the mean of triplicates ± standard deviation. Dunnett's multiple comparison test was carried out for data in the *Salmonella* assay. The value of $p < 0.05$ was considered statistically significant.

In silico methods

Molecular modeling methods

The structures of 40 experimentally determined molecules and two reference molecules (**MK-886** and **4b** [1]) were modeled using the Biovia Discovery Studio 4.5 (DS) (Dassault Systemes BIOVIA, 2017) program and optimized with using DS ligand preparation tool. The enzymes used in molecular docking studies are, respectively, mPGES-1 (PDB ID: 5K0I, resolution: 1.30 Å) [95], COX-1 (PDB ID: 5WBE, resolution: 2.75 Å) [96] and COX-2 (PDB ID: 3NT1, resolution: 1.73 Å) [97] retrieved from Protein Data Bank (https://www.rcsb.org), an online protein database. Proteins were cleared of co–Crystallized inhibitors, non-interacting ions, and water molecules. All missing residues and hydrogens were added. Proteins were prepared with BIOVIA "Prepare Macromolecule" toolkit. The prepared ligand and enzyme structures were used as input files in docking studies. AutoDock 4.2.6 docking program (http://autodock.scripps.edu) [98] was used for all docking experiments. The studies were arranged to make the proteins rigid and all ligands flexible. The grid center coordinates of the mPGES-1 enzyme were, respectively, 9.697, 15.296, and 27.28 (x, y, z); the grid center coordinates of the COX-1 enzyme were 37.205, 163.297, and 27.409 (x, y, z); and the grid center coordinates of the COX-2 enzyme were formed as − 54.506, − 55.797, and − 11.193 (x, y, z). An energy grid box of 50 × 50 × 50 Å was chosen in all studies. Ten independent runs were randomly performed for each ligand. Autodock 4.2's Lamarckian Genetic Algorithm [99] was used with a 20,000,000 energy rating. Visualization was performed using the BIOVIA program to process interactions between ligands and active sites of protein complexes.

Determination of predicted ADMET profile

In this study, water solubility and molecular descriptors (molecular weight, LogP, number of hydrogen bond donors/acceptors, topological polar surface area, number of rotatable bonds, %ABS …) of compounds **7–46** were evaluated, besides Lipinski's Rule of 5 and Veber's rules. All of these data were obtained from the online web server SwissADME [100], while estimated intestinal absorption (%ABS) was calculated as follows: %ABS = 109 − (0.345 × TPSA) according to the method of Zhao et al. [101]. In addition, graphical distribution of lipophilicity and polarity of compounds

7–46 were prepared using the boiled egg predictive model from the online web server SwissADME [86]. Finally, the predicted toxicity risk profiles (mutagenicity, tumorigenicity, irritant, and reproductive effects) of compounds **11–46** were evaluated using OSIRIS DataWarrior software [102].

Supplementary Information The online version contains supplementary material available at https://doi.org/10.1007/s11030-022-10551-0.

Funding This work has been supported by Marmara University Scientific Research Projects Coordination Unit under grant number SAG-A-070617-0336.

Declarations

Conflicts of interest The authors declare that they have no conflict of interest.

References

1. Bülbül B, Küçükgüzel İ (2019) Microsomal prostaglandin E2 synthase-1 as a new macromolecular drug target in the prevention of inflammation and cancer. Anticancer Agents Med Chem 19:1205–1222. https://doi.org/10.2174/1871520619666190227174137
2. Larsson K, Jakobsson PJ (2015) Inhibition of microsomal prostaglandin E synthase-1 as targeted therapy in cancer treatment. Prostagland Other Lipid Mediat 120:161–165. https://doi.org/10.1016/j.prostaglandins.2015.06.002
3. Eibl G, Bruemmer D, Okada Y, Duffy JP, Law RE, Reber HA, Hines OJ (2003) PGE2 is generated by specific COX-2 activity and increases VEGF production in COX-2-expressing human pancreatic cancer cells. Biochem Biophys Res Commun 306:887–897. https://doi.org/10.1016/S0006-291X(03)01079-9
4. Dufour M, Faes S, Dormond-Meuwly A, Demartines N, Dormond O (2014) PGE2-induced colon cancer growth is mediated by MTORC1. Biochem Biophys Res Commun 451:587–591. https://doi.org/10.1016/j.bbrc.2014.08.032
5. Zhang S, Da L, Yang X, Feng D, Yin R, Li M, Zhang Z, Jiang F, Xu L (2014) Celecoxib potentially inhibits metastasis of lung cancer promoted by surgery in mice, via suppression of the PGE2-modulated β-catenin pathway. Toxicol Lett 225:201–207. https://doi.org/10.1016/j.toxlet.2013.12.014
6. Chen EP, Smyth EM (2011) COX-2 and PGE2-dependent immunomodulation in breast cancer. Prostagland Other Lipid Mediat 96:14–20. https://doi.org/10.1016/j.prostaglandins.2011.08.005
7. Ruan D, So SP (2014) Prostaglandin E2 produced by inducible COX-2 and MPGES-1 promoting cancer cell proliferation in vitro and in vivo. Life Sci 116:43–50. https://doi.org/10.1016/j.lfs.2014.07.042
8. Nakanishi M, Gokhale V, Meuillet EJ, Rosenberg DW (2010) MPGES-1 as a target for cancer suppression. Biochimie 92:660–664. https://doi.org/10.1016/j.biochi.2010.02.006
9. Mattila S, Tuominen H, Koivukangas J, Stenbäck F (2009) The terminal prostaglandin synthases MPGES-1, MPGES-2, and CPGES are all overexpressed in human gliomas. Neuropathology 29:156–165. https://doi.org/10.1111/j.1440-1789.2008.00963.x
10. Hanaka H, Pawelzik SC, Johnsen JI, Rakonjac M, Terawaki K, Rasmuson A, Sveinbjörnsson B, Schumacher MC, Hamberg M, Samuelsson B, Jakobsson PJ, Kogner P, Rådmark O (2009) Microsomal prostaglandin E synthase 1 determines tumor growth in vivo of prostate and lung cancer cells. Proc Natl Acad Sci 106:18757–18762. https://doi.org/10.1073/pnas.0910218106
11. Salvado MD, Alfranca A, Haeggström JZ, Redondo JM (2012) Prostanoids in tumor angiogenesis: therapeutic intervention beyond COX-2. Trends Mol Med 18:233–243. https://doi.org/10.1016/j.molmed.2012.02.002
12. Ricciotti E, FitzGerald GA (2011) Prostaglandins and inflammation. Arterioscl Thromb Vasc Biol 31:986–1000. https://doi.org/10.1161/ATVBAHA.110.207449
13. El-Husseiny WM, El-Sayed MAA, Abdel-Aziz NI, El-Azab AS, Asiri YA, Abdel-Aziz AAM (2018) Structural alterations based on naproxen scaffold: synthesis, evaluation of antitumor activity and COX-2 inhibition, and molecular docking. Eur J Med Chem 158:134–143. https://doi.org/10.1016/j.ejmech.2018.09.007
14. Matos P, Kotelevets L, Jordan P, Gonçalves V, Henriques A, Zerbib P, Moyer MP, Chastre E (2013) Ibuprofen inhibits colitis-induced overexpression of tumorrelated Rac1b. Neoplasia 15:102–111. https://doi.org/10.1593/neo.121890
15. Greenspan EJ, Madigan JP, Boardman LA, Rosenberg DW (2011) Ibuprofen ınhibits activation of nuclear β-catenin in human colon adenomas and ınduces the phosphorylation of GSK-3β. Cancer Prev Res 4:161–171. https://doi.org/10.1158/1940-6207.CAPR-10-0021
16. Endo H, Yano M, Okumura Y, Kido H (2014) Ibuprofen enhances the anticancer activity of cisplatin in lung cancer cells by inhibiting the heat shock protein 70. Cell Death Dis 5:e1027–e1027. https://doi.org/10.1038/cddis.2013.550
17. Sujith KV, Rao JN, Shetty P, Kalluraya B (2009) Regioselective reaction: synthesis and pharmacological study of mannich bases containing ibuprofen moiety. Eur J Med Chem 44:3697–3702. https://doi.org/10.1016/j.ejmech.2009.03.044
18. Abbas SE, Awadallah FM, Ibrahim NA, Gouda AM (2010) Novel substituted and fused pyrrolizine derivatives: synthesis, anti-inflammatory and ulcerogenecity studies. Eur J Med Chem 45:482–491. https://doi.org/10.1016/j.ejmech.2009.10.031
19. Küçükgüzel İ, Küçükgüzel ŞG, Rollas S, Ötük-Sanış G, Özdemir O, Bayrak İ, Altuğ T, Stables JP (2004) Synthesis of some 3-(arylalkylthio)-4-alkyl/aryl-5-(4-aminophenyl)-4H-1,2,4-triazole derivatives and their anticonvulsant activity. Il Farm 59:893–901. https://doi.org/10.1016/j.farmac.2004.07.005
20. Küçükgüzel İ, Tatar E, Küçükgüzel ŞG, Rollas S, De Clercq E (2008) Synthesis of some novel thiourea derivatives obtained from 5-[(4-aminophenoxy)methyl]-4-alkyl/aryl-2,4-dihydro-3h-1,2,4-triazole-3-thiones and evaluation as antiviral/anti-HIV and anti-tuberculosis agents. Eur J Med Chem 43:381–392. https://doi.org/10.1016/j.ejmech.2007.04.010
21. Navidpour L, Shafaroodi H, Abdi K, Amini M, Ghahremani MH, Dehpour AR, Shafiee A (2006) Design, synthesis, and biological evaluation of substituted 3-alkylthio-4,5-diaryl-4H-1,2,4-triazoles as selective COX-2 inhibitors. Bioorg Med Chem 14:2507–2517. https://doi.org/10.1016/j.bmc.2005.11.029
22. Salgın-Gökşen U, Gökhan-Kelekçi N, Göktaş Ö, Köysal Y, Kılıç E, Işık Ş, Aktay G, Özalp M (2007) 1-Acylthiosemicarbazides, 1,2,4-triazole-5(4H)-thiones, 1,3,4-thiadiazoles and hydrazones containing 5-methyl-2-benzoxazolinones: synthesis, analgesic-anti-inflammatory and antimicrobial activities. Bioorg Med Chem 15:5738–5751. https://doi.org/10.1016/j.bmc.2007.06.006
23. Küçükgüzel ŞG, Küçükgüzel İ, Tatar E, Rollas S, Şahin F, Güllüce M, De Clercq E, Kabasakal L (2007) Synthesis of some novel heterocyclic compounds derived from diflunisal hydrazide as potential anti-infective and anti-inflammatory agents. Eur J Med Chem 42:893–901. https://doi.org/10.1016/j.ejmech.2006.12.038
24. Sakya SM, Shavnya A, Cheng H, Li C, Rast B, Li J, Koss DA, Jaynes BH, Mann DW, Petras CF, Seibel SB, Haven ML, Lynch

MP (2008) comparative structure-activity relationship studies of 1-(5-methylsulfonylpyrid-2-Yl)-5-alkyl and (hetero)aryl triazoles and pyrazoles in canine COX inhibition. Bioorg Med Chem Lett 18:1042–1045. https://doi.org/10.1016/j.bmcl.2007.12.025
25. Hassan GS, Hegazy GH, Ibrahim NM, Fahim SH (2019) New ibuprofen derivatives as H_2S and NO donors as safer anti-inflammatory agents. Future Med Chem 11:3029–3045. https://doi.org/10.4155/fmc-2018-0467
26. Kulabaş N, Tatar E, Bingöl Özakpınar Ö, Özsavcı D, Pannecouque C, De Clercq E, Küçükgüzel İ (2016) Synthesis and antiproliferative evaluation of novel 2-(4H–1,2,4-triazole-3-ylthio) acetamide derivatives as inducers of apoptosis in cancer cells. Eur J Med Chem 121:58–70. https://doi.org/10.1016/j.ejmech.2016.05.017
27. Erensoy G, Ding K, Zhan C-G, Elmezayen A, Yelekçi K (2020) Synthesis, in silico studies and cytotoxicity evaluation of novel 1,3,4-oxadiazole derivatives designed as potential MPGES-1 ınhibitors. J Res Pharm 24:436–451
28. Turky A, Bayoumi AH, Sherbiny FF, El-Adl K, Abulkhair HS (2021) Unravelling the anticancer potency of 1,2,4-triazole-N-arylamide hybrids through Inhibition of STAT3: synthesis and in silico mechanistic studies. Mol Divers 25:403–420. https://doi.org/10.1007/s11030-020-10131-0
29. Turky A, Sherbiny FF, Bayoumi AH, Ahmed HEA, Abulkhair HS (2020) Novel 1,2,4-triazole derivatives: design, synthesis, anticancer evaluation, molecular docking, and pharmacokinetic profiling studies. Arch Pharm (Weinheim) 353:e2000170. https://doi.org/10.1002/ardp.202000170
30. He S, Li C, Liu Y, Lai L (2013) Discovery of highly potent microsomal prostaglandin E 2 synthase 1 inhibitors using the active conformation structural model and virtual screen. J Med Chem 56:3296–3309. https://doi.org/10.1021/jm301900x
31. Vasincu I, Apotrosoaei M, Tuchiluş C, Pânzariu AT, Dragostin O, Lupaşcu D (2013) Profire, L new derıvatıves of aryl-propıonıc acıd. Synthesıs and bıologıcal evaluatıon. Rev Med Chir Soc Med Nat Iaşi 117:532–537
32. Dhall E, Jain S, Mishra A, Dwivedi J, Sharma S (2018) Synthesis and evaluation of some phenyl substituted azetidine containing 1, 2, 4-triazole derivatives as antibacterial agents. J Heterocycl Chem 55:2859–2869. https://doi.org/10.1002/jhet.3357
33. Raviprabha K, Manjunatha K, Poojary B, Kumar V, Harish N (2015) Synthesis, characterisation and antimicrobial activities of newer 3,4,5-trisubstitued [1,2,4]-triazoles derivatives. Int J Pharm Res Sch 4:96–104
34. Manjunatha K, Poojary B, Kumar V, Lobo PL, Fernandes J, Chandrashekhar C (2015) Synthesis, characterization and antimicrobial activities of imidazo-[2,1, b][1,3,4]-thiadiazoles. Pharma Chem 7:207–215
35. Nargund LVG, Reddy GRN, Hariprasad V (1994) Anti-inflammatory activity of substituted 1,3,4-oxadiazoles. J Pharm Sci 83:246–248. https://doi.org/10.1002/jps.2600830226
36. Durgun BB, Rollas S, Apaydın S, Öztürk R (1995) Synthesis and antimicrobial activity of some new 1-[4-(4-fluorobenzoylamino) benzoyl)-4-substituted thiosemicarbazides. Drug Metabol Drug Interact 12:145. https://doi.org/10.1515/DMDI.1995.12.2.145
37. Doğan H, Duran A, Yemni E (1999) Synthesıs and antıbacterıal actıvıty of l-(3-hydroxy-2-naphthoyl)-4-substıtuted thıosemıcarbazıdes. Drug Metabol Drug Interact 15:10
38. Küçükgüzel ŞG, Oruç EE, Rollas S, Şahin F, Özbek A (2002) Synthesis, characterisation and biological activity of novel 4-thiazolidinones, 1,3,4-oxadiazoles and some related compounds. Eur J Med Chem 37:197–206. https://doi.org/10.1016/S0223-5234(01)01326-5
39. Cesur N, Birteksöz S, Ötük G (2002) Synthesis and biological evulation of some new thiosemicarbazides, 4-thiazolidinone, 1,3,4-oxadiazole and 1,2,4-triazole-3-thione derivatives bearing imidazo[1,2-α]pyridine moiety. Acta Pharm Turc 44:23–41
40. Çoruh I, Rollas S, Turan S, Akbuğa J (2012) Synthesis and evaluation of cytotoxic activities of some 1,4-disubstituted thiosemicarbazides, 2,5-disubstituted-1,3,4-thiadiazoles and 1,2,4-triazole-5-thiones derived from benzilic acid hydrazide. Marmara Pharm J 1:56–63
41. Omar F, Mahfouz N, Rahman M (1996) Design, synthesis and antiinflammatory activity of some 1,3,4-oxadiazole derivatives. Eur J Med Chem 31:819–825. https://doi.org/10.1016/0223-5234(96)83976-6
42. Tutoveanu M, Constantinescu C, Maerean V (1973) New semi- and thiosemicarbazides and cyclization products. Rev Chim 24:155–158
43. Vasilev G (1991) Synthesis and growth-regulating activity of some hydrazides and thiosemicarbazides of the benzoic, phenylacetic, and 1-naphthylacetic acids. Dokl Na Bulg Akad Na Nauk 44:101–104
44. Dobosz M, Pachuta-Stec A (1996) Synthesis of new derivatives of 3-benzyl-δ2-1,2,4-triazoline-5thione and 5-benzyl-1,3,4-thiadiazole. Act Pol Pharm Drug Res 53:123–131
45. Wujec M, Pachuta-Stec A, Stefańska J, Kuśmierz E, Siwek A (2013) Synthesis and antibacterial activity of some new derivatives of thiosemicarbazide and 1,2,4-triazole. Phosph Sulfur Silicon Relat Elem 188:1661–1669. https://doi.org/10.1080/10426507.2012.757612
46. Küçükgüzel ŞG, Çıkla-Süzgün P (2015) Recent advances bioactive 1,2,4-triazole-3-thiones. Eur J Med Chem 97:830–870. https://doi.org/10.1016/j.ejmech.2014.11.033
47. Ulusoy N, Çapan G, Ergenç N, Ekinci A, Vidin A (1998) Synthesis, characterization and anticonvulsant activity of new 4-thiazolidinone and 1,2,4-triazole-3-thione derivatives. Acta Pharm Turc 40:5–8
48. Coşkun G, Djikic T, Hayal T, Türkel N, Yelekçi K, Şahin F, Küçükgüzel Ş (2018) Synthesis, molecular docking and anticancer activity of diflunisal derivatives as cyclooxygenase enzyme inhibitors. Molecules 23:1969. https://doi.org/10.3390/molecules23081969
49. Marcel P, Bellon R (1961) Erfectionnements Au Procédé de Préparation Des Mercapto 3 Triazoles 1. 2. 4. Etproduits Fabriqués Selon Le Procédé. FR1273881(A) 1961-10-20.
50. Abdel-Aziz M, Abuo-Rahma GEDAA, Beshr EAM, Ali TFS (2013) New nitric oxide donating 1,2,4-triazole/oxime hybrids: synthesis, investigation of anti-inflammatory, ulceroginic liability and antiproliferative activities. Bioorg Med Chem 21:3839–3849. https://doi.org/10.1016/j.bmc.2013.04.022
51. Mohassab AM, Hassan HA, Abdelhamid D, Abdel-Aziz M, Dalby KN, Kaoud TS (2017) Novel quinoline incorporating 1,2,4-triazole/oxime hybrids: synthesis, molecular docking, anti-inflammatory, cox inhibition, ulceroginicity and histopathological investigations. Bioorg Chem 75:242–259. https://doi.org/10.1016/j.bioorg.2017.09.018
52. Karakurt A, Dalkara S (1999) Oksim ve Oksim Eterler: I. Sentezleri ve Farmakolojik Özellikleri. FABAD J Pharm Sci 24:143–156
53. Rollas S, Kalyoncuoğlu N, Altıner D, Yeğenoğlu Y (1993) 5-(4-Aminophenyl)-4-substitued 2,4-dihydro-3H-1,2,4-triazole-3-thiones: synthesis and antibacterial and antifungal activities. Pharmazie 48(308):309
54. Bayrak H, Demirbas A, Karaoglu SA, Demirbas N (2009) Synthesis of some new 1,2,4-triazoles, their Mannich and Schiff bases and evaluation of their antimicrobial activities. Eur J Med Chem 44:1057–1066. https://doi.org/10.1016/j.ejmech.2008.06.019
55. Kumar H, Javed SA, Khan SA, Amir M (2008) 1,3,4-Oxadiazole/thiadiazole and 1,2,4-triazole derivatives of biphenyl-4-yloxy

acetic acid: synthesis and preliminary evaluation of biological properties. Eur J Med Chem 43:2688–2698. https://doi.org/10.1016/j.ejmech.2008.01.039
56. Amir M, Kumar S (2007) Synthesis and evaluation of anti-inflammatory, analgesic, ulcerogenic and lipid peroxidation properties of ibuprofen derivatives. Acta Pharm 57:31–45. https://doi.org/10.2478/v10007-007-0003-y
57. Baji H, Flammang M, Kimny T, Gasquez F, Compagnon P, Delcourt A (1995) Synthesis and antifungal activity of novel (l-aryl-2-heterocyclyl)ethylideneaminooxymethyl-substituted dioxolanes. Eur J Med Chem 30:617–626
58. Ansari MS, Rama NH, Hussain MT, Raza AR (2000) Diastereotopy in some 3,4-dihydroisocoumarins—effect of changing the substituents on the chiral centre. Spectrochim Acta A Mol Biomol Spectrosc 56:1385–1389. https://doi.org/10.1016/S1386-1425(99)00266-8
59. Khan N, Ansari MS, Baber Z (2002) Diastereotopic effect in some N-Substituted-3-methyl-4,1-benzoxazepine-2,5-diones. Spectrochim Acta A Mol Biomol Spectrosc 58:2265–2269. https://doi.org/10.1016/S1386-1425(01)00698-9
60. Frączek T, Paneth A, Kamiński R, Krakowiak A, Paneth P (2015) Searching for novel scaffold of triazole non-nucleoside inhibitors of HIV-1 reverse transcriptase. J Enzyme Inhib Med Chem 31:1–9. https://doi.org/10.3109/14756366.2015.1039531
61. Saal C, Becker A, Krier M, Fuchß T (2021) Atropisomerism: a neglected way to escape out of solubility flatlands. J Pharm Sci 111:206–213. https://doi.org/10.1016/j.xphs.2021.10.011
62. Laoufi A, Belboukhari N, Sekkoum K, Aboul-Enein HY (2021) Synthesis and chiral separation of atropisomers of 4,5-di methyl Δ 4 N-phenyl N-aryl Imidazoline-2-thione derivatives. Chirality 33:264–273. https://doi.org/10.1002/chir.23306
63. Silverstein R, Webster F, Kiemle J (2005) In Spectrometric identification of organic compounds. Wiley, New Jersey, pp 171–172
64. Balcı M (2005) Basic 1 H- and 13 C-NMR spectroscopy, 1 edn, transferred to digital print. Elsevier, Amsterdam, Heidelberg
65. Günay NS, Çapan G, Ulusoy N, Ergenç N, Ötük G, Kaya D (1999) 5-Nitroimidazole derivatives as possible antibacterial and antifungal agents. Il Farm 54:826–831. https://doi.org/10.1016/S0014-827X(99)00109-3
66. Karczmarzyk Z, Pitucha M, Wysocki W, Pachuta-Stec A, Stańczuk A (2013) 3-Benzyl-4-ethyl-1 H-1,2,4-triazole-5(4 H)-thione. Acta Crystallogr Sect E Struct Rep Online 69:o155–o156. https://doi.org/10.1107/S1600536812051276
67. Andersen HKG, Christensen I, Mogensen J, Larsen (2004) Pharmaceutical use of substituted 1,2,4-triazoles. WO2004/089367(A1).
68. Kampen G, Andersen H (2004) Combination therapy using an 11-beta-hydroxysteroid dehydrogenase type 1 ınhibitor and an antihypertansive agent for the treatment of metabolic syndrome and related diseases and disorders. Patent No: WO2004/089416(A2).
69. Kampen G Andersen H (2004) Combination therapy using an 11β-hydroxysteroid dehydrogenase type 1 ınhibitor and a glucocorticoid receptor agonist to minimize the side effects associated with glucocorticoid receptor agonist therapy. WO2004/089415(A2)
70. Wobst I, Schiffmann S, Birod K, Maier TJ, Schmidt R, Angioni C, Geisslinger G, Grösch S (2008) Dimethylcelecoxib inhibits prostaglandin E2 production. Biochem Pharmacol 76:62–69. https://doi.org/10.1016/j.bcp.2008.04.008
71. Hanke T, Rörsch F, Thieme TM, Ferreiros N, Schneider G, Geisslinger G, Proschak E, Grösch S, Schubert-Zsilavecz M (2013) Synthesis and pharmacological characterization of benzenesulfonamides as dual species inhibitors of human and murine MPGES-1. Bioorg Med Chem 21:7874–7883. https://doi.org/10.1016/j.bmc.2013.10.006
72. Howe LR, Subbaramaiah K, Kent CV, Zhou XK, Chang S-H, Hla T, Jakobsson P-J, Hudis CA, Dannenberg AJ (2013) Genetic deletion of microsomal prostaglandin E synthase-1 suppresses mouse mammary tumor growth and angiogenesis. Prostaglandins Other Lipid Mediat 106:99–105. https://doi.org/10.1016/j.prostaglandins.2013.04.002
73. Olesch C, Sha W, Angioni C, Sha LK, Açaf E, Patrignani P, Jakobsson P-J, Radeke HH, Grösch S, Geisslinger G, von Knethen A, Weigert A, Brüne B (2015) MPGES-1-derived PGE2 suppresses CD80 expression on tumor-associated phagocytes to ınhibit anti-tumor ımmune responses in breast cancer. Oncotarget 6:10284–10296
74. Li Y, Chen J, Yin S, Nie D, He Z, Xie S, Wang X, Wu Y, Xiao J, Liu H, Wang J, Yang W, Ma L (2018) Regulation of MPGES-1 composition and cell growth via the MAPK signaling pathway in jurkat cells. Exp Ther Med 16:3211–3219. https://doi.org/10.3892/etm.2018.6538
75. Othman EM, Fayed EA, Husseiny EM, Abulkhair HS (2022) The effect of novel synthetic semicarbazone- and thiosemicarbazone-linked 1,2,3-triazoles on the apoptotic markers, VEGFR-2, and cell cycle of myeloid leukemia. Bioorganic Chem 127:105968. https://doi.org/10.1016/j.bioorg.2022.105968
76. Othman EM, Fayed EA, Husseiny EM, Abulkhair HS (2022) Apoptosis induction, PARP-1 inhibition, and cell cycle analysis of leukemia cancer cells treated with novel synthetic 1,2,3-triazole–chalcone conjugates. Bioorg Chem 123:105762. https://doi.org/10.1016/j.bioorg.2022.105762
77. Özsavcí D, Erşahin M, Şener A, Özakpinar ÖB, Toklu HZ, Akakín D, Şener G, Yeğen BÇ (2011) The novel function of nesfatin-1 as an anti-inflammatory and antiapoptotic peptide in subarachnoid hemorrhage-induced oxidative brain damage in rats. Neurosurgery 68:1699–1708. https://doi.org/10.1227/NEU.0b013e318210f258
78. Ding K, Zhou Z, Hou S, Yuan Y, Zhou S, Zheng X, Chen J, Loftin C, Zheng F, Zhan C-G (2018) Structure-based discovery of MPGES-1 ınhibitors suitable for preclinical testing in wild-type mice as a new generation of anti-ınflammatory drugs. Sci Rep 8:5205. https://doi.org/10.1038/s41598-018-23482-4
79. Kubota Y, Kleinman HK, Martin GR, Lawley TJ (1988) Role of laminin and basement membrane in the morphological differentiation of human endothelial cells into capillary-like structures. J Cell Biol 107:1589–1598. https://doi.org/10.1083/jcb.107.4.1589
80. Kamei D, Murakami M, Sasaki Y, Nakatani Y, Majima M, Ishikawa Y, Ishii T, Uematsu S, Akira S, Hara S, Kudo I (2010) Microsomal prostaglandin E synthase-1 in both cancer cells and hosts contributes to tumour growth, invasion and metastasis. Biochem J 425:361–371. https://doi.org/10.1042/BJ20090045
81. Wu K-M, Dou J, Ghantous H, Chen S, Bigger A, Birnkrant D (2010) Current regulatory perspectives on genotoxicity testing for botanical drug product development in the U.S.A. Regul Toxicol Pharmacol 56:1–3. https://doi.org/10.1016/j.yrtph.2009.09.012
82. Khurana P, Jachak SM (2016) Chemistry and biology of microsomal prostaglandin E 2 synthase-1 (MPGES-1) inhibitors as novel anti-inflammatory agents: recent developments and current status. RSC Adv 6:28343–28369. https://doi.org/10.1039/C5RA25186A
83. Stoyanov S, Petkov I, Antonov L, Stoyanova T, Karagiannidis P, Aslanidis P (1990) Thione-thiol tautomerism and stability of 2- and 4-mercaptopyridines and 2-mercaptopyrimidines. Can J Chem 68:1482–1489. https://doi.org/10.1139/v90-227
84. Lipinski CA, Lombardo F, Dominy BW, Feeney PJ (2001) Experimental and computational approaches to estimate solubility and permeability in drug discovery and development settings. Adv Drug Deliv Rev 46:3–26

85. Veber DF, Johnson SR, Cheng H-Y, Smith BR, Ward KW, Kopple KD (2002) Molecular properties that influence the oral bioavailability of drug candidates. J Med Chem 45:2615–2623. https://doi.org/10.1021/jm020017n
86. Daina A, Zoete VA (2016) BOILED-egg to predict gastrointestinal absorption and brain penetration of small molecules. Chem Med Chem 11:1117–1121. https://doi.org/10.1002/cmdc.201600182
87. Lin JH, Yamazaki M (2003) Role of P-glycoprotein in pharmacokinetics: clinical implications. Clin Pharmacokinet 42:59–98. https://doi.org/10.2165/00003088-200342010-00003
88. Hamza A, Tong M, AbdulHameed MDM, Liu J, Goren AC, Tai H-H, Zhan C-G (2010) Understanding microscopic binding of human microsomal prostaglandin E synthase-1 (MPGES-1) trimer with substrate PGH 2 and cofactor GSH: insights from computational alanine scanning and site-directed mutagenesis. J Phys Chem B 114:5605–5616. https://doi.org/10.1021/jp100668y
89. Ding K, Zhou Z, Zhou S, Yuan Y, Kim K, Zhang T, Zheng X, Zheng F, Zhan C-G (2018) Design, synthesis, and discovery of 5-((1,3-diphenyl-1 H-pyrazol-4-Yl)methylene)pyrimidine-2,4,6(1 H,3 H,5 H)-triones and related derivatives as novel inhibitors of MPGES-1. Bioorg Med Chem Lett 28:858–862. https://doi.org/10.1016/j.bmcl.2018.02.011
90. Hamza A, Zhao X, Tong M, Tai H-H, Zhan C-G (2011) Novel human MPGES-1 inhibitors identified through structure-based virtual screening. Bioorg Med Chem 19:6077–6086. https://doi.org/10.1016/j.bmc.2011.08.040
91. Zhou Z, Yuan Y, Zhou S, Ding K, Zheng F, Zhan C-G (2017) Selective inhibitors of human MPGES-1 from structure-based computational screening. Bioorg Med Chem Lett 27:3739–3743. https://doi.org/10.1016/j.bmcl.2017.06.075
92. Harding L, Wang Z, Tai H-H (1996) Stimulation of prostaglandin E2 synthesis by interleukin-1/3 is amplified by interferons but inhibited by interleukin-4 in human amnion-derived wish cells. Biochim Biophys Acta 1310:48–52
93. No T (2020) 471: Bacterial reverse mutation test, in OECD guidelines for the testing of chemicals. OECD Publishing, Paris
94. Maron DM, Ames BN (1983) Revised methods for the salmonella mutagenicity test. Mutat Res 113:173–215
95. Kuklish SL, Antonysamy S, Bhattachar SN, Chandrasekhar S, Fisher MJ, Fretland AJ, Gooding K, Harvey A, Hughes NE, Luz JG, Manninen PR, McGee JE, Navarro A, Norman BH, Partridge KM, Quimby SJ, Schiffler MA, Sloan AV, Warshawsky AM, York JS, Yu XP (2016) Characterization of 3,3-dimethyl substituted N-aryl piperidines as potent microsomal prostaglandin E synthase-1 inhibitors. Bioorg Med Chem Lett 26:4824–4828. https://doi.org/10.1016/j.bmcl.2016.08.023
96. Cingolani G, Panella A, Perrone MG, Vitale P, di Mauro G, Fortuna CG, Armen RS, Ferorelli S, Smith WL, Scilimati A (2017) Structural basis for selective ınhibition of cyclooxygenase-1 (COX-1) by diarylisoxazoles mofezolac and 3-(5-chlorofuran-2-Yl)-5-methyl-4-phenylisoxazole (P6). Eur J Med Chem 138:661–668. https://doi.org/10.1016/j.ejmech.2017.06.045
97. Duggan KC, Walters MJ, Musee J, Harp JM, Kiefer JR, Oates JA, Marnett LJ (2010) Molecular basis for cyclooxygenase inhibition by the non-steroidal anti-inflammatory drug naproxen. J Biol Chem 285:34950–34959. https://doi.org/10.1074/jbc.M110.162982
98. Morris GM, Huey R, Lindstrom W, Sanner MF, Belew RK, Goodsell DS, Olson AJ (2009) AutoDock4 and AutoDockTools4: automated docking with selective receptor flexibility. J Comput Chem 30:2785–2791. https://doi.org/10.1002/jcc.21256
99. Morris G, Goodsell D, Halliday R, Huey R, Hart W, Belew Olson A (1998) Automated docking using a lamarckian genetic algorithm and an empirical binding free energy function. J Comp Chem 19:1639–1662
100. Daina A, Michielin O, Zoete V (2017) SwissADME: a free web tool to evaluate pharmacokinetics, drug-likeness and medicinal chemistry friendliness of small molecules. Sci Rep 7:42717. https://doi.org/10.1038/srep42717
101. Zhao YH, Abraham MH, Le J, Hersey A, Luscombe CN, Beck G, Sherborne B, Cooper I (2002) Rate-limited steps of human oral absorption and QSAR studies. Pharm Res 19:1446–1457
102. Sander T, Freyss J, von Korff M, Rufener C (2015) DataWarrior: an open-source program for chemistry aware data visualization and analysis. J Chem Inf Model 55:460–473. https://doi.org/10.1021/ci500588j